UNIVERSITY OF
BIRMINGHAM

EFFECTS OF SPLIT INJECTION AND EXHAUST GAS RECIRCULATION STRATEGIES ON COMBUSTION AND EMISSIONS CHARACTERISTICS IN A MODERN V6 DIESEL ENGINE

By

NIK ROSLI ABDULLAH

A Thesis submitted to
The University of Birmingham
For the degree of
DOCTOR OF PHILOSOPHY

School of Mechanical Engineering
The University of Birmingham
March 2011

UNIVERSITY OF
BIRMINGHAM

University of Birmingham Research Archive

e-theses repository

This unpublished thesis/dissertation is copyright of the author and/or third parties. The intellectual property rights of the author or third parties in respect of this work are as defined by The Copyright Designs and Patents Act 1988 or as modified by any successor legislation.

Any use made of information contained in this thesis/dissertation must be in accordance with that legislation and must be properly acknowledged. Further distribution or reproduction in any format is prohibited without the permission of the copyright holder.

ABSTRACT

The thesis presents investigations of advanced combustion strategies in a modern V6 diesel engine fuelled with mineral diesel and Tallow Methyl Ester (TME)-diesel blends, in order to meet future emissions legislation. One of the main objectives of this research is to improve fuel consumption whilst minimising engine emissions through the combined effects of injection strategy (fuel injection pressure, dwell period, pilot fuel quantity) and cooled Exhaust Gas Recirculation (EGR) on a modern V6 common rail direct injection diesel engine.

In the case of using EGR (49–52%) at 1500 rpm and 10% of engine peak torque, by increasing the fuel injection pressure from 300 to 800 bar, engine thermal efficiency increased from 16.5 to 19.1% and 17.1 to 19.7%, BSFC decreased by 13.5% and 13.2%, smoke level decreased by 74.3% and 70.1% and NO_x emissions increased by 69.6% and 68.0%, respectively for a short (5 CAD) and a long (40 CAD) dwell period. In addition, the study of a variation of pilot fuel quantities (0.8–3.0 mg/stroke) with a fixed dwell period (5 CAD) at two different fuel injection pressures (250 bar and 800 bar) shows that the smaller pilot quantity with the higher fuel injection pressure can be considered as an enhanced strategy to control engine performance and emissions simultaneously. Therefore, the combination of higher injection pressure, longer dwell, smaller pilot quantity and the use of EGR could potentially improve fuel consumption and minimise engine emissions.

The use of TME-diesel blends results in lower engine thermal efficiency and higher fuel consumption and NO_x emissions. In the case of 1500 rpm and 25% of engine peak torque, the combustion of TME10 and TME30 reduced the engine thermal efficiency from

35.3 to 33.7% and 35.3 to 33.2% and increased the BSFC by 4.9% and 6.5%, respectively. At the same engine condition, the combustion of TME-diesel blends increased NO_x emissions by 1.8% and 10.0% and reduced CO by 0.9% and 1.8%, THCs by 18.0% and 23.9 %, smoke by 30% and 51.7% for TME10 and TME30 respectively. However, the engine thermal efficiency, BSFC and NO_x emissions could be improved with the application of the combined effect of injection strategy (fuel injection pressure, dwell period, pilot fuel quantity) and EGR as shown in the first phase of this study.

DEDICATION

dedicated to my parents Abdullah Che Noh and Raja Fatimah Raja Daud, my parents in-law Jamal Bun and Sri Hartati Jajuli, my wife Hanny Jamal, my lovely daughters Nik Hidayah & Nik Hanisah, my brothers, my sisters and motherland, Malaysia.

ACKNOWLEDGMENTS

I would like to express my deep gratitude to my supervisors Professor M.L. Wyszynski and Dr A. Tsolakis for their guidance and encouragement throughout my study. Without their great patience and attention to detail, this work would not be possible to complete with a good ending. A sincere thank to Professor H.M. Xu for his great support in my research work.

I would like to express my gratitude to my sponsors:

- The Malaysia Government and Universiti Teknologi MARA (UiTM) for the provision of my Ph.D. scholarship and maintenance grant,
- Jaguar Land Rover (JLR) for financial and technical support towards the research project,
    - Mr T. Gardiner for his excellent experimental work management,
    - Mr R. Rudra for his helpful technical support on the engine management system (EMS) setting-up and calibration,
- Shell Global Solutions UK through Prof. R. F. Cracknell for the supply of ULSD and biodiesel blends, and
- Green Fuel for biodiesel through Mr C. Hygate

I owe a big thank you to Mr C. Hingley, Mr P. Thornton and Mr L. Gauntlett for a wonderful support during engine set up. Also, my acknowledgements would be incomplete without acknowledging to my colleagues Dr R. Mamat, Dr G. Tian, Dr K. Theinnoi, Mr P. Rounce and Mr J. Zhang for their support as well as my social welfare.

TABLE OF CONTENTS

LIST OF FIGURES

LIST OF TABLES

LIST OF ABBREVIATIONS

AFR	Air fuel ratio
AT	Actuator of throttle
ATDC	After top dead centre
BMEP	Brake mean effective pressure
BP	Boost pressure
BSFC	Brake specific fuel consumption
BSN	Bosch smoke number
BTDC	Before top dead centre
BV	Butterfly valve
CA	Crank angle
CAD	Crank angle degree
CI	Compression ignition
CR	Common rail
CYL	Cylinder
D	Engine cylinder bore
DI	Direct injection
DOC	Diesel oxidation catalyst
DPF	Diesel particulate filter
DSG ltd	Dynamometer Services Group Limited
ECU	Electronic control unit
EDC	Electronic diesel control
EGR	Exhaust gas recirculation
EMS	Engine management system
FAME	Fatty acid methyl ester
FCU	Fuel cooling unit
FMS	Fuel measuring system
FSN	Filter smoke number
HCCI	Homogeneous charge compression ignition
HCLD	Heated chemiluminescent detector

HCN	Hydrogen cynide
HFID	Heated flame ionisation detector
IC	Internal combustion
ID	Ignition delay
IEA	International Energy Agency
IMEP	Indicated mean effective pressure
IOP	Injection of pressure
IP	Injection pressure
JLR	Jaguar-Land Rover
JOME	Jatropha oil methyl ester
LHV	Lower heating value
MFB	Mass fraction burnt
MK	Modulated kinetics
NAC	NO_x Adsorber Catalysts
NDIR	Non-dispersive infrared
NEDC	New European Driving Cycle
NI	National Instrument
PAH	Polycyclic aromatic hydrocarbon
PCI	Premixed compression ignition
PM	Particulate matter
PV	Process value
RME	Rapeseed methyl ester
RH	Relative humidity
ROHR	Rate of heat release
SCR	Selective Catalytic Reduction
SFC	Specific fuel consumption
SI	Spark ignition
SOC	Start of combustion
SOI	Start of injection
STK	Stroke
SV	Set value
TDC	Top dead centre

TME	Tallow methyl ester
ULSD	Ultra low sulphur diesel
UIS	Unit injector system
UPS	Unit pump system
VGT	Variable geometry turbocharger

LIST OF SYMBOLS

SYMBOL	UNIT	
g	m/s^2	Acceleration due to gravity
m_a	kg/s	Air mass flow rate
λ	-	Air excess ratio
N	rpm	Crankshaft rotational speed
ρ	kg/m^3	Density
μ	kg/ms	Dynamics viscosity
m_{EGR}	kg/s	EGR mass flow rate
P_b	kW	Engine brake power
T_b	Nm	Engine brake torque
η_{th}	%	Engine thermal efficiency
m_f	kg/s	Fuel mass flow rate
Φ	-	Fuel-to-air equivalence ratio
V	cm^3	Instantaneous volume of the engine cylinder
p	bar	In-cylinder pressure
$\Delta\theta_{delay}$	deg	Ignition delay
κ	joules	Kinetic energy
p_{max}	bar	Peak in-cylinder pressure
p_{drop}	bar	Pressure drop
γ	-	Ratio of specific heats
R_{swirl}	-	Swirl ratio
t	s	Time
m_{Total}	kg/s	Total air mass flow rate
R	J/mol. K	Universal gas constant
V	V	Voltage signal

CHAPTER 1
INTRODUCTION

Diesel engines have high thermal efficiency, high fuel economy, high durability and reliability which have resulted in them becoming the preferred engines in all heavy and many light duty vehicles. The high thermal efficiency results from the high power output with lower fuel consumption due to a high compression ratio [1]. However, diesel engines emit a higher level of emissions as compared with gasoline engines, especially oxides of nitrogen (NO_x) and Particulate Matter (PM) emissions. The application of direct injection (DI) diesel engines has expanded rapidly from commercial vehicles to passenger cars due to substantial improvements, with respect to emissions, fuel consumption and engine noise levels. The common rail direct fuel injection system has a capability of increasing the injection pressure up to 2000 bar, contributing to a cleaner and quieter diesel engine and having a positive impact on the environment [2-8]**.** The ultra high pressures enable complete combustion leading to less harmful emissions. In fact, a highly precise multiple injections strategy is favourable for NO_x-PM reduction, fuel consumption and engine noise.

The primary challenges in diesel engine research are exhaust emissions and engine noise. The NO_x emissions are related to the combustion temperature while the smoke level is related to the Air-Fuel ratio (AFR) or mixing process [9-13]. In the near future, fossil diesel fuel will be in short supply. In fact, a forecast of world oil consumption (oil-based fuels) by the International Energy Agency (IEA) suggests a dramatic increase in fuel consumption from 82.1 (2004) to 115.4 million barrels per day (2030) [14]. Therefore,

much research has been done on biodiesel as an alternative renewable fuel since both fuels have similar characteristics [15-36]. Biodiesel has special advantages in terms of higher cetane number, lower sulphur (sulphur-free), and lower aromatic hydrocarbons [16, 30, 31, 33, 37, 38]. The fuel is easy to combine with fossil diesel and can be used on diesel engines without requiring any engine modification. In fact, several engine manufacturers have declared that biodiesel was included in their warranty. In general, engines fuelled with biodiesel emit a lower level of emissions, except NO_x, as compared with fossil diesel fuel [16, 31, 39, 40]. Alternatively, the use of biodiesel can be combined with exhaust gas recirculation (EGR) to improve the NO_x emissions. Exhaust gas recirculation is an effective technique to reduce NO_x emissions emitted from diesel engines [10, 12, 41-44]. However, the technique tends to produce high particulate matter emissions, specific fuel consumption and degrade the lubrication oil quality and engine durability [45, 46]. Therefore, more research is required to study the effects of combustion strategy and exhaust gas recirculation on diesel engine performance and emissions when fuelled by biodiesel-diesel blends.

Based on the above discussion, this study has been developed to investigate the effects of injection timing (dwell period), fuel injection pressure, pilot fuel quantity and EGR rates on engine performance and emissions. These strategies are key in solving the initial problems encountered with diesel engines which are associated with a poor mixing process and an incomplete combustion. The experimental work has been done on fossil diesel and biodiesel blends fuel through a combustion strategy at a variety of engine speeds and loads chosen to comply with selected points of the New European Driving Cycle (NEDC). The main objective is to improve engine performance and emissions

accompanied by low fuel consumption in a wide range of fuel types and engine test conditions.

1.1. Background

In the following section, the background information about emissions regulation, diesel engine operation, injection modes and emissions control in diesel engines are discussed. The first subsection presents the latest information about the emissions regulation. In the last subsection, the emissions control in diesel engines is described.

1.1.1 Emission Regulations

The most challenging task in diesel emissions controls is the combination of NO_x and PM emissions. The emissions which constitute the major part of PM are characterized by a carbonic mixture composed of approximately 18,000 different high-molecular-weight organic compounds [3]. PM consists of a mixture of solid and liquid species differing in origin, dimension and composition. The fraction of soot in the PM from diesel exhaust varies, but it is typically higher than 50% [4]. This pollutant is strongly correlated with adverse effects on the respiratory system and it can be classified by size as PM10 and PM2.5, which means that the particles diameter is less than 10 and 2.5 µm respectively [3]. Therefore, the reduction of the emissions level is always regarded as an important target to be achieved for human stability and to be environmentally friendly.

Soot is a solid substance consisting of roughly eight parts carbon and one part hydrogen, most primary particles range in size from about 20 to 70 nm [4]. It is formed from unburned fuel, which nucleates from the vapour phase to a solid phase in fuel-rich regions at elevated temperatures. Soot absorbs hydrocarbons or other available molecules

in the exhaust system. Soot is quite complicated to control. The higher temperatures at the end of combustion enhance the burnout of soot, while high temperatures at the time of injection reduce air entrainment and increase soot formation due to incomplete combustion [4]. In the diffusion combustion phase, the amount of soot formed increases monotonically with the increasing temperature, particularly for the case of oxygen deficiency [10, 11, 13] and decreases with high oxygen availability [26, 44].

Table 1.1 shows that European Union emission standards for passenger cars diesel engines have tightened since EURO 1 which came into force in 1992 up to EURO 6 for the year of 2014 in the future. It is evident from the Table 1.1 that the major challenges raised in diesel engines are NO_x and PM emissions.

Table 1.1. European Union emission standards for diesel engine passenger cars [47]

Tier	Year	g/km				
		CO	**HC**	**NOx**	**HC+ NOx**	**PM**
EURO 1*	July 1992	2.72 (3.16)	-	-	0.97(1.13)	0.14 (0.18)
EURO 2	January 1996	1.00	-	-	0.70	0.08
EURO 3	January 2000	0.64	-	0.50	0.56	0.05
EURO 4	January 2005	0.50	-	0.25	0.30	0.025
EURO 5	September 2009	0.500	-	0.180	0.230	0.005
EURO 6	September 2014	0.500	-	0.080	0.170	0.0025

* Values in brackets are conformity of production (COP) limits.

1.1.2. 4- Stroke Diesel Engine Operation

Diesel engines produce high pressure during compression stroke due to their operation with high compression ratio. The engine converts the chemical energy stored in fuel into mechanical energy through the crankshaft. One complete 4-stroke engine cycle consists of four events (intake, compression, power and expansion). Each event requires 180 crank angle degrees (CAD), so that the complete cycle requires two rotations of the crankshaft which is 720 crank angle degrees (CAD). The combustion process occurs when

the fuel is injected into the hot compressed air near the end of the compression stroke. The high compression ratio up to 25:1 is used to compress the fresh air while simultaneously heating the mixture up to approximately 627 ^{0}C before injection [48]. The engine power is controlled by the amount of fuel injected into the combustion chamber. In general, diesel engines combustion occurs with a lean mixture up to 1.5-1.8 of lambda value on full load and higher lambda values at lower loads [1, 49]. However, in the whole mixture there still remain spot regions of rich mixture, which contributes to higher emissions. The engine firing order is defined as the order of combustion in each cylinder of multi-cylinder engines. For example, in a six cylinder as shown in Figure 1.1, the engine's firing order is 1, 4, 2, 5, 3, 6. This means that the cylinder 1 is fired first and cylinder 6 is fired last within the 2-revolution cycle. Thus, there is a combustion event every 120 degrees of the crankshaft revolution.

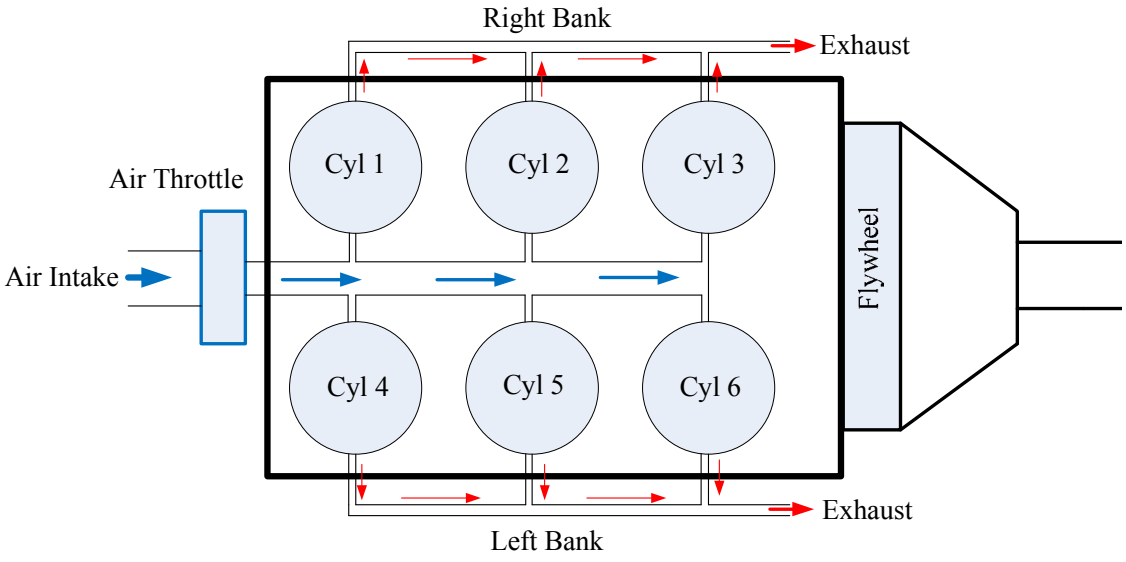

Figure 1.1. Cylinder arrangement in V6 diesel engine.

In diesel engines, heat is generated during a compression stroke to produce hot compressed air to ignite the mixture. Therefore, the injected fuel needs to be a finely dispersed spray for fast evaporation and mixing process to promote complete combustion.

1.1.3. Summary of 4- Strokes Diesel Engines

Intake stroke: The piston moves from top dead centre (TDC) to bottom dead centre (BDC) to draw in the fresh air from the atmosphere. During this period, the intake valve(s) open and the exhaust valve is still open for a few degrees to allow the scavenging process.

Compression Stroke: The piston moves from BDC to TDC to compress the charged air before the fuel is injected into the combustion chamber. The fuel is injected at the end of the compression stroke when the temperature of compressed air is high enough to ignite the mixture.

Power Stroke: The combustion process occurs in this stroke. It consists of two types of combustion modes. The first phase is called premixed combustion and the second phase is called diffusion combustion. The expanding gases from combustion force the piston downward to rotate the crankshaft to produce power. Any high pressure condition in the crankcase shows that the engine is in poor condition due to blow-by mechanism (leakage around the piston rings).

Exhaust Stroke: The piston moves from BDC to TDC to remove all residual gas to flow out of the cylinder. The cycle is completed after the piston reaches TDC.

1.1.4. Mixture Formation in Diesel Engines

Local Air-Fuel ratio (AFR) highly influences the engine emissions, particularly NOx emissions and smoke level. In this case, the timing of start of injection has a major contribution to the formation of the partial homogenous mixture. The mixture quality has a significant effect to produce a cleaner combustion. The improved mixture can be formed through the optimisation of nozzle parameters, increased injection pressure, and

optimization of the injection timing. In the combustion process, only 80% of charge air is burned with fuel and the rest is not fully utilised due to the limited available contact time between fuel and air. In fact, combustion methods such as homogenous charge compression ignition HCCI, premixed compression ignition (PCI) and modulated kinetics (MK) use a combined effect of injection timing and EGR to create a long contact time (long ignition delay) for a complete mixing process. As is well accepted, the longer ignition delay can reduce the PM emissions due to the complete mixing process [50].

The most important injection characteristics are injection timing, injection pressure, fuel quantity and injection duration. All these factors affect the engine performance and emissions directly. The injection pressure has a direct impact on spray formation and the mixing process. In diesel spray, the fuel is evaporated and then mixed with compressed air before being ignited. The evaporation rate can also be improved through a smaller injector nozzle diameter that leads to smaller droplets which tend to evaporate and mix faster. The fuel distribution is largely determined by the local conditions such as air motion, density, injection pressure and temperature, with the fuel spray penetration decreasing along with increasing local temperatures. This is because the high temperature of the entrained compressed air leads to the quicker fuel evaporation process. The injection pressure and nozzle parameters significantly influence the behaviour of the fuel spray during the formation and breakup process.

The diesel spray structure can be investigated both macroscopically and microscopically. The overall spray behaviour such as penetration length, spray angle and profile can be classified under macroscopic characteristics. Meanwhile, the microscopic characteristics are the droplets size and fuel distribution. It is well accepted that the spray consists of cold fuel, rich regions, ignition zones and combustion products as shown in

Figure 1.2. The high injection pressure contributes to the fine atomisation that induces high air entrainment leading to the complete mixing process. The complete mixing process can suppress the soot formation. The effect of air entrainment on the spray structure is important for engine performance and emissions improvement. This is due to fuel evaporation rate being dominantly controlled by air entrainment in the spray structure.

In steady spray condition, the spray surface is smooth near the spray tip and uneven rugged structures develop at the downstream of the nozzle. Air near the spray surface is forced by spray to flow along the spray before entering the spray envelope. The surrounding gas in front of the spray is pushed outward resulting in a large-scale vortex around the spray structure to enhance the mixing process. The premixed combustion phase occurs at the middle of the spray envelope and the diffusion combustion phase occurs at the outer surface as shown in Figure 1.2. This is due to Air-Fuel ratio distribution along the spray envelope. The soot formation is high due to oxygen deficiency and the high level of NO_x is due to high combustion temperatures.

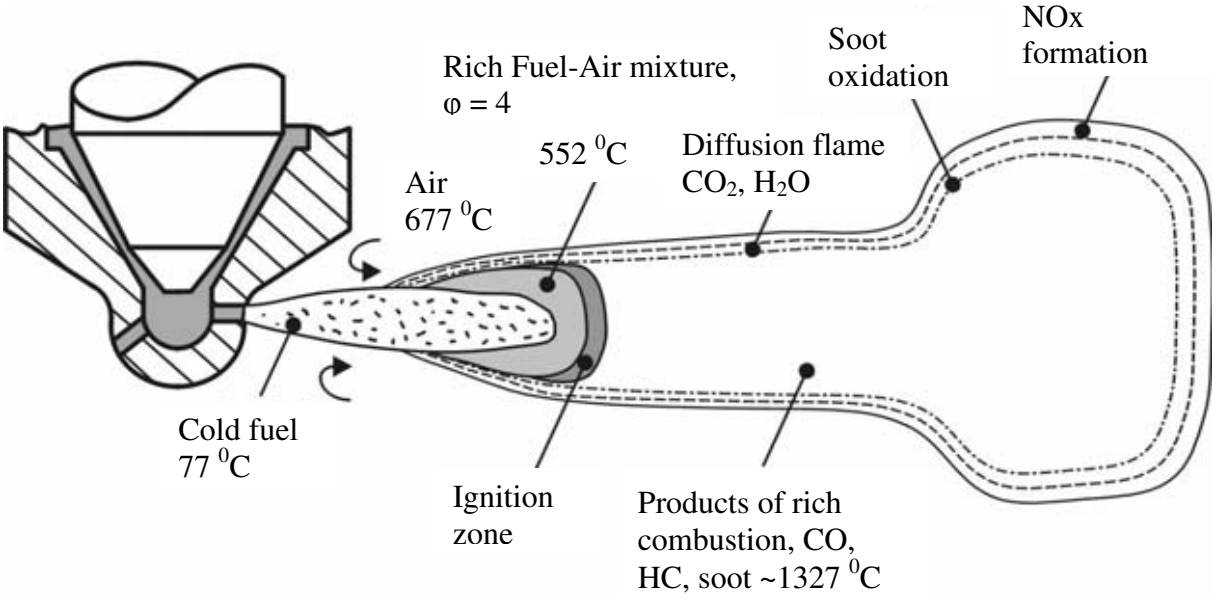

Figure 1.2. Conventional diesel spray and production of NO_x and soot (PM) [48]

PM emissions are formed in the middle of the spray structure where there occurs pyrolysis of fuel by hot burned gases. This region consists of liquid core and fuel-rich zones with flame temperatures between 727 and 2527 ^{0}C [48]. At the end, a large portion of the PM is oxidised by oxygen with the yellow colour of the flame being a visual effect of the glowing soot. The high temperatures from the diffusion combustion phase can increase PM oxidisation, thus reducing the total PM emissions. Only a small portion of PM exits to the exhaust manifold as visible smoke.

1.1.5. Injection Modes

The technology of common rail direct injection offers flexibility in injection strategy such as injection durations, fuel quantities and pressures. The significant improvement in the fuel injection systems improves the engine performance and emissions. In fact, the multiple injections strategy has a potential of simultaneous reduction of NOx and PM emissions. The term of multiple injections has a wide meaning which includes pilot injection, split injections and multiple injections. The pilot injection (pre-injection) has a relatively small fuel quantity injected earlier than the main injection. Split injections consist of two injections with a small dwell period and larger fuel quantity at the first injection. Meanwhile, the multiple injections consist of double injections and are more of variation in fuel quantities and dwell periods. The multiple injections have a capability to increase the Fuel-Air interactions to form a complete mixture. Figure 1.3 shows an example of multiple injections strategy which is commonly used in diesel engines.

The optimization of pilot injection (pre-injection) is a significant strategy for NOx reduction and engine noise level [48]. The strategy also improves the engine thermal efficiency and specific fuel consumption. However, the pilot injection introduces an

increase in soot formation especially at part load due to the low initial combustion temperatures. Nevertheless, this effect is completely compensated by a post-injection strategy without affecting the fuel consumption [48].

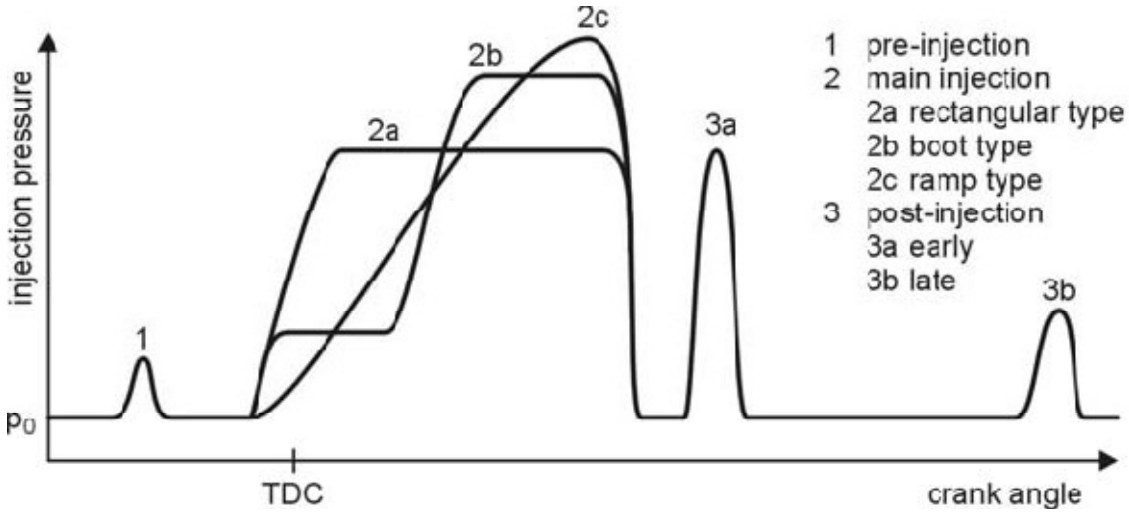

Figure 1.3. Injection modes in multiple injection strategy [48]

1.1.6. Combustion in Diesel Engines

Combustion in diesel engines can be divided into two phases. The first phase is called premixed combustion and the second phase is called diffusion combustion as shown in Figure 1.4 [48]. The appearance of a double peak on the rate of heat release analysis shows the combustion consists of two phases. The overall combustion process can be identified through the rate of heat release analysis and cylinder pressure traces as shown in Figure 1.4. Ignition delay is the time period between start of injection (SOI) and start of combustion (SOC). The SOI can be dictated through the engine management system (EMS). Meanwhile, the SOC can be indentified through a heat-release analysis against crank angle degrees which represent the time scale. The duration of the ignition delay

period depends on a number of factors such as evaporation process, mixing process, Air-Fuel ratio, cetane number, fuel amount and local temperatures.

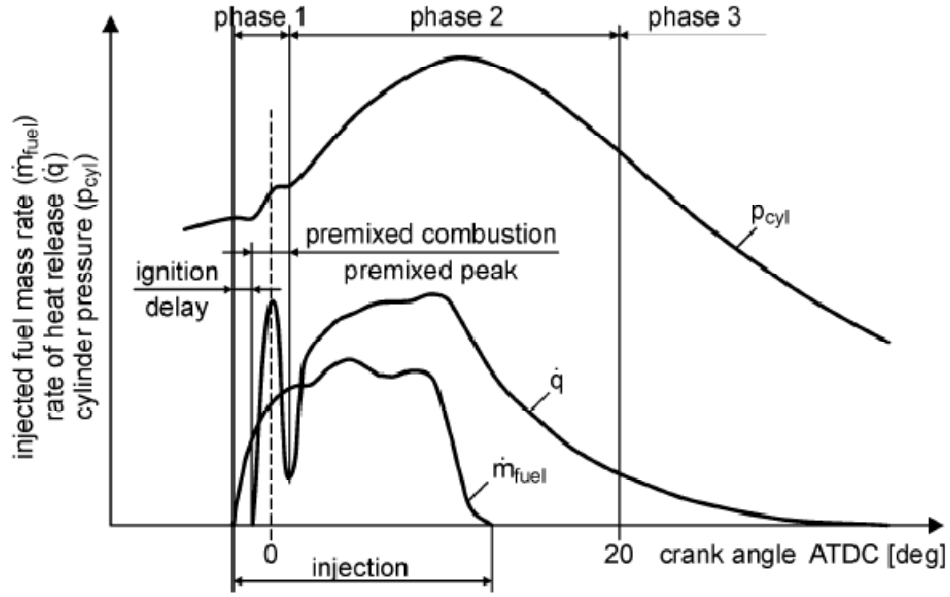

Figure 1.4. Conventional diesel engine combustion (injected fuel mass rate, rate of heat release and cylinder pressure [48].

The injected fuel breaks up into sub-micron size droplets, and then spreads, evaporates and mixes with the hot compressed air during the ignition delay period. The fuel mixes with the compressed air and undergoes a series of spontaneous chemical reactions that result in auto-ignition. The portion of the fuel that had been mixed with air burns very rapidly during a period known as premixed combustion. A rapid rise in the in-cylinder pressure during premixed combustion promotes high NO_x formation. The rate and duration of the in-cylinder pressure increase as the amount of fuel burned during premixed combustion is increased. This combustion phase is useful to increase the combustion temperatures that contribute to the oxidation of particulates. The remaining fuel and burnt gas mix together in a diffusion combustion phase. The air and partially

burnt products diffuse from the centre of the spray area to the outer regions to form the diffusion flame as shown in Figure 1.3. In Figure 1.4, the diffusion combustion is categorised under phases 2 and 3. The combustion is slower than in the premixed phase due to limited mixing of partially burnt products and air. In phase 2, the fuel evaporates and partially oxidises to increase soot formation due to the lack of oxygen and high combustion temperatures. The particles are formed in high temperatures particularly in fuel-rich regions. The early post-injection can be considered as an alternative option to reduce soot emissions.

The final oxidation of the remaining unburned and partially oxidized fuel fragments as well as soot particles occurs in phase 3. The chemical reaction rates decrease dramatically in phase 3 due to low gas temperature in the expansion stroke and due to lack of oxygen. However, the engines fuelled with biodiesel have a capability to increase this combustion rate due to extra oxygen content in the fuel.

1.1.7. Emissions Control in Diesel engines

In diesel engines, there are possible several advanced technologies which have been introduced in order to eliminate emissions. They can be classified into four strategies: (1) fuel development and modification, (2) combustion optimisation strategy, (3) engine oil development, and (4) after-treatment devices. In this work, the emissions reduction strategy is focused on combustion optimisation and its effect on engine performance and emissions fuelled with fossil diesel and Tallow Methyl Ester (TME) blends. The literature results show that the advanced combustion system consisting of high injection pressure, cooled EGR, piston-bowl geometries, and in-cylinder flows have produced substantial reductions in engine emissions [12].

This work uses exhaust gas recirculation (EGR) to control high NO_x emissions that are produced by high injection pressure and biodiesel-diesel blend fuels. Alternatively, PM and smoke can be reduced by using biodiesel due to high oxygen content. The injection strategies consisting of double injections (pilot and main), variable dwell period between pilot and main injection, variable fuel injection pressure, variable pilot fuel quantity followed by cooled EGR and without cooled EGR have all been presented in this work.

1.2. Objectives and Approaches

The aim of this research is to investigate the combustion characteristics and exhaust emissions through combustion strategies using 2.7l and 3.0l modern V6 diesel engines fuelled with fossil diesel and TME-diesel blends. Objectives that related to the research are as below:

1. To study a combined effect of injection strategy (variable fuel injection pressure, variable dwell period and variable pilot fuel quantity) and cooled exhaust gas recirculation (EGR) on the engine performance and emissions.
2. To study the effect of fuel properties on engine performance and emissions fuelled with TME-diesel blends at a variety of engine test conditions with unmodified EMS calibration.
3. To develop an improved understanding of in-cylinder combustion behaviour of TME-diesel blends through analysis of in-cylinder pressure traces and rate of heat release.

1.3. Research outline

The initial work is based on the advanced combustion strategy on a modern V6 diesel engine fuelled with fossil diesel and TME-diesel blends in order to meet future emissions legislation. The principle relies on high fuel injection pressure, variation of injection timings, variation of pilot fuel quantities and cooled EGR. This approach leads to a new advanced combustion strategy that offers low emissions, high power output and low fuel consumption. This work is a collaboration of University of Birmingham with other parties such as Jaguar Land Rover, Shell Global Solution UK, Green Fuel Ltd, Johnson Matthey Plc and partly funded by Technology Strategy Board (Department of Industry, UK Government). The present work detailed in this thesis is divided into the following chapters:

CHAPTER 1: INTRODUCTION

Chapter 1 gives a brief explanation about the emissions regulation and the concept of combustion in diesel engines. The concept of combustion strategy is also explained in this chapter. This chapter ends with the objectives of this study and research outline.

CHAPTER 2: LITERATURE-REVIEW

An overview of current diesel engine technology in terms of common rail direct injection system, injection strategy, cooled exhaust gas recirculation as well as emissions and after-treatment devices are presented. This chapter also briefly describes biodiesel fuel as a renewable potential alternative fuel. The aims of the experimental work are to improve engine power output, exhaust emissions and fuel economy. All of these rely on

the optimisation of the combustion strategy (injection strategy and cooled EGR) and fuel characteristics.

CHAPTER 3: EXPERIMENTAL FACILITIES

Chapter 3 introduces the experimental set up, data acquisition and facilities of the engine work bench. The specifications of modern V6 engines (2.7l and 3.0l), equipment and measurement devices are shown in this chapter. This chapter also explains the detail of the experimental procedure, data collection and data analysis.

CHAPTER 4: COMBINED EFFECT OF FUEL INJECTION PRESSURE AND EGR ON THE ENGINE PERFORMANCE AND EMISSIONS

Chapter 4 reports the combined effect of injection pressure and EGR on combustion characteristics and emissions of a modern 2.7l V6 diesel engine. The experiments were carried out with different injection pressures (300 – 700 bar) and EGR mode at different engine test conditions by fuelling with ultra low sulphur diesel fuel. The fuel injection pressure for the pilot and main injection are the same. The fuel quantity ratio between pilot and main is approximately 10:90 by mass.

CHAPTER 5: COMBINED EFFECT OF FUEL INJECTION PRESSURE, DWELL PERIOD (INTERVAL BETWEEN PILOT AND MAIN) AND EGR ON THE ENGINE PERFORMANCE AND EMISSIONS

This chapter discusses the analysis of short and long dwell periods between the pilot and main fuel injection at different fuel injection pressures (300 – 800 bar) and EGR mode. The fuel injection pressure for the pilot and main injection are the same. The fuel quantity ratio between pilot and main is approximately 10:90 by mass. Short and long

dwell periods are 5 CAD and 40 CAD respectively, are controlled by INCA V5.3 software to communicate with the engine management system (EMS). The effects of these changes are evaluated by repeating the experiments at different engine test conditions. Finally, the results from in-cylinder pressures, rate of heat release, engine performance (ignition delay, fuel consumption etc.) and emissions are explained.

CHAPTER 6: COMBINED EFFECTS OF PILOT FUEL QUANTITY, FUEL INJECTION PRESSURE AND DWELL TIMING ON THE ENGINE PERFORMANCE AND EMISSIONS

Chapter 6 presents a further investigation of injection strategies. The effect of pilot fuel quantity (0.8 - 3.0 mg/stroke) and dwell timing (5 - 30 CAD) were carried out at different engine test conditions. In this case, the pilot fuel quantity was changed from 0.8 to 3.0 mg/stroke, while the main fuel quantity was controlled by the EMS in order to meet the required power output. The fuel injection pressure for the pilot and main injection the same. In the dwell timing study, advanced pilot injection timing delivers promising emissions reduction it in terms of smoke, THCs and CO emissions. This confirms that the main purpose of the pilot injection is to reduce engine noise, fuel consumption and exhaust emissions.

CHAPTER 7: COMBUSTION BEHAVIOUR AND EMISSIONS CHARACTERISTICS OF TME BLENDS FUELLING

Chapter 7 reports the combustion and emissions analysis of a 3.0 l V6 diesel engine fuelled with TME-diesel blends. The experiments were conducted with unmodified EMS calibration for a wide range of engine test conditions. The selected fuel blends are TME10 and TME30 (10% and 30% TME with ULSD). The output from this study can be used to

develop a new engine mapping specifically for the engines fuelled with a wide range of fuels.

CHAPTER 8: CONCLUSIONS AND RECOMENDATIONS

The key parameters for understanding the observed trends are the in-cylinder pressure trace, mass of fuel burnt, rate of heat release (premixed and diffusion phase), ignition delay, fuel consumption and exhaust emissions. By combining EGR with optimised injection strategies, it is possible to minimise both smoke and NO_x at a wide range of engine conditions. A further study with TME10 and TME30 was carried out in order to investigate the effects of fuel properties on the combustion and emissions. Both TME-diesel blends result in higher NO_x emissions and in higher BSFC. The potential solution to improve fuel consumption and minimise NO_x emissions in engine fuelled with TME-diesel blends is a combined strategy between injection strategy (fuel injection pressure, dwell period and pilot fuel quantity) and cooled EGR.

CHAPTER 2
LITERATURE REVIEW

In this chapter, a review of literature used in this study is presented. The chapter is divided into five sections which include fuel injection system and strategies, exhaust gas recirculation and combustion strategy, biodiesel as renewable fuel, engine emissions and lastly after-treatment technology development is also being expressed in each subsection respectively.

2.1 Review of Fuel Injection System

The main focus in the development of diesel engine technologies is on the fuel injection system in order to improve performance and emissions. A high injection pressure is the most important factor in a diesel engine leading to complete combustion. In modern engines, the injection pressures can be increased up to 2000 bar for a specific combustion configuration [4, 51]. The high injection pressure results in generating small-sized fuel droplets, leading to fast fuel evaporation and mixing processes leading to active combustion. The fast mixing process is significantly important in diesel engines since only 80 percent of air is utilised in combustion due to limited available contact time between fuel and air [36]. Traditionally, the injection pump is driven by gears, chains or a toothed belt which indirectly connects to the crankshaft or the camshaft. A rotary pump or distributor pump is usually used in cars and light trucks. The system uses a rotary distribution valve to distribute the fuel to the individual cylinders. The system allows more fuel to be injected into the cylinder with the application of a turbocharger or supercharger on the engines.

The in-line fuel-injection pump was used on diesel engines during the last development stage especially in passenger cars. In-line fuel-injection pump systems use one pump element for each engine cylinder. The camshaft of the in-line fuel-injection pump is driven by the gear wheels or chains from the combustion engine. The in-line fuel-injection pump runs at half of the engine speed (four stroke) and always synchronously with the piston movements. The fuel reaches the nozzle-holder assemblies via high-pressure lines before being injected into the cylinder. The common rail direct injection system is the latest technology in diesel fuel injection that is widely used in modern diesel engines. The high injection pressures and the precisely-metered amount of fuel in a common rail system introduce high combustion efficiency, low fuel consumption and low engine emissions. The rail is always filled with pressurised fuel supplied by a high pressure pump, while, a conventional direct-injection systems take time to build up the pressure in the rail before a next cycle of injection process.

The nozzle is the heart of the injection systems. The nozzle components consist of nozzle body or nozzle-holder assembly and the nozzle needle. The injector receives a signal from the Engine Management System (EMS) to open and close the nozzle needle. The injectors are connected to the rail (high-pressure connection) via short lines. The piezo-electric injectors can operate at fast injection timing with a precise fuel metering. This type of injector can operate almost five times faster than the most modern magnetic injector systems.

2.1.1 Types of Fuel Injection Pumps

2.1.1.1 In-line Fuel Pump

The nozzle is arranged in an inline position. The pump consists of separate units i.e. barrel, plunger, and inlet port. The plunger continues to move upwards and downwards to increase the fuel pressure before the fuel is injected through the injector.

2.1.1.2 Distributor fuel pump

Only one pump serves all engine cylinders. An axial piston is used to increase fuel pressure. The rotating shaft at the centre of the pump is used to distribute the fuel to the specific cylinder.

2.1.1.3 Individual Pumps Type PE

The pump is driven by a camshaft. They are usually used in marine engines, diesel locomotives and construction machinery.

2.1.1.4 Unit Injector System (UIS)

It consists of a pump and nozzle as shown in Figure 2.1. The pump is driven by a tappet or rocker arm that links to the camshaft. The pump is usually fitted on commercial vehicles [48].

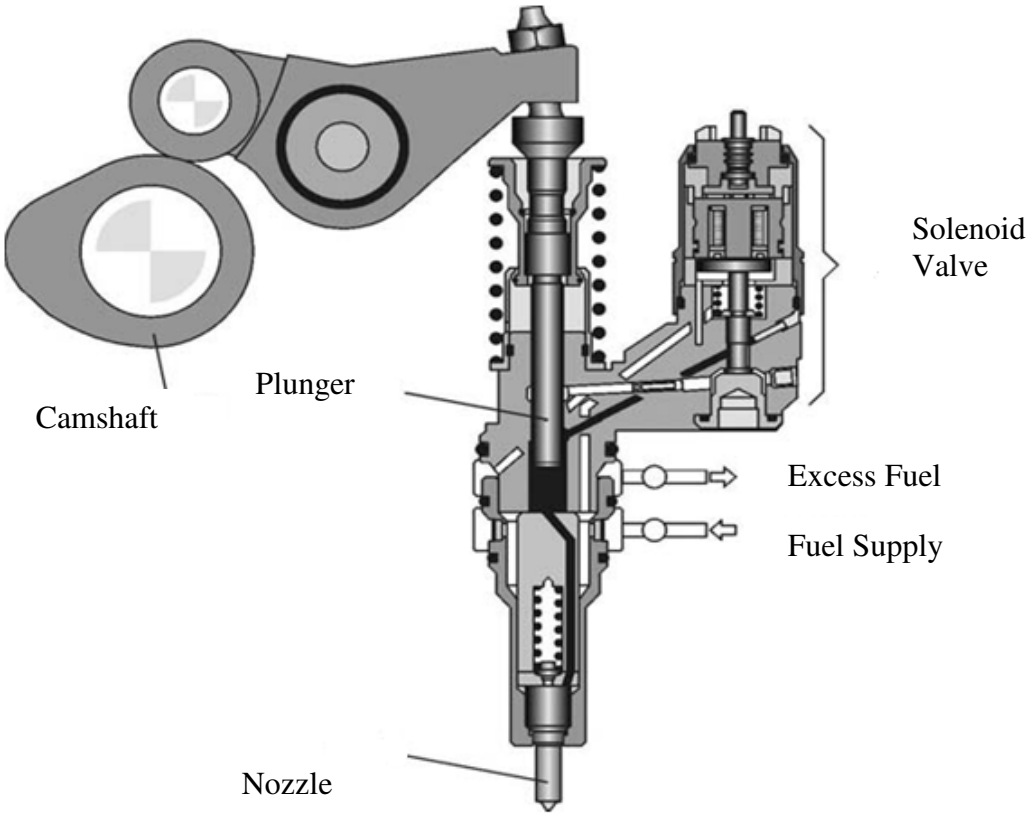

Figure 2.1. Unit injector system [48].

2.1.1.5 Unit Pump System (UPS)

This pump operates on the same principle as the UIS. However, the pump and nozzle is connected through a short high pressure line as schematically shown in Figure 2.2. It is driven by a camshaft.

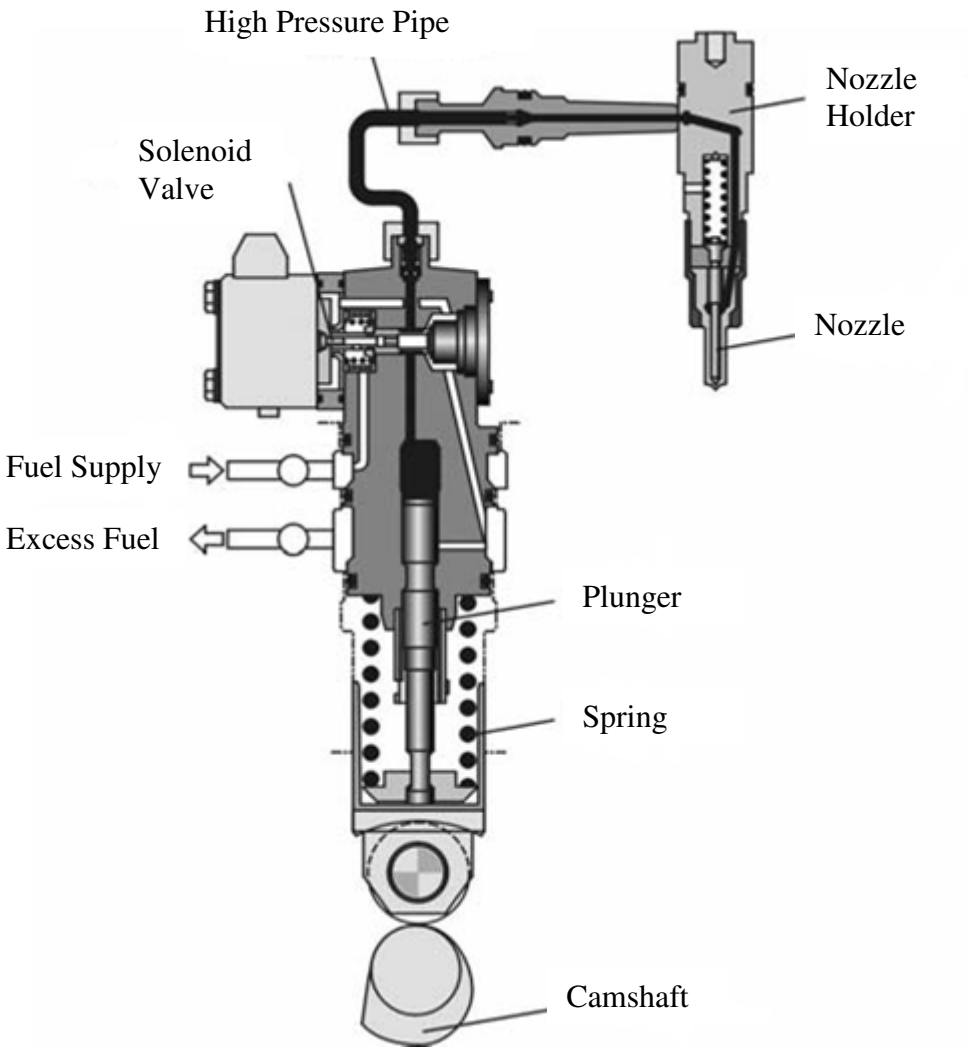

Figure 2.2. Unit pump system [48].

2.1.2 Common Rail Direct Injection Systems

The common rail offers flexibility in pressure, switching times and variable rate of fuel to be injected in the cylinder. The main advantage of common rail is its ability to change the injection pressure and timing over a wider scale. In this case, the common rail system increases a specific power output, lowers fuel consumption, engine noise and emissions [52-54].

Diesel engines have associated problems with emissions (NO_x-PM trade-off), cold start, engine noise and vibration. However, the innovative technology in the common rail direct injection system greatly reduces diesel's environmental impact. The system consists of one high pressure pump, common rail, fuel rail and an electronic control unit. It offers a high degree of flexibility in the injection strategies. The common rail direct injection system has a capability to increase the injection pressure that leads to cleaner and quieter diesel engines [2-8]**.** Common rail (CR) direct injection fuel systems provide a significant increase in injection pressure as compared with the previous rotary and inline pump systems [4]. The high injection pressures enable complete combustion resulting in less harmful engine emissions. In addition, highly precise multiple injection strategies are favourable for NO_x reduction and engine noise. In fact, the common rail direct injection systems are less sensitive to the fuel properties as compared with the in-line injection systems [16]. This is due to a constant pressure supplied in a fuel rail by the high pressure pump. The generated pressure in the fuel rail is independent of the engine speed and fuel quantity. The required injection pressure in the fuel rail is controlled by the rail pressure sensor located in front of the rail as shown in Figure 2.3. The fuel metering unit on the high pressure pump is used to determine the amount of fuel delivered by the pump.

There are presently three different injector types available as a serial product:

1. Solenoid-valve injectors with one-part armature.

2. Solenoid-valve injectors with two-part armature.

3. Injector with piezo actuator.

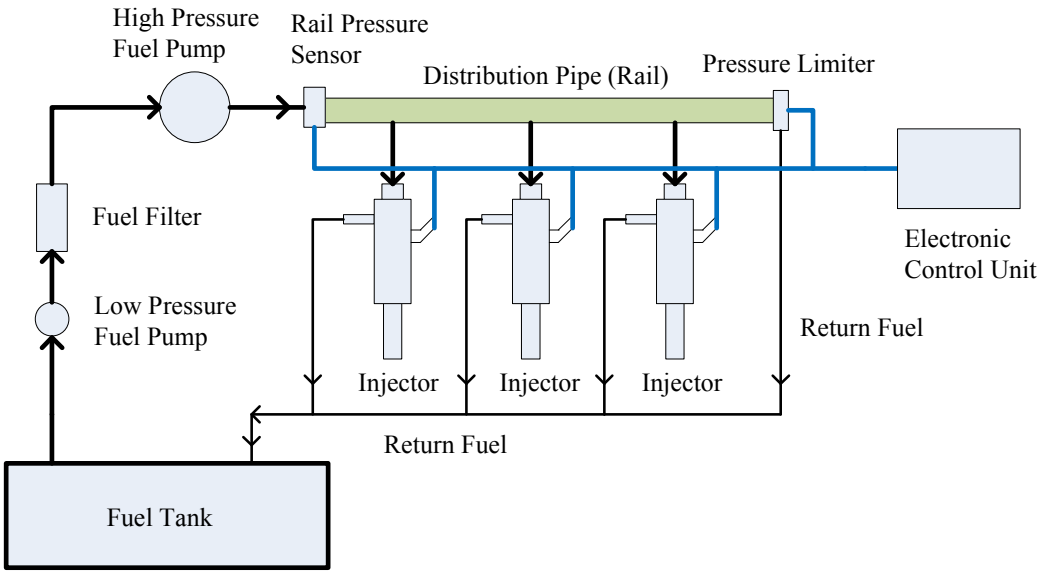

Figure 2.3. Common rail direct injection system.

2.1.3 Multiple Injection Strategy with High Injection Pressure

Diesel engine performance and emissions are significantly influenced by the amount of fuel burnt in the premixed combustion, peak in-cylinder pressure and combustion temperatures. All of these are highly related to the start of injection (SOI) timing, fuel evaporation and mixing process and start of combustion (SOC) timing. Previous study shows that the injection timing in a single injection strategy is one of the most influential factors on the engine emissions particularly in NO_x [16]. The retardation of the SOI timing in a single injection strategy results in lower NO_x emissions but brings also a high level of PM due to the poor mixing process [39, 55]. Meanwhile, the advanced SOI timing yields lower PM but introduces a higher level of NO_x emissions due to high combustion temperatures [55-57]. The strategy also increases the CO and THCs emissions and specific fuel consumption (SFC) due to wall wetting. The injection timing strategy in a multi injection system also shows a similar effect on engine emissions. Late SOI timing in the multiple injection strategy tends to increase smoke due to poor evaporation while

early SOI timing minimises the smoke level [58]. The early injection timing in a multi injection strategy reduces the smoke level due to long ignition delay (ID) that allows a complete mixing process. However an early SOI timing induces wall wetting results in higher THCs, CO, smoke level and fuel consumption. In the worst case, the fuel that accumulates in the oil sump will result in a degradation of engine oil [9]. Therefore, the injection timing requires further investigations in order to reduce NO_x -PM trade-off.

In other injection strategy studies, the results show that the higher injection pressure is positively influencing the combustion behaviour and engine emissions [2, 59-64]. The higher injection pressures induced faster combustion rates resulting in higher combustion temperatures. Faster combustion occurs due to better fuel evaporation and faster mixing process. The high injection pressure has a potential to reduce the particulate matter up to 80% without a significant increment in NO_x and THCs emissions. Indeed, the combination of injection timing and injection pressure promises a better result in terms of engine performance and emissions [65]. The advanced injection timing shows better results in terms of brake specific fuel consumption (BSFC) as compared with retarded injection timing in conjunction with a high injection pressure on a multi injection strategy [59]. This is strongly related to the long ignition delay that provides longer reaction time for the fuel and air mixed together. Moreover, the effect of high injection pressure can be clearly observed at low engine speed and load [59]. At low engine speed, the availability of oxygen is lower leading to the poor mixing process resulting in higher emissions. Therefore, the application of high injection pressure at low engine speed has tremendous effects on the mixing process leading to cleaner combustion due to complete mixture formation. The combined effects of the high injection pressures and EGR rates have potential results in the simultaneous reduction of PM and NO_x emissions [5, 11, 66, 67]. A

small difference in injection pressure allows further increase in EGR rates resulting in further reduction in NO_x emissions.

An increased injection pressure tends to reduce the smoke level due to improved fuel evaporation leading to complete combustion and high combustion temperatures for soot oxidation [14, 59, 61, 68-70]. However, the increase in spray penetration with increasing injection pressure results in high THCs and CO due to wall wetting [68]. This drawback can be controlled by using a multiple pilot injection strategy [58] with a special nozzle to reduce the fuel penetration force [71]. The pilot injection strategy shows a reduction in the ignition delay of the main injection leading to less fuel burnt in the premixed combustion phase. This leads to lower peak combustion temperatures and results in a significant reduction of the NO_x emissions [8, 72].

Okude et al. [58] researched the effect of multiple injections on a single-cylinder diesel engine. Their results showed that multiple pilot injections substantially reduced THCs and CO emissions. This is due to a better mixture resulting from improved turbulent effect between the two pilot injections [6]. In fact, the advanced pilot injection timing tends to reduce NO_x emissions due to lower combustion temperatures. However, the advanced pilot injection contributes to the wall wetting resulting in higher THCs and CO emissions. In addition, the wall wetting also induced the higher fuel consumption. Alternatively, the injection strategy through the small quantity of pilot injection is promising in term of improvement in CO and THCs emissions and fuel consumption [6, 58, 60, 73].

Recently, the multiple and split injection strategies are the most effective strategies for diesel emissions reduction with the exception of NO_x emissions [3, 6, 8, 58, 74-76]. Other studies showed an advanced combustion strategy possible with the common rail

direct injection system has a potential to control NO_x-PM trade-off [5-8, 11, 58, 60, 66, 67, 74, 77-79]. In line with these studies, the NO_x emissions can effectively be reduced by using EGR [12, 41, 43, 80-82]. In addition, the introduction of cooled EGR has a potential for further NO_x reduction with less soot formation [10, 41, 77, 83, 84]. In conclusion, the application of multiple injection strategies is beneficial for the PM reduction and the EGR is beneficial for NO_x emissions. Therefore, the combination of injection strategies and EGR has a promising output in the simultaneous reduction in NO_x and soot emissions [77, 78, 85-87]. In fact, both of these affect heavily on the combustion behaviour and engine emissions.

2.1.4 Injector Nozzle Development

The most important component of the common rail direct injection system is the injector nozzle. In the common rail direct injection system, each injector located in the cylinder is fitted with a rapid action valve (solenoid or piezo-triggered actuator). The injector nozzle is designed to atomise the fuel that introduces a high evaporation rate. Two different types of nozzles normally used in direct injection diesel engines are a valve covered orifice (VCO) nozzle and a sac hole nozzle. The schematic diagram of both nozzles is showed in Figure 2.4. The large volume below the needle seat of the sac hole nozzle can increase THCs and soot emissions due to fuel enter the combustion chamber after the end of injection process [48]. The fuel evaporation of the residual fuel inside the sac hole nozzle at a later stage of combustion can also increases the THCs emissions. Meanwhile, the VCO nozzle has the smaller volume below the needle seat as compared to the sac hole nozzle as shown in Figure 2.4.

Nozzle geometry affects spray characteristics that resulting in better air fuel mixing. The solenoid or piezo actuator is used to open and close the nozzle to inject and pressurise the fuel respectively. The timing interval between injection events can be controlled up to 0.4 ms. In fact, the system also has a capability to perform up to six injection events per cycle with appropriate fuel quantity. The high needle speeds can deliver a complete closing in order to avoid a deteriorated mixture formation and unintended post-injections at the end of each injection process. The small holes of the nozzle are not suitable for the larger amounts of the injected fuel but favourable for the small quantity of injected fuel. Therefore, the effective cross-sectional area of the nozzle will be a variable for every fuel quantity. The experimental work has found that the wide injection angles and high injection pressures tend to emit a higher level of NO_x emissions due to the lean mixture and high combustion temperatures [88]. A conventional injector is often suitable for the injection timings close to the top dead centre (TDC) and is quite limited in application to the early or late injection timings. However, the modern injector comes with narrow angles, low penetration, and high dispersion that offer a better solution to the emissions. The application of two coaxial needles seems possible to open and close the nozzle at a different timing of each hole. The outer needle is used to control the smaller amount of pilot injection and the inner needle is used to control the main injection with a larger fuel quantity.

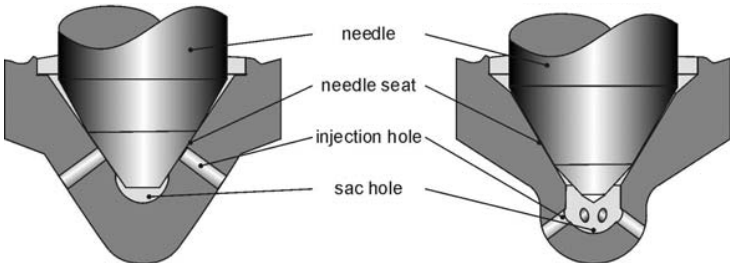

a) b)

Figure 2.4. Two types of nozzles a) VCO nozzle and b) Sac hole nozzle [48].

2.2. Exhaust Gas Recirculation (EGR)

Exhaust gas recirculation (EGR) technique is used in both diesel and gasoline engines. A small fraction of exhaust gases is recycled from the exhaust manifold to the engine intake system via a control valve (EGR valve). In both types of engines, the main objective is to reduce NO_x emissions through lower combustion temperatures. However, the way EGR is being applied to these engines is quite different. In gasoline engines, the total amount of charge is increased as the EGR is applied in order to maintain a required power output. Air throttle is open wider to provide more mixture enters to the combustion chamber as can be clearly seen in Figure 2.5 [89]. Meanwhile, in diesel engines, the total amount of charge air is constant even with EGR due to the engine operating without a throttle (fully open). Therefore, the EGR technique tends to replace some of the inlet air resulting in less oxygen availability for the combustion. The amount of fuel injected to the engine is similar to maintain a required power output. This condition affects heavily on the air fuel ratio of diesel engines which resulting in lower NO_x emissions. The difference in EGR in both engines is shown in Figure 2.5.

Nowadays, the introduction of the combustion strategy and EGR seems to be mandatory in order to meet the future stringent emission legislations. The EGR reduces

the combustion temperatures through high specific heat of inert gases in the flame and a retardation of the combustion rate. The total amount of fuel burnt in the premixed combustion phase is decreased as the hot EGR rate increases due to short ignition delay caused by hot charge air [90]. The shorter ignition delay tends to form a larger local rich region during the start of combustion (SOC) due to less time available for the mixing process. This condition promotes high NO_x formation due to high combustion temperatures coming from rapid combustion. Alternatively, the cooled EGR can reduce the inlet charge air temperature even at high EGR rates contributing to the low NO_x emissions [41, 46].

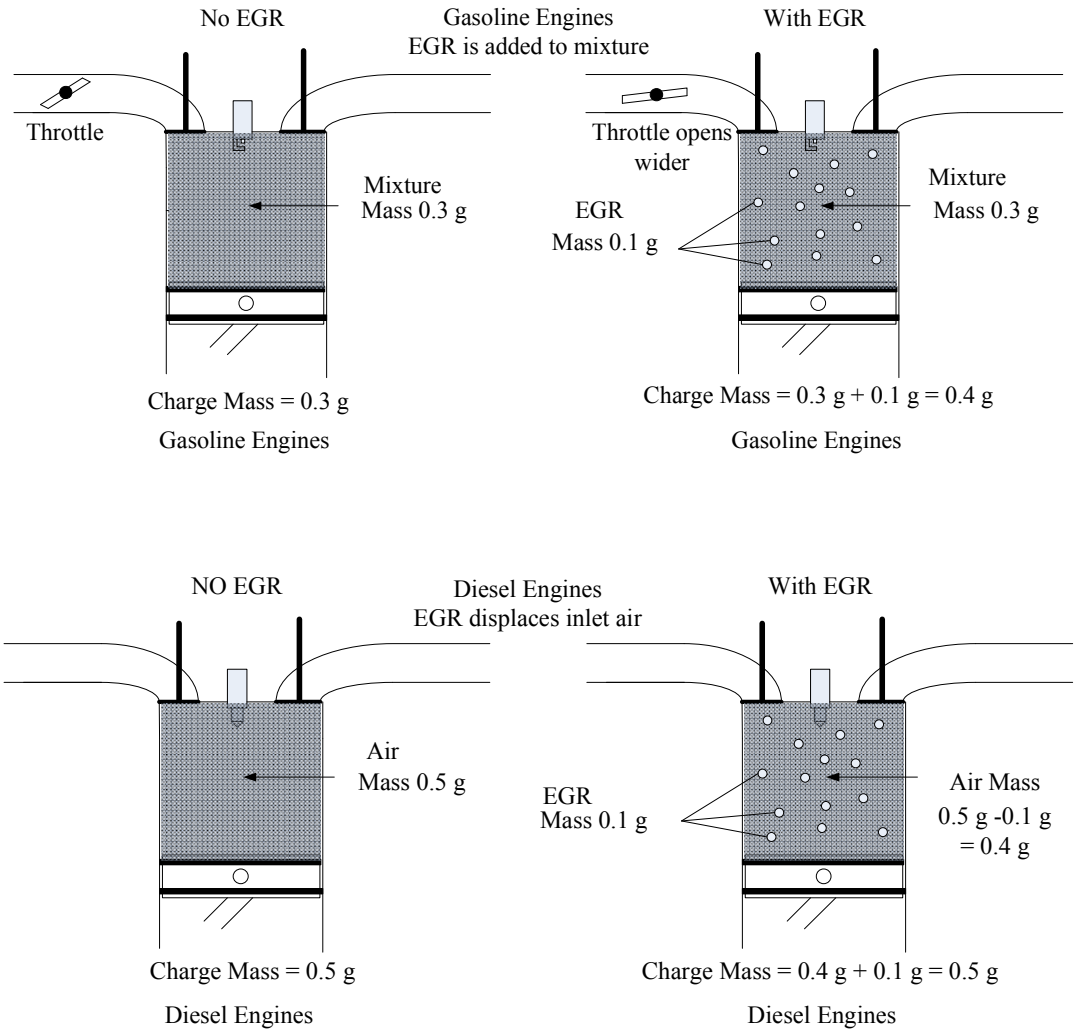

Figure 2.5 Comparison of EGR in Gasoline and Diesel engines [46, 89].

2.2.1 Effects of Exhaust Gas Recirculation (EGR) on Emissions

EGR was established as a standard method for NO_x reduction in both single and multi cylinder engines [1]. With the use of EGR, the rate of NO_x reduction increases as engine load increases. The experimental results showed that the lower NO_x emissions are contributed by the dilution effect and both the chemical and thermal effects had very little influence [89]. In fact, a number of reports use simulated EGR by injecting CO_2 into the intake air to investigate the effect on the NO_x emissions [91, 92]. The results showed that

the increase in CO_2 decreased the NO_x emissions. The EGR techniques could also possibly control the combustion quality and engine noise [53, 54, 93]. EGR can prolong the ignition delay thus preventing rapid combustion and keeping the local peak combustion temperatures low to reduce the engine noise.

The combustion with a short ignition delay induces higher level of soot due to the poor mixing process. In this condition, the fuel has insufficient time to evaporate and mix with air. The soot formation is also promoted by the rich regions due to air deficiency caused by EGR. However, the problem can be controlled by using high injection pressure strategies to promote the fuel vaporization and fast mixing process since diesel engine combustion is significantly influenced by the rate of mixture formation [94]. The high temperatures from complete combustion are beneficial for the soot oxidation**.** Even the application of high EGR rates decreased the soot emissions that were due to oxygen deficiency [86, 95]. An initial increase followed by a decrease in the smoke level with increasing EGR rates has been observed in both single and multi cylinder engines operating with common rail injection systems [96, 97]. A simultaneous reduction of soot and NO_x can be obtained through the high EGR rates due to low combustion temperatures. The soot formation freezes at low combustion temperatures even at rich regions [97]. Other combustion methods such as premixed charge compression ignition (PCCI), modulated kinetics (MK) combustion and homogeneous charge compression ignition (HCCI) [42, 67, 98] show that simultaneous reduction in NO_x and soot can be achieved through the injection timing strategy and EGR. The primary reason for the above method is the longer ignition delay leading to a more complete mixing process.

A number of studies have found that EGR in general tends to produce high particulate matter emissions (soot), specific fuel consumption and degrades the lubrication

oil quality and engine durability [5, 14, 44-46, 50, 68, 78, 86, 91, 99]. Other experimental studies prove that the increase in EGR rates increases the engine wear rate particularly on the piston ring and cylinder liner due to higher carbon and sulphur oxide content in the cylinder [1, 100, 101]. The formation of an abrasive surface by a large amount of soot leads to the lubricant film being removed resulting in high wear rate on the surface [99, 100, 102-104]. High EGR rates also increase cycle-by-cycle variations which result in poor engine stability.

From the above studies, it is seen that the proper strategies on EGR have a potential for better outputs reducing all these drawbacks simultaneously. This work strongly proves that the combined effects of injection strategies and EGR on engines fuelled with biodiesel-diesel blends can demonstrate new scientific knowledge which explores engine performance and emissions. More benefits can be abstracted from EGR techniques when these are combined with injection strategy on engines fuelled with biodiesel-diesel blends.

2.2.2 Variable Geometry Turbocharger and Boost Pressure

The main function of a variable geometry turbocharger (VGT) is to provide increased boost pressure at lower loads and speeds while constantly maintaining this value at high engine loads and speeds [14, 105]. The combustion deterioration is minimal even at an increased EGR rate due to a high enough boost pressure that is generated by VGT and variable speed superchargers [105, 106]. The increased boost pressure is important for the mixing process especially at high EGR rates. The conventional EGR system has drawback effects in terms of increased back pressure and fuel consumption. However, three advanced turbo-charging technologies such as variable nozzle turbochargers, integral EGR pump and an ultra-high pressure ratio long life compressor, are effectively used to

reduce back pressure and fuel consumption [106]. The latest systems such as sequential hydro supercharging and hydraulic pump are more flexible making it possible to control the boost pressure at all engine conditions.

The increased boost pressure is significant to increase air entrainment resulting in a faster mixing process leading to smoke reduction [77]. The faster mixing process at higher boost pressure results in complete combustion due to high air density [107]. Therefore, the start of combustion occurs earlier and promotes energy release which takes place closer to TDC, which increases the thermodynamic efficiency resulting in lower fuel consumption [61]. The high boost pressure leads to complete combustion resulting in lower particulate matter and fuel consumption [90, 105]. This is due to better fuel distribution resulting in a complete mixing process.

2.3 Biodiesel as a Renewable Fuel

Biodiesel offers several advantages such as lower sulphur content, generally higher flash point, lower aromatic content and higher oxygen content [108-110]. A study by Mittelbach [111] showed that biodiesel characteristics are highly dependent on the origin of the vegetable oil. The lower sulphur content results in low engine corrosion and environmental pollution. The combustion of biodiesel does not add to the net CO_2 in the atmosphere, because the next crop will reuse CO_2 to grow.

2.3.1 Production of Biodiesel

Biodiesel is a renewable fuel that consists of the alkyl monoesters of fatty acids. In 1999, biodiesel was certified as a provisional standard by ASTM. Later on in 2002, it received a full standard from the same board as ASTM D6751. It has been considered as

an alternative diesel fuel for internal combustion engines due to its efficiency, cleanliness and biodegradability [1-4, 8]. Besides that, it as significant environmental benefits as an oxygenated fuel being biodegradable and essentially free of sulphur and compounds of ring structures (aromatics) [109].

Biodiesel is composed of large molecules consisting of carbon chains with sixteen to eighteen carbon atoms [24]. It can be derived from fresh-pressed vegetable oil, waste oils, waste restaurant greases, non-food grade vegetable oils and animal fat through a transesterification process by using alcohol and sodium hydroxide [109]. In the chemical reaction, the fatty acid radicals of the triglyceride molecule split away from the main (glycerine) backbone as shown in Figure 2.6. The fatty acid radicals form a new bonding with the alcohol molecule to form fatty acid esters known as biodiesel. Vegetable oils and animal fats are composed of triglycerides. The fatty acids have the greatest impact on the physical properties of oil due to 90% of total oil mass contributed by fatty acids.

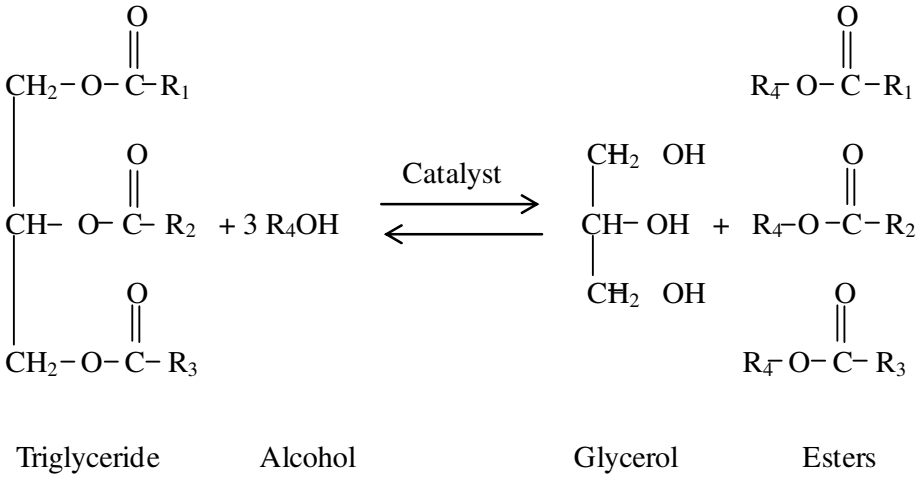

Figure 2.6. Transesterification reaction [108]

2.3.2 Fuel Characteristics

Biodiesels are classified based on the proportions of unsaturated and saturated methyl esters measured by Iodine Value (IV). The iodine value of soy-derived biodiesel is 130 and decreases with increasing degree of saturation [112]. The iodine number increases as the number of double bond increases. The chain length becomes shorter as there is an increase in the number of double bonds. The viscosity increases as the chain length increases. Biodiesel produced from vegetable oils is higher in esters of unsaturated fatty acids but biodiesel from animal fats is higher in esters of saturated fatty acids [113, 114]. Both of them have advantages and disadvantages in terms of engine performance and emissions. An unsaturated biodiesel tends to increase NO_x emissions and decreases particle mass emissions. The increase of NO_x with unsaturated biodiesel is due to higher flame temperature [40]. However, it produces a smaller mean diameter of particulate matter [32]. A large degree of unsaturation in fuels affects the start of combustion due to their lower cetane number resulting in longer ignition delays as compared to the saturated biodiesel. However, the unsaturated biodiesel has low viscosity as a result of a better atomization process and tends to produce cleaner combustion [32].

Previous studies by Lapuerta et al. [32] showed that the unsaturated esters have higher adiabatic flame temperature which contributes to the higher soot oxidation rate and higher NO_x formation. On the other hand, the saturated biodiesel has lower NO_x emissions than ordinary soy-derived biodiesel, but essentially with the same level of PM emissions [112] due to higher cetane number and shorter ignition delay. A higher cetane number fuel has a shortened ignition delay period thereby allowing less time for the air/fuel mixing before the premixed burning phase. Consequently, a weaker mixture would be generated and burnt during the premixed phase resulting in a relatively lower NO_x formation [34].

2.3.3 Combustion Characteristics of Biodiesel

Biodiesel has high oxygen content (10-11%) that leads to a complete combustion [23, 32, 35, 115-117]. It has a potential to become an additive to petroleum diesel fuel for the reduction of emissions and improved lubrication of the fuel injectors. The improved fuel lubrication properties can reduce the engine wear [118]. Biodiesel is completely soluble in commercial petroleum-based diesel fuel. Therefore, it can be used as a blend in one fuel tank. The blended fuels can be used directly in the diesel engines without engine modification. In fact diesel engines were originally designed to use vegetable oils [119].

Previous studies have shown that biodiesel produces comparable engine performance with fossil diesel [120, 121]. However, biodiesel showed higher fuel consumption [55, 117, 122-125]. Biodiesel has a higher cetane number, no aromatics, almost zero sulphur and a high oxygen content [55, 123, 126] that is favourable to emissions. The earlier start of combustion in biodiesel leads to higher NO_x emissions. This is due to the burned gases being exposed to the high temperature and pressure for a longer time period as compared with burned gas from fossil diesel fuel. The oxygen availability in the fuel boosted the NO_x formation. However, the higher oxygen content contributes to the reduction of smoke due to complete combustion [45]. It has been reported in the previous studies [23, 39, 45, 127] that biodiesel has lower emissions in THCs, CO, soot and PM as compared with petroleum-based diesel fuel. In addition, it has almost zero sulphur oxide (SO_x) due to sulphur free fuel. However, biodiesel has higher NO_x emissions than diesel fuel [40] due to fuel properties. This commonly occurs with an in-line fuel pump but not with a common rail fuel injection system [16]. However, some studies [16, 128] showed that NO_x is increased even with common rail. In fact the increase of NO_x with biodiesel is dependent on fuel injection type [112].

The result was confirmed through a detailed study on injection pressure and injector needle movement with biodiesel [129]. A pump-nozzle fuel injection system for biodiesel has been used with advanced injection timing [26, 39, 130]. However, the advanced injection timing also occurred in a diesel engine equipped with a common rail fuel injection system [131]. The advanced injection timing with biodiesels tends to increase the ignition delay and prolong the combustion duration, leading to higher NO_x emissions. The higher cetane number in biodiesel can reduce premixed combustion resulting in lower combustion temperatures that are favourable for NO_x emissions. The volumetric efficiency also increases in engines fuelled with biodiesel due to low combustion temperature [132]. However, the disadvantages of biodiesel such as cold start problems, lower energy content and fuel pumping difficulty need to be improved for future effective fuel.

2.3.4 Tallow Methyl Ester (TME)

The alternative feedstocks for producing Tallow Methyl Ester (TME) are beef, mutton, and pork. A study by Nelson and Schrock [133] shows that the tallow from animal fat offered a wide range of energy, environmental and economic benefits. Tallow from beef contains high levels of saturated fatty acids and low levels of polyunsaturated fatty acids [134]. The high content of saturated fatty acids in tallow contributed to high fuel sensitivity at the low temperature range [135]. The main components of fatty acids in the tallow are palmitic (28.7%), stearic (19.5%), and oleic (44.4%) [118]. The details about the beef tallow composition are given in Table 2.1. The high melting point and viscosity of tallow are due to the higher palmitic and stearic acid. But, the melting point was dramatically reduced from 45 to 15.9 °C after transesterification process [136]. A study by

Oner et al. [137] shows that the viscosity, density and calorific value of TME are very close to that of fossil diesel. Meanwhile, the higher cetane number and oxygen content compensates the disadvantages of TME such as high viscosity and low volatility. This is because the higher cetane number and oxygen content contributes to a cleaner and more efficient of combustion process [110, 138].

The experimental results show that engine fuelled with TME consumed higher fuel as compared to fossil diesel due to lower calorific value and higher fuel density [139]. However, other study by Winther [135] shows that the difference in BSFC does not change significantly with TME. TME emits lower emissions of THCs and smoke as compared to fossil diesel [135, 139] but not so with NO_x emissions [139]. However, study by McCormick et al. [128] found that the engine fuelled with TME decreased the NO_x emissions due to the high cetane number. This finding was confirmed by Kalligeros et al. [110] who mentioned that the high cetane number in TME can reduce the ignition delay, resulting in low quantity of fuel burnt in premixed combustion.

Table 2.1. Fatty acid composition of beef tallow and TME [136]

Carbon chain (Acid name)	Edible beef tallow (%)	Tallow Methyl Ester (%)
$C_{14:0}$ (Myristic)	4.8	3.6
$C_{16:0}$ (Palmitic)	28.4	26.8
$C_{16:1}$ (Palmitoleic)	4.7	3.5
$C_{18:0}$ (Stearic)	14.8	18.1
$C_{18:1}$ (Oleic)	44.6	46.2
$C_{18:2}$ (Linoleic)	2.7	1.8
Total saturated	48.0	48.5
Total unsaturated	52.0	51.5

2.4 Emissions of Diesel Engines

2.4.1 Oxides of Nitrogen (NO_x)

Nitric oxide (NO) and nitrogen dioxide (NO_2) are non-flammable gases. The mixture of both of them is called oxides of nitrogen (NO_x). NO_x can combine with other chemicals to form smog and acid rain. NO_x emissions in diesel engines are increased when fuel cetane number and fatty acid are decreased. However, the primary reasons for high NO_x emissions are high temperature and pressure in the combustion chamber during fuel combustion [140]. In addition, the higher air to fuel ratio operation in diesel engines will increase NO_x emissions due to excess air at high combustion temperatures. The combination of lean mixtures and high local temperatures significantly influences the higher NO_x formation. However, the lean Air-Fuel ratio can also reverse this behaviour. The lean mixture induced by the swirl motion at high engine speed promotes a reduction of the local temperatures around the spray that leads to the lower NO_x formation [61]. The retardation of injection timing strategy reduces the NO_x emissions due to low combustion temperatures [141]. The shorter ignition delay from high injection pressure reduces the NO_x formation as less fuel is burnt in the premixed phase [36]. However, other studies showed that the increased injection pressure increased the NO_x emissions due to faster combustion leading to higher combustion temperatures and rapid pressure rise [64, 142].

The primary principle of NO formation has been explained by the Zeldovich mechanism as below:

$$O + N_2 \Leftrightarrow NO + N \qquad (2.1)$$

$$N + O_2 \Leftrightarrow NO + O \qquad (2.2)$$

Another possible mechanism for the formation of NO_2 is $NO + HO_2 \Rightarrow NO_2 + OH$ and all of them together are called the extended Zeldovich mechanism. In the normal combustion, the amount of NO_2 is approximately 10 to 30 percent of the total exhaust oxides of nitrogen emissions. A conversion of this NO_2 to NO occurs via $NO_2 + O \Rightarrow NO + O_2$ reaction.

2.4.2 Particulate Matter

In diesel engines exhaust emissions, the combination of soot, liquid and other absorbed or adsorbed condensed substances is called particulate matter (PM). The structure of PM is illustrated schematically in Figure 2.7. The soot comes from the incomplete combustion of hydrocarbon fuel. It is strongly dependent on air-fuel ratio and mixture distribution; the fuel composition also affects the smoke formation and oxidation. The low sulphur content in biodiesel is favourable for low smoke formation and high oxygen content is favourable for smoke oxidation [143]. Exposure to the fine PM can cause a variety of health effects including heart and lung disease.

In general, the formation of soot emissions consists of two opposing processes, i.e. soot formation and soot oxidation. Therefore, the net soot emission appearing in the exhaust is dependent on the dominant process. The soot formation occurs inside the fuel spray at the rich fuel regions whereas the soot oxidation occurs at the late combustion phase (diffusion combustion). The high temperatures at the rich fuel regions tend to increase soot formation while the lean fuel regions contribute to the soot oxidation. The soot formation can be reduced by inducing a better prepared mixture, e.g. through injection strategy and swirl ratios. The injection strategy with pilot injection increases the ignition delay of the main fuel injection to allow a complete mixing process. Meanwhile, soot

oxidation can be increased by introducing high temperatures at late combustion, i.e post injection. The air entrainment and turbulence intensity can minimize the fuel-rich regions that favour soot formation [84].

Studies by Svensson et al. [144] showed that the higher boost pressure and oxygenate content of the fuel are favourable in smoke reduction. In general, almost all (over 90 percent) of the soot formed during the combustion process is subsequently oxidised prior to exhaust [145].

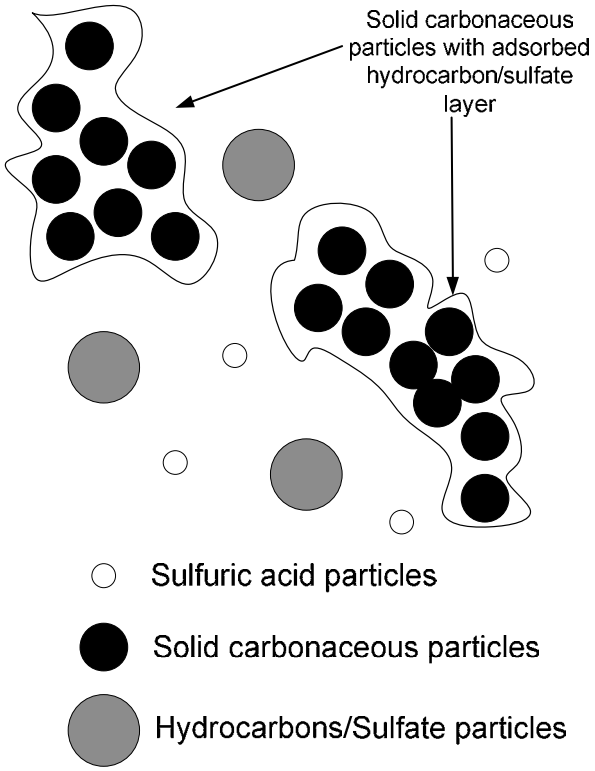

Figure 2.7. Schematic diagram of PM's structure [146].

2.4.3 Total Hydrocarbons

Total hydrocarbons (THCs) in diesel emissions are the result of incomplete fuel combustion due to heavier hydrocarbon [64]. Imaging studies showed that the THC's

source is dominated by engine conditions and geometry [147, 148]. Poor fuel oxidation in the combustion chamber can be considered as a main contributor to the THC's emissions. The condition is created by the lower wall temperature, fuel impingement on the cylinder wall, over-lean mixture and lower temperature due to the poor mixing process. Meanwhile, the well-prepared mixture tends to promote a cleaner combustion resulting in a low level of THCs [142].

THCs emissions are decreased with biodiesel fuels. This is due to the higher oxygen (10 – 11%) content in the fuel [35, 115-117, 149, 150]. The fuel properties also influence the atomization process that leads to the homogeneous mixture formation resulting in lower THCs emissions [151]. Therefore, the application of injection strategy in terms of injection pressure, injection timing and pilot quantity is a potential solution to reduce the THCs in diesel emissions through homogenous mixture formation.

2.4.4 Carbon Monoxide

Carbon monoxide (CO) emissions are odourless, colourless, tasteless and noncorrosive but they are poisonous. They are generated in either too lean or too rich fuel-air mixtures [152-154]. In lean mixture regions, the low temperatures can cause partial fuel oxidation that leads to higher CO. In the rich mixture regions, the low oxygen concentration can cause partial fuel oxidation that also increases the CO emissions. In this case, the higher boost pressure is favourable for CO emissions [155]. Therefore, the complete mixing process between fuel and air is significantly important for a reduction of CO emissions. The smaller droplets can increase the mixing rate which results in active combustion favourable for the low CO emissions [36]. The increase in CO emissions indicates poor fuel combustion caused by lower oxygen concentration and lower local

temperatures [156]. The lower local temperatures during cold start can be considered as a reason for the higher CO emissions as compared with the higher local temperatures during fully hot-soak, i.e, when engine has been running for a period.

2.4.5 Carbon Dioxide

The amount of carbon dioxide (CO_2) in exhaust emissions is an indication of complete combustion [36]. The emission level is proportional to the amount of fuel burned during combustion. The higher injection pressure tends to promote smaller droplets for complete combustion that are favourable for high CO_2 emissions. Oxygenated fuel like biodiesel, can increase the CO_2 emissions due to better combustion [36]. Increasing the engine load at a constant speed decreases the CO_2 emissions due to high quantities of injected fuel resulting in incomplete combustion.

2.5. After-treatment Development

The major harmful substances from diesel emissions are particulate matter (PM), oxides of nitrogen (NO_x), carbon monoxide (CO) and total hydrocarbons (THCs). A particulate filter is effective for PM reduction and NO_x reduction can be achieved through after-treatment devices. High temperatures at the diffusion-combustion phase significantly lower the PM oxidation resulting in low total emissions. There are several after-treatment techniques available for diesel's emissions treatment such as diesel particulate filters (DPF), selective catalytic reduction (SCR), NO_x adsorber catalyst (NAC), diesel oxidation catalysts (DOC) and NO_x storage reduction (NSR) catalyst and four-way catalyst.

2.5.1. Diesel Particulate Filter

Diesel particulate filter (DPF) is one of the most technically feasible solutions to reduce diesel particulate matter. The DPF is fitted in the exhaust line and collects particulate matter through a deep-bed filtration process. Unlike a catalytic converter which is a flow-through device, a DPF cleans exhaust emissions by forcing them to flow through the filter. In emission studies, the filtration process has shown to be an effective method to remove particles in exhaust emissions up to 97% depending on the porosity of the filter material [157]. The collected PM in the filter is then periodically combusted by oxidizing agents in the exhaust gas which is supplied much hotter. This is called a regeneration process. In general, the process of filtration can be divided into three major stages. First, the particle filtration, which leads to a deposition of particulate matter in the filter, then the occasional regeneration of the collected particle and finally, the rearrangement of the soot deposition ash collected from the regeneration process.

The DPF consists either of porous ceramic or sintered metal and is made up of a large number of parallel channels that are open and closed at alternate ends. This structure can withstand high temperatures of exhaust gases. The most popular materials to make a filter are Cordierite and Silicon Carbide (SiC). The filters can be ceramic wall-flow monoliths, ceramic and metallic yarns, or ceramic and metallic foams. The exhaust gas is forced to flow through the porous walls of the honeycomb structure as shown in Figure 2.8. The particle loading of the filter makes the back pressure increase over the time, therefore the particulate filter must be regenerated regularly to avoid back pressure increases. The negative effect from poor regeneration is increased pumping work, and consequently the deterioration of fuel consumption. Usually, for supercharged engines, a noticeable

deterioration of combustion can occur at back-pressures higher than 200 - 250 mbar [158] and the normal value of back pressure is less than 100 mbar [159].

The main considerations that need to be emphasized in connection with the after-treatment system's performance are methods, operating conditions and effectiveness of the regeneration process. Based on a previous study, regeneration can't occur naturally due to the high ignition temperature of soot [160]. The soot oxidation process can occur at temperature levels exceeding 550 °C. However, various approaches have been tried in order to burn the collected particles on the filter to avoid exceeding back pressure limits in order to maintain good engine performance. The concept is either to increase the exhaust gas temperature or to reduce the soot oxidation temperature. There are several practical techniques used such as raised temperature using a burner or by electrical heating, or a catalyst may be employed either on the DPF or in the fuel [160]. In automatic dual filter systems one clean filter is loaded by the particulate exhaust and automatically the second filter is regenerated off-line by a burner [161]. The process can be done by using a conducting material for the filters or by equipping the filter with heating wires. However, the filter fitted with a heater is very costly to use in the active regeneration process [162]. Another method is to use an oxidation catalyst to increase NO_2 concentration to oxidise more soot in the exhaust system.

The flow resistance represents an important performance parameter for DPF. It can be divided into four major components: inlet/exit effects, frictional losses flow through the filtration wall and the particulate layer. There are two types of filter normally used, these are Segmented and Monolithic filters. In general, segmented filters generate higher pressure drop than monolithic filters due to smaller filtration wall area, thus yielding higher flow resistance by up to 30% for clean cases and up to 35% when loaded with particulate

[163]. Almost all the total pressure drop in the filter is contributed by the particulate packing layer and the filtration walls [163] while effects from channel friction and flow contraction/ expansion are less significant.

The combustion strategy needs to be improved in order to control the engine emissions even though the after-treatment devices could take care of all of these emissions. This is due to limitations in after-treatment techniques such as the requirement of high exhaust temperature, low filtration efficiency and high fuel consumption. The devices work with a low efficiency at cold start and low load conditions due to the lower exhaust gas temperature. Therefore, the combustion strategy remains as an important technique to control the engine emissions before passing it into the atmosphere through the after-treatment devices and the exhaust pipe.

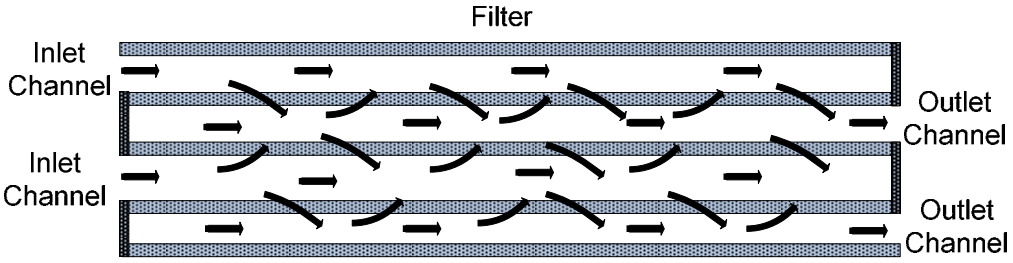

Figure 2.8. Schematic diagram of DPF channels from side view [164].

2.5.2. Selective Catalytic Reduction

The main solution in NO_x after-treatment technologies is the selective catalytic reduction (SCR) [165]. This technique does not suffer from sulphur poisoning that is present in fossil diesel fuel. It's main function is to reduce NO_x from diesel emissions to N_2 by using a catalyst. The catalysts are classified into two types. The first type is called the Urea-SCR system which uses ammonia produced from urea as a reducing agent. The

second type is called the HC-SCR system since the reductant of NOx is a hydrocarbon (HC)The Urea-SCR system has been widely attached to heavy duty trucks and buses due to high NO_x purification efficiency [166, 167]. Currently some research has been performed in replacing ammonia with hydrocarbons (HC-SCR) [165, 168]. The HC-SCR system has been used widely on passenger cars. The catalyst materials and fuel deterioration are the major concerns in the SCR application. Besides that, the SCR still has a number of associated problems, such as the high cost, the lack of low temperature performance, and deactivation through ageing.

2.5.3. NOx Adsorber Catalysts

The principle of NO_x adsorbers involves the adsorption and storage of NO_x on the catalyst during lean conditions and its release under locally rich operating conditions [169, 170]. The higher NO_x emissions in a diesel engine are difficult to control due to excess air and high combustion temperatures. The usual reductants applied in a NO_x adsorber are HC and CO. In this technique, the NO is catalytically oxidized to NO_2 and stored as a nitrate [171]. The rich condition in the exhaust pipe is created by post injection in order to release the stored NO_x. The released NO_x is quickly converted to N_2 by the reaction with CO on a rhodium catalyst.

2.5.4. Diesel Oxidation Catalyst

Diesel Oxidation Catalyst (DOC) is the lowest cost device in after-treatment systems. DOCs have been used in off-road applications since the 1960s and widely used in on-road applications since the 1980s. A DOC is a flow-through device that consists of a porous ceramic monolith honeycomb substrate. The substrate has a large surface area that

is coated with an active catalyst layer such as platinum or palladium to enhance the chemical process to reduce some harmful substances in diesel emissions. The system has a capability to oxidise diesel emissions such as carbon moNOxide (CO), total hydrocarbons (THCs) and liquid hydrocarbon particles (unburned fuel and oil) resulting in lower particulate matter emissions. The devices work effectively in emissions reduction without introducing any penalty to the engine performance.

2.5.5. NOx Reduction System and Four-way Catalyst

This is also known as the Diesel Particulate – NO_x Reduction system (DPNR). The system has great potential to simultaneously purify the four harmful diesel emissions (PM, NO_x, CO and THCs). This system uses a DPF where the filter surface is coated by a kind of NO_x storage reduction (NSR) catalyst. The PM is oxidised by active oxygen from the NO_x storage and reduction processes or oxygen from excess air due to lean combustion.

CHAPTER 3

EXPERIMENTAL FACILITY SET-UP AND APPARATUS

This section describes the experimental facilities that have been used in this study. The experimental facilities consist of a modern V6 2.7l and a 3.0l common rail direct injection Jaguar diesel engine. The engine cooling system (engine cooler and intercooler) had a fully automated control system that utilised a 3-way valve from Honeywell and a PID controller from TC Direct. The CADET V14 software from CP Engineering is used to control the engine speed and torque. This chapter details the apparatus and measuring devices that have been used in this work such as thermocouples, pressure sensors, exhaust gas monitoring (Horiba MEXA 7100EGR), AVL 415S smoke meter, 365CC AVL encoder, AVL in-cylinder pressure transducer, AVL Indi Master 420 (combustion analyser) and CADET V14 software. The experiments were conducted at various engine operating conditions in order to analyse the combustion characteristics and emissions level.

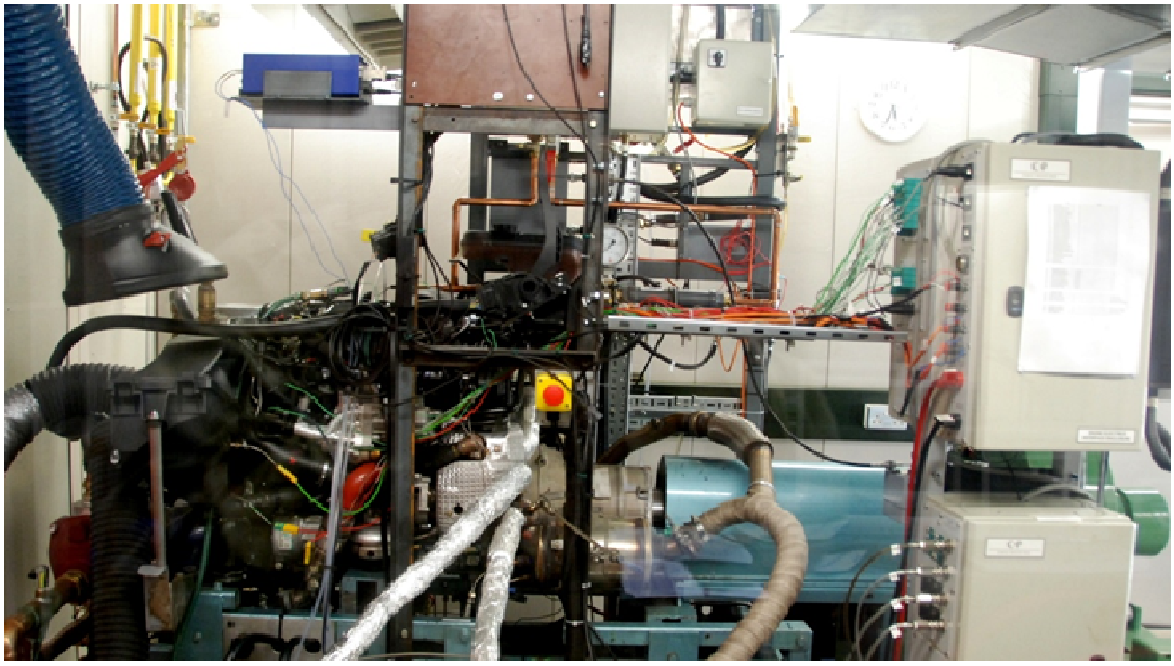

Figure 3.1. The Jaguar V6 3.0l diesel engine

3.1. Engine Set Up

3.1.1. 2.7L and 3.0L V6 Diesel Engines

The experiments were conducted using a modern V6 2.7l and a 3.0l Jaguar diesel engine, which is twin-turbocharged, water-cooled, and equipped with a common rail direct injection system. The engine is fully equipped with emission control devices such as variable geometry turbochargers, cooled EGR, twin DOCs and DPFs. The engine geometry and characteristics for the 2.7l and 3.0l diesel engines used for engine testing are summarised in Table 3.1 and Figure 3.2 respectively.

Table 3.1. Engine specifications 2.7l and 3.0l

	Jaguar V6 2.7l	Jaguar V6 3.0l
Bore	81.0 mm	84.0 mm
Stroke	88.0 mm	90.0 mm
Displacement volume	2720 cm^3	2993 cm^3
Maximum torque	435 Nm @ 1900 rpm	600 Nm @ 2000 rpm
Maximum power	152 kW @ 4000 rpm	199.1 kW @ 4000 rpm
Compression ratio	17.3:1	16.1:1
Connecting rod length	160.0 mm	160.0 mm

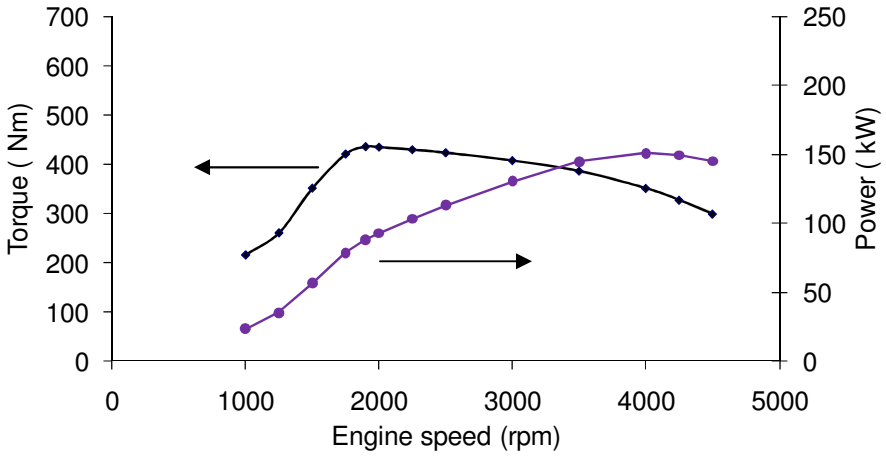

a)

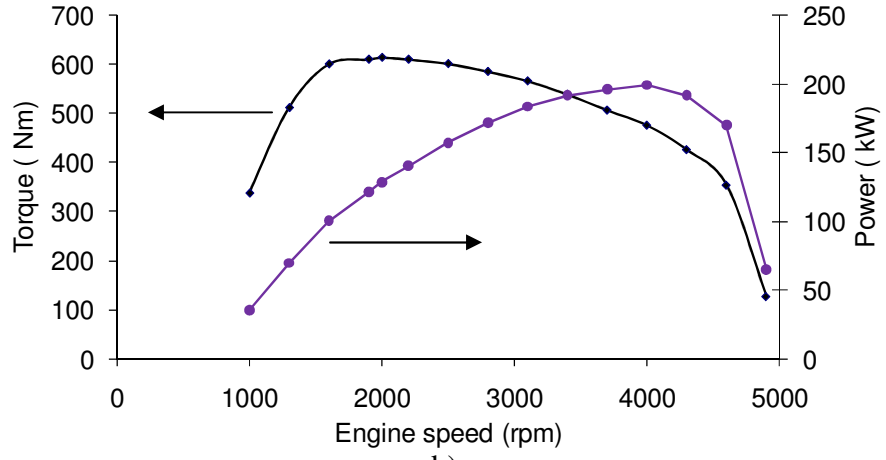

b)

Figure 3.2. Engine torque and power versus speed a) 2.7l and b) 3.0l

3.1.2. Dynamometer and Controller

The dynamometer used to load the engine is an eddy-current water-cooled provided by the Dynamometer Services Group Limited (DSG Ltd), model number W230. The main specifications and performance envelope for the engine dynamometer are listed and depicted in Table 3.2 and Figure 3.3, respectively. The dynamometer has a capacity to cover the full-load and full-speed of both engines (see Figures 3.2 and 3.3). A flow switch is attached on the cooling water feed line circuit to monitor water flow inside the dynamometer which is required for safety purposes. The dynamometer was calibrated up to 500 Nm with the controller CP128 installed. Engine load and speed are digitally controlled by the dynamometer's controller CP 128 through the CADET V14 software. The dynamometer controller consists of CADET computer, transducer box, engine electrics box and AT12 throttle actuator as shown in Figure 3.4. The electrics box is used to connect the engine wiring system such as battery, engine management system (EMS), ignition, starter motor, fuel supply, AT12 throttle actuator, engine coolant temperature and oil temperature sensors. The engine oil pressure sensor is connected to the transducer box for safety reasons. This allows for the engine pressure to be read during cranking and running. The controller communicates with the dynamometer through the CADET V14 software.

The additional electronics box is used to record and monitor the temperatures and pressures from the selected engine components such as air intake, exhaust, compressor etc, as this is important to monitor the engine's health and standards during engine operation.

Table 3.2. Dynamometer specifications

Model	W230
Rated torque	750 Nm
Maximum speed	7500 rpm
Power	230 kW
Moment of inertia	0.53 kgm^2
Torsional stiffness	0.593×10^6 Nm/rad
Weight	480 kg

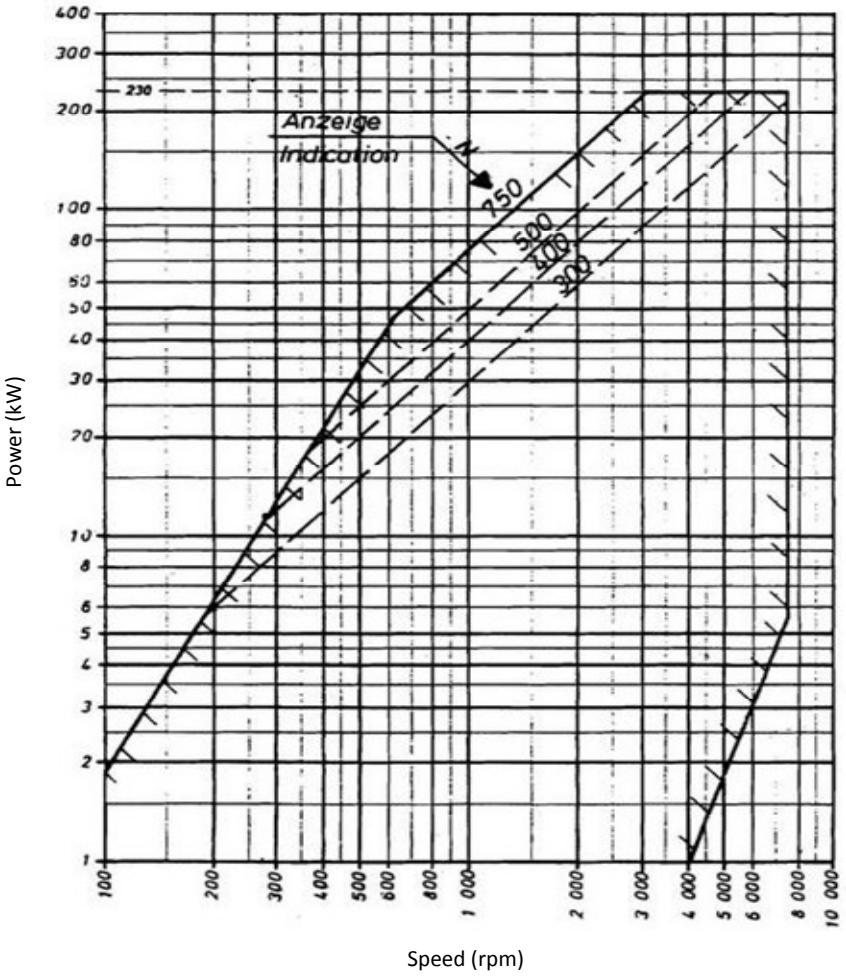

Figure 3.3. Engine dynamometer performance envelope from DSG Ltd

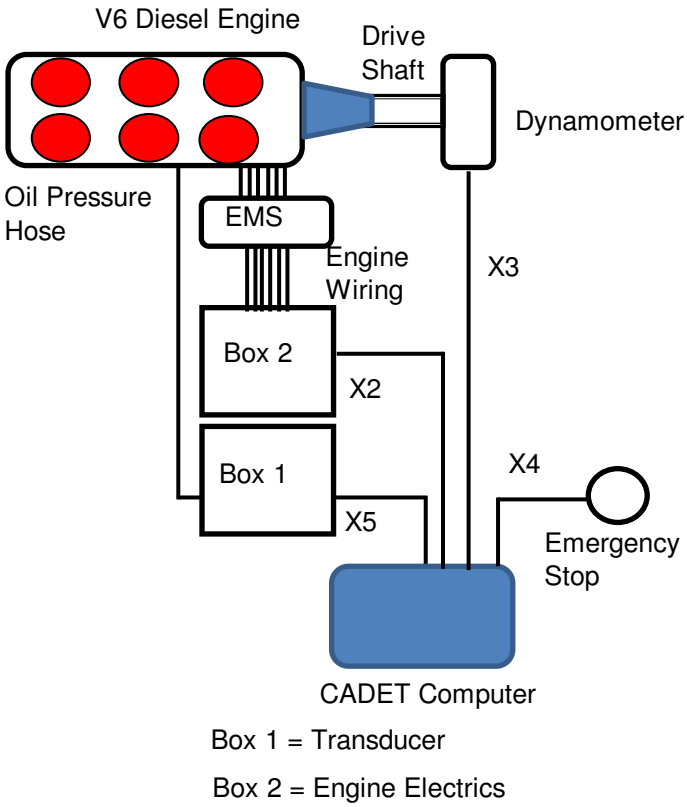

Figure 3.4. Schematic diagram of the CP 128 dynamometer controller.

CADET V14 software is a computer based system designed to perform engine testing under automatic or manual control. The actuator is connected to the electronics box then driven by a DC motor to control the engine speed. The unit contains a permanent magnet DC motor which drives a cable drum through an integral reduction gearbox. A servo-potentiometer, directly coupled to the output shaft provides a signal that is dependent on the throttle lever position. The position control loop maintains the required throttle position by comparing this feedback signal with the demand and outputting a corrected demand signal.

3.1.3. Engine Cooling System and Controllers

There are two additional cooling systems for the engine test rig: engine cooler and charged air cooler (intercooler). The heat exchanger, model GL320-1428-5 from EJ Bowman (Birmingham) Ltd is used as the engine cooler. The standard heat exchanger is made from many materials, e.g. cuprum-nickel tubes, cast aluminium shell, and cast iron end covers.

Figure 3.5 shows that the available plant water from the main tank located on top of the building flows through a Bowman GL320 heat exchanger to absorb heat from engine coolant. The counter-flow is applied between plant water and engine coolant circulation. The counter-flow regime is more efficient in removing the heat as compared with cross-flow and parallel flow. Water flow rate is controlled by a constant flow rate cartridge (60 l/min) that is located at the end of the Bowman heat exchanger.

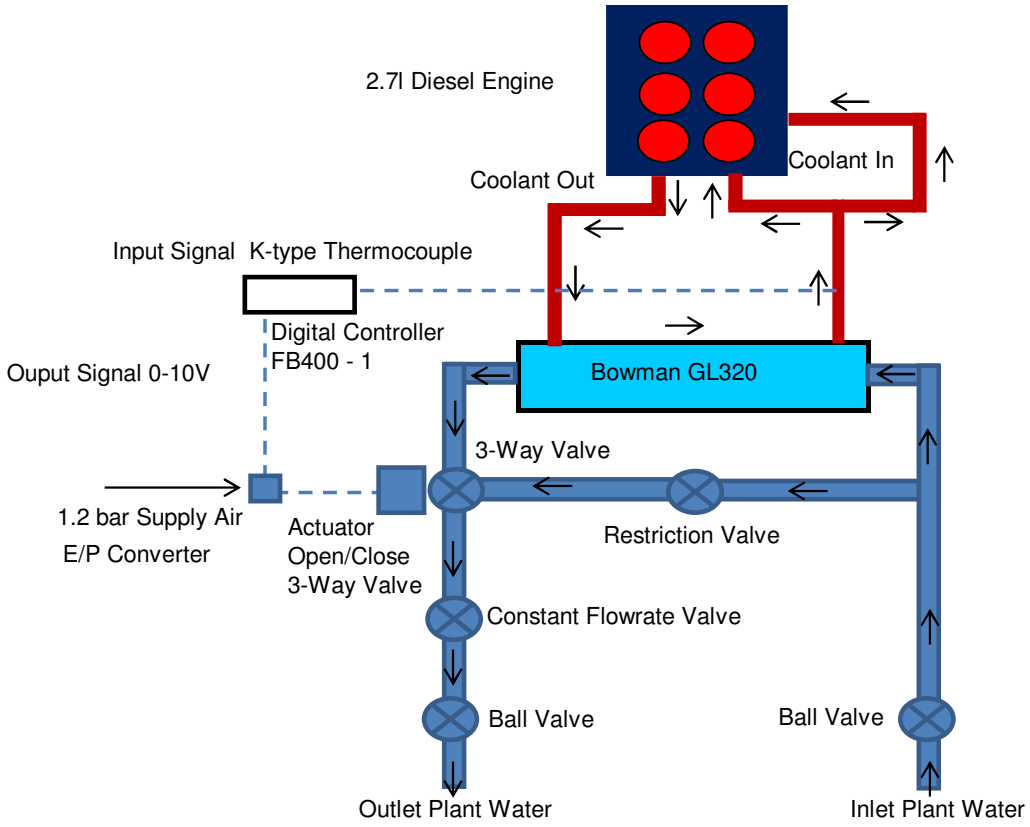

Figure 3.5. Schematic diagram of the engine cooler controller based on the Bowman GL320 heat exchanger.

The Bowman model FG100-4075-2 heat exchanger is used as an intercooler to cool the charged air after the compressor. Counter-flow arrangement is applied to cool the charge air up to between 21 and 51 °C. The constant water flow rate is induced by a constant auto-flow valve located at the end of the pipeline (120 l/min) as shown in Figure 3.6. The valve consists of the main body with the special cartridge inside controlling the flow rate. The actuator on the 3-way valve is controlled by an FB400-2 controller supplied by TC Direct. The measured input temperature from a K-type thermocouple is registered as input into the controller. The output from the controller is in voltage signal (0-10V) transmitted to the EP transducer RP751A 1009-1 to activate the 3-way valve MP 953C5084 supplied by Honeywell. The actuator on the 3-way valve is activated by

compressed air (1.25 bar) to control the amount of water flow rate flowing from the Bowman FG100-4075-2 heat exchanger and the restriction valve in order to keep the required charge air temperature. The charge air temperature is set on the controller as a set value (SV) and the process value displays on the controller as process value (PV).

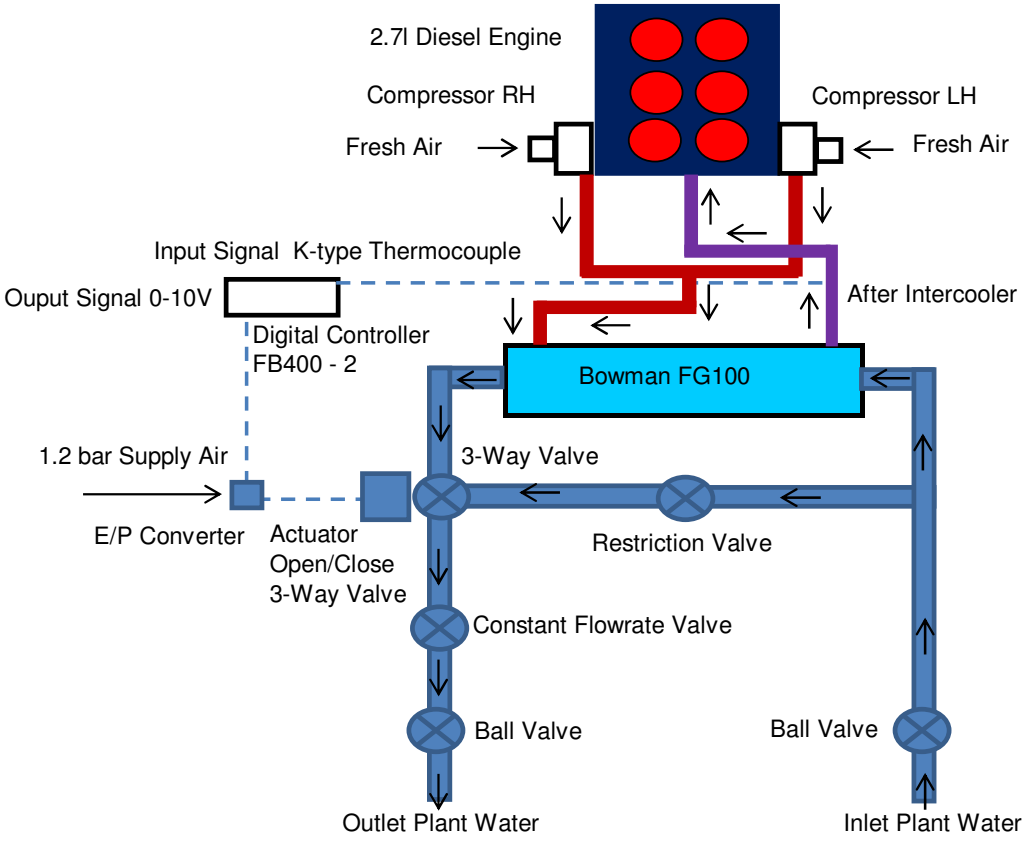

Figure 3.6. Schematic diagram of the intercooler controller based on the Bowman FG100 heat exchanger.

3.1.4. Fuel Measuring Unit (FMS) and Fuel Cooling Unit (FCU)

Figure 3.7 shows the fuel layout of the engine test bench. The engine is provided with two 15.0l and 25.0l of stainless steel tanks for diesel and biodiesel respectively. As it is seen in the layout, the fuel flows to the fuel measuring system through a solenoid valve.

The low pressure fuel line is pressured by a 12V low pressure pump in order to supply constant pressurised fuel at approximately 0.5 bar to the engine. The fuel pressure is manually controlled by a fuel pressure regulator as shown in Figure 3.7. The supply fuel is cooled by the "Bowman 1" heat exchanger and filtered through a fine filter before being fed to the high pressure pump. The hot return fuel from the common rail and injectors are cooled by the "Bowman 2" heat exchanger before mixing with fresh supply fuel in the next delivery. The temperature range for the return fuel is 35 to 80 °C depending on engine speed and load. The input temperature measured by a K-type thermocouple is used as an input signal to the controller through the CADET V14 software as an interface. The output signal from the controller is connected to the solenoid valve in order to control the water flow-rate to achieve the required temperature. The feed fuel temperature is controlled at 20 to 25 °C by the fuel cooling unit (FCU). The mixed fuel flows through the "Bowman 1" heat exchanger and fine filter again before entering the high pressure pump.

The fuel measuring system (FMS1000) is controlled and monitored by the CADET V14 software which also records and displays the data on the computer screen. The FMS1000 uses a 20N load cell to measure the fuel consumption. The system has capability to stabilize any vibration as the construction is stiff and has no moving parts. Inside the box, the system has a 1.0l tank that is mounted on top of the 20N load cell. The FMS has four ports which are for fuel feed, fuel supply, fuel return and vent, as shown in Figure 3.7.

During the measuring process, the CADET V14 software shuts down the fuel flowing from the tank through the solenoid valve. This is so that the fuel is taken only from the small tank (1.0l) inside the box during this stage. After a short settling time, the net mass of fuel taken from the small tank (over the desired sampling time) is measured.

The CP128 card samples data at 10 kHz and returns the averaged value back to the CADET V14 at a frequency of up to 10 Hz. At steady state conditions the engine power is known and the CADET V14 software calculates brake specific fuel consumption (BSFC). The FMS1000 is capable of monitoring fuel during a period of a test stage, or cycle, for a specific time as short as 100 ms. The stage, or cycle, is then repeated and the average fuel consumption rate is calculated as a true dynamic reading.

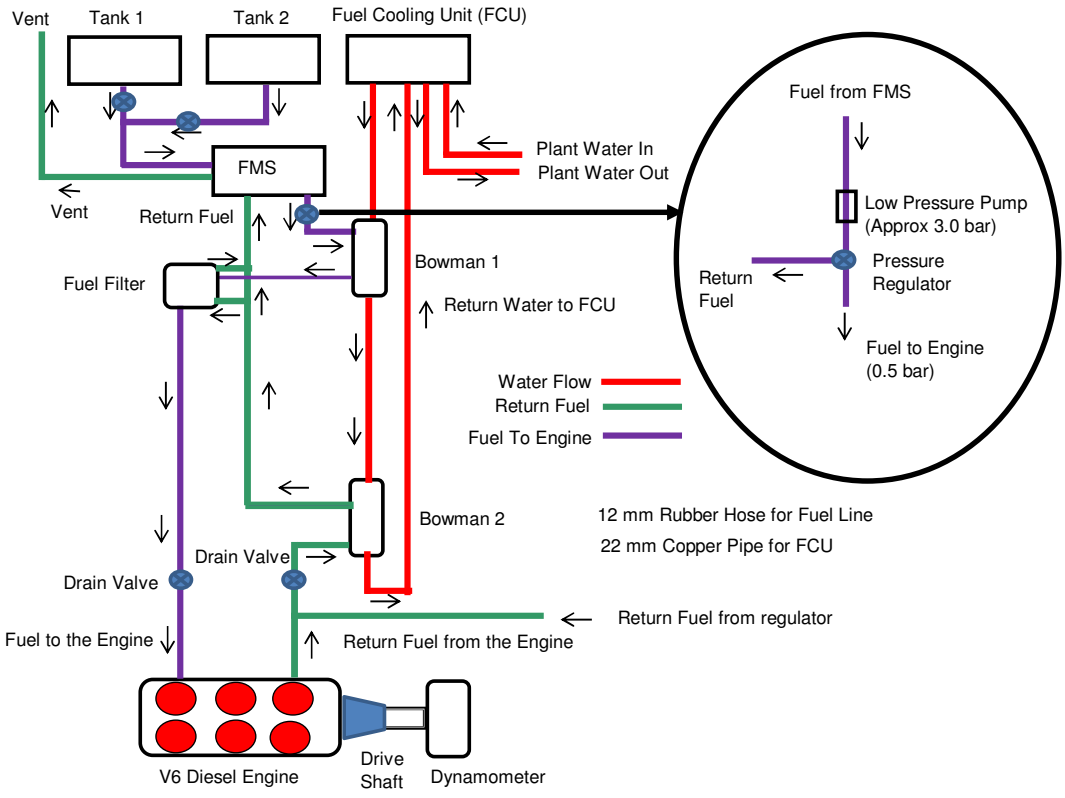

Figure 3.7. Schematic diagram of the fuel measuring system (FMS) and fuel cooling unit (FCU)

A fuel cooling unit is used to control the temperature of supply fuel to the engine. The temperature of supply fuel is high when the return fuel is piped back to the fuel measurement unit. Both fuels, fresh and return, mix together and cool down after passing through the heat exchanger and are filtered by the fine filter before being injected in the

engine cylinder. Figure 3.7 shows the fuel conditioning system process enclosure and the associated heat exchangers. The principle of work is based on generating a conditioned fluid (water or water glycol mix) that can be pumped through one or more fuel heat exchangers. The conditioned fluid is pumped from a vented header tank through the heat exchangers and returned to the header tank. When heating is required a 3 kW heater fitted in the header tank is activated by the control system. When cooling is required two solenoid valves operating in tandem are activated to allow the conditioned fluid through the conditioned fluid heat exchanger. The conditioned fluid temperature in the header tank is monitored by a PRT.

3.1.5. Engine and Controller Wirings

The main features of the engine wiring system such as ignition, engine management system, starter motor and engine emergency stop are explained as below. A schematic diagram of the whole engine wiring system is displayed in Figure 3.8. For the engine starting system, power from a battery is used to turn the engine crank via the starter motor. The re-charging system fully works as the alternator circuit is connected to the charging system. During the cranking process, a high-current power supply from the battery is connected directly to the starter motor and is triggered by a solenoid coil in the starter motor to turn the engine crank via the flywheel.

The ignition and engine management system (EMS) switches are wired to the CADET V14 software through box 2. The battery is expected to supply a constant 12-13.8VDC all the time. The primary ignition switch functions are to switch the EMS (start/stop the engine) and to be used during cranking the engine for top dead centre (TDC) identification. Two emergency stop buttons are attached in the engine wiring system, one

of which is placed in the control room in front of the control panel whilst the second is located in the engine test cell. These two stop buttons are used only for emergencies to stop the engine by isolating the power supply to the EMS.

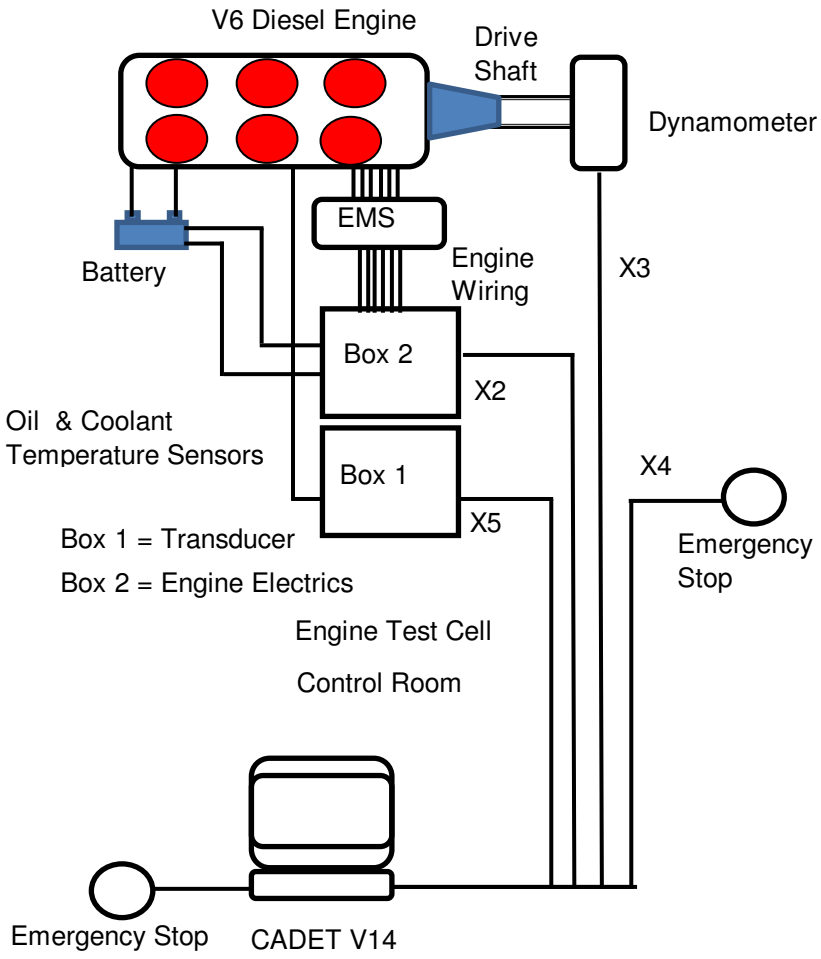

Figure 3.8. Schematic diagram of engine and controller wiring

3.2 Instrumentation and Control

3.2.1. In-cylinder Pressure Data Acquisition Devices

The layout of the cylinder pressure transducers and optical encoder is displayed in Figure 3.9. The air shut off throttle and oil filter are removed from the engine top before

the glow plug is dismantled. The glow plug at cylinder 2 and cylinder 5 are replaced by AVL GU13G piezo pressure transducers. The glow plug bores are matched with pressure transducer adaptors. Each transducer is mounted into a glow plug adaptor before being fitted into cylinder 2 and cylinder 5. Key technical data of the transducers are listed in Table 3.3.

Table 3.3. In-cylinder pressure transducer specification

Measuring range (FSO)	0 to 200 bar
Sensitivity for S/N 6045	15.53 pC/bar
Sensitivity for S/N6046	15.44 pC/bar
Linearity	≤ ± 0.3% FS
Operating temperature range	up to 400°C
Natural frequency	130 kHz
Tighten torque	1.5 Nm

An amplifier model AVL 3066A03 with two-channels is used to rectify the raw signals from the piezo-electric transducer. The amplified cylinder pressure signal and encoder signal are connected to the AVL Indi Master 620 combustion analyser and the data is recorded by IndiCom 2010 software. The key technical data of the amplifier are listed in Table 3.4.

Table 3.4. Charge amplifier specification

Measurement range (for 10V output voltage)	100 pC to 16000 pC
Measurement range settings	1, 2, 5, 10, 20, 50 bar/V
Transducer sensitivity	1.00 pC/bar to 99.9 pC/bar
Linearity error	≤ ± 0.01% FS
Upper cut-off frequency (low-pass)	200 kHz
Output voltage	-10V to +10V

The crankshaft position is determined by the optical encoder 365CC from AVL by using IndiCom 2010 software. The encoder is attached into the bracket and mounted on to the main pulley of the engine crankshaft. The engine crankshaft and the encoder are connected by an adapter flange. The encoder generates 720 pulses for each complete revolution of the crank shaft. Therefore, for a complete 4-stroke engine cycle the 1440 pulses have been transmitted by the encoder. The encoder shaft with double bearing is built with high strength materials (titanium and high strength aluminium alloy) as the housing. Technical data of the AVL 365CC encoder is given in Table 3.5.

Table 3.5. Shaft encoder specification (AVL 365CC)

Speed range	50 rpm – 20,000 rpm
Vibration-resistance axial and radial	500 – 1000 g x 9.81 m/s^2
Permissible ambient temperature	-40 deg C – 120 deg C
Mass load of crank shaft	300 g horizontal, 350 g
Moment of inertia of rotating masses	3.8 x 10^{-5} kgm^2

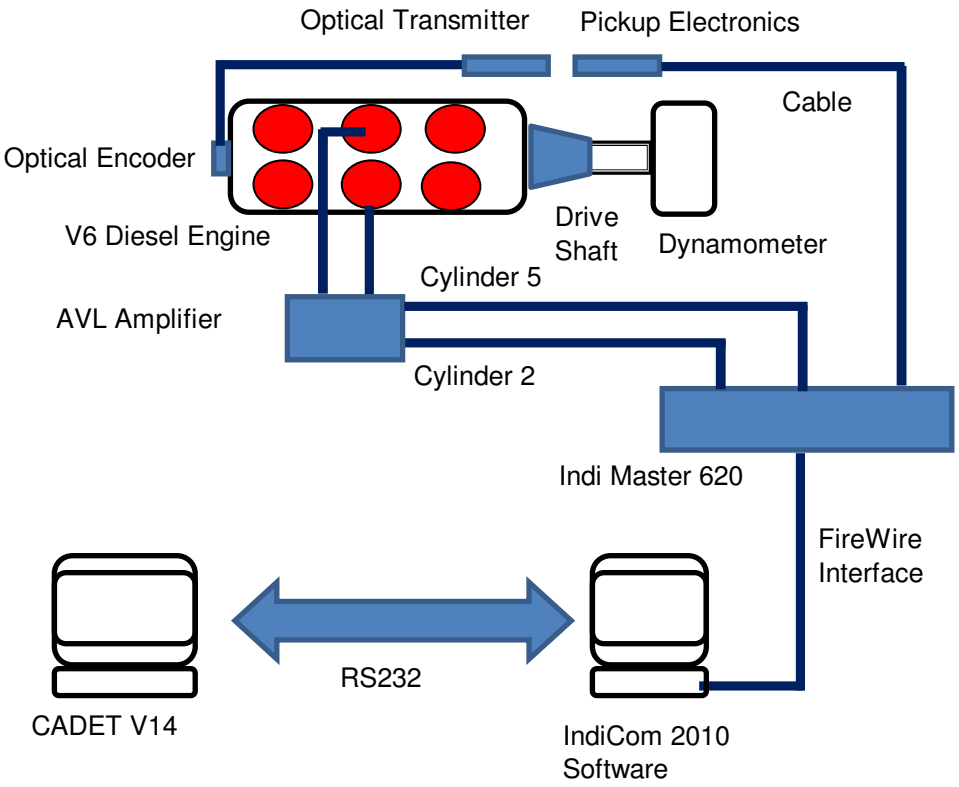

Figure 3.9. Schematic diagram and wirings of the in-cylinder pressure data acquisition

3.2.2. Engine Management System Acquisition and Calibration

Figure 3.10 shows the connection of the INCA management system from ETAS with the CADET V 14 software. The engine management system (EMS) is connected to the computer for data monitoring, calibration and recording. The INCA V5.3 software from ETAS has been used to communicate with the EMS through a specific file provided by Jaguar Land Rover. The EMS signals for engine operating parameters such as air mass flow, fuel mass flow, fuel injection pressure, start of pre-, main-, and post- injection, temperature of coolant and lubrication, intake manifold pressure etc, can be monitored, calibrated, and recorded through the computer.

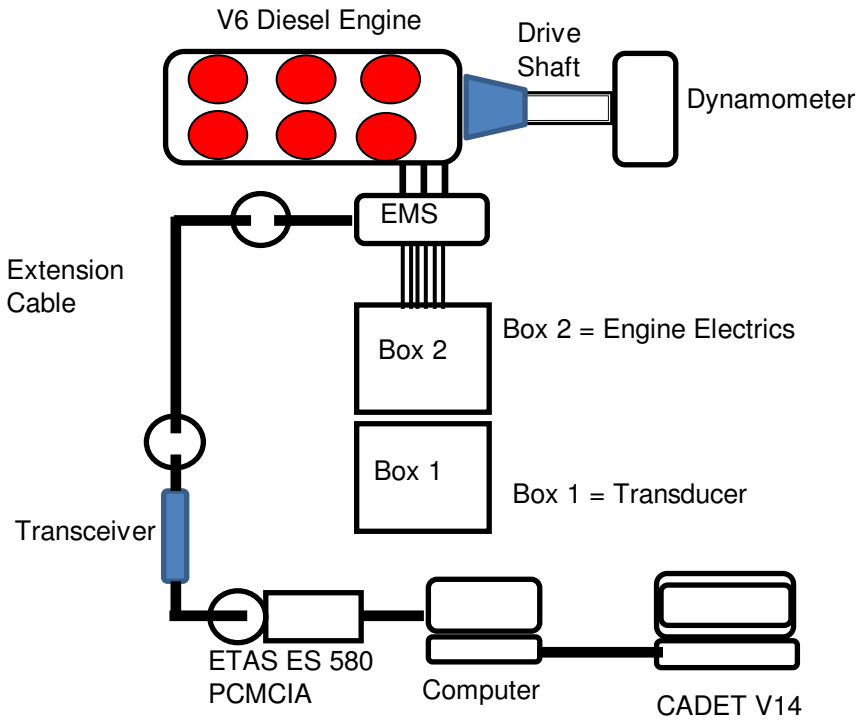

Figure 3.10. Schematic diagram of the engine management system (EMS).

The data was recorded in the CADET V14 software by using ASAP 3 command provided by CP Engineering. The specification of the ETAS ES 580 CAN card interface is displayed in Table 3.6.

Table 3.6. CAN card interface module specification

CAN No. of channels	2 (V2.0B extended format)
Maximum baud rate	1 Mbit/s
Resolution	1 µs
PC interface	16-bit PC-Card Version 2.0 (PCMCIA)
Current consumption	150 mA for ES580 and typical 30 mA for CAN cable
Temperature range	Operation: 0°C to 55°C, Storage: -40°C to 125°C

3.2.3. Temperature and Pressure Data Acquisition Devices

The additional data acquisition systems for pressures and temperatures are shown in Figures 3.11 and 3.12 respectively. Thermocouples and pressures are located at

strategic points in the engine as listed in the Appendix C. The temperatures signal acquired by K-type thermocouple and the output signals in voltage are connected to the CP box and recorded on CADET V14 software.

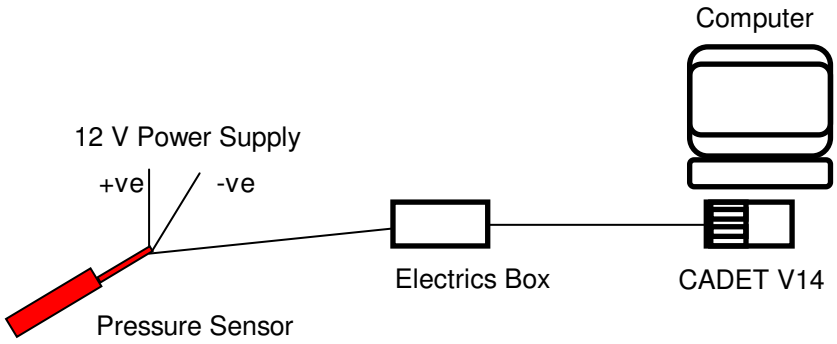

Figure 3.11. Schematic diagram and wirings of pressure data acquisition

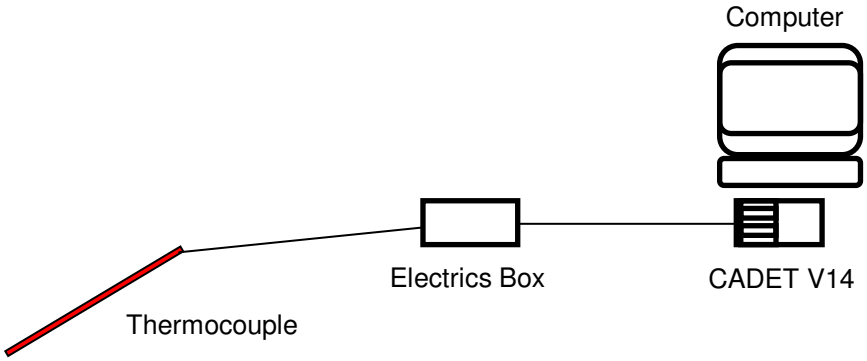

Figure 3.12. Schematic diagram and wirings of temperature data acquisition

3.2.4 Relative Humidity and Atmosphere Pressure

The relative humidity and ambient temperature are monitored by hygrometer from VAISALA. The atmosphere's pressure is measured by using a barometer also provided by VAISALA. The data is recorded by the CADET V14 software.

3.2.5 Engine Load and Speed Control

The engine is loaded with an eddy current dynamometer using the CADET V14 control software and hardware. The complete test plan is created in the CADET V14 software to run the experiments. The engine load is measured from the IMEP calculated by the CADET V14 software. The dynamometer automatically balances the changes in the engine load and speed during the settling time.

3.2.6 Injection Pressure Control

The 2.7l V6 engine is equipped with a Siemens common rail direct injection system and the 3.0l V6 engine is equipped with a Bosch common rail direct injection system. The summary of both injection systems are displayed in Table 3.7.

Table 3.7. Summary of injection system

Injection System Parameters	**2.7 l Engine**	**3.0 l Engine**
Control System	Siemens	Bosch
Maximum Rating (bar)	1600	2000
Injector Type	Siemens Piezo Actuator	Bosch Piezo Actuator
Injector Pipe (mm)	Inner Diameter 3	Inner Diameter 3
Nozzle Type	6 Holes	8 Holes

The injection strategies control the injection timing, injection pressure, injection quantity, injection events, injection duration and dwell period between injection events. The injection strategies can be controlled by using the INCA V5.3 software that communicates through the Engine Management System (EMS). The user can modify these values on the calibration window of the INCA software. The engine operation will automatically change based on the modifications made in the calibration window. The

EMS has a capability of executing up to 6 injection events per cycle. All the injection parameters such as duration, pressure etc, can be controlled.

3.2.7 EGR Ratio Control

The exhaust gas recirculation (EGR) ratio is also electronically controlled by the INCA V5.3 software. The EGR operation can be changed in the calibration window of the INCA software and the engine automatically responds to the modification. In this case, the EGR rate is totally controlled by engine calibration. The EGR configuration used in this engine is shown in Figures 3.13a and 3.13b. The exhaust gas diverted before turbines (high pressure EGR) flows through the EGR valve and then mixes with charge air downstream of the compressor.

$$EGR = 100 \times \left[1 - \left(\frac{m_a RT}{pV\eta_v} \right) \right] \tag{3.1}$$

The EGR set-point is calculated using Equation 3.1 [131], where m_a represents the air mass flow rate, p is the manifold pressure, V is the volume, η_v is the volumetric efficiency, and R is the gas constant. The main parameters' influences on the EGR set-point are the air mass flow rate, boost pressure and volumetric efficiency. These parameters are changing according to the engine speed, load and feedback signals such as smoke, fuel consumption, engine power, etc. Therefore, the EGR set-point is slightly different with different injection strategy (injection pressure, dwell period and pilot quantity) due to the different values in the air mass flow rate, manifold pressure and volumetric efficiency.

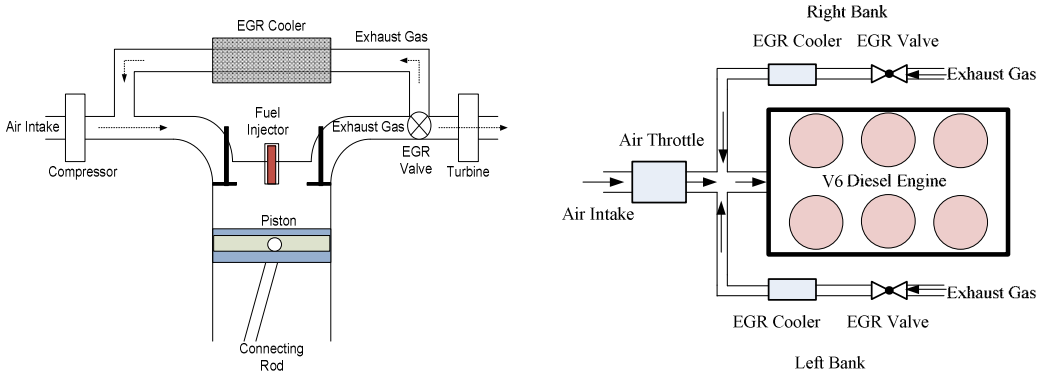

a) b)

Figure 3.13. Schematic diagram of the EGR system on V6 diesel engine a) general view b) top view.

3.2.8 Engine Cooler and Intercooler

The details about the engine cooler and intercooler were described in Section 3.1.3. Both temperatures are fully controlled by the PID controller. In this study, the engine coolant inlet temperature is set at 90 °C. However, the temperature of the intercooler outlet is set based on engine speed and load.

3.2.9 Fuel Measuring System (FMS)

Fuel consumption is measured by using a Fuel Measuring System (FMS) supplied by CP Engineering. The details about the FMS were explained in Section 3.1.4. The fuel consumption is monitored and recorded by the CADET V14 software. The reading of fuel flow rate is recorded in gram per second (g/s).

3.3. Exhaust Gas Monitoring Analysis and Instrumentation

3.3.1. Exhaust Gaseous Instrumentation (Horiba MEXA 7100EGR)

Emissions of CO, CO_2, THC and NO_x are measured from the exhaust sample line by an exhaust gas analyzer (Horiba MEXA-7100EGR). The different exhaust gas components are measured using different measuring techniques as shown in Table 3.8. The heated line and pre-filter are maintained at 191 °C. The system has to be calibrated by suitable bottled span and zero calibration gases. After this process, the system is ready to use.

Table 3.8. Exhaust emissions measurement methods

Emissions components	Measurement method
Carbon MoNOxide (CO)	Non-dispersive Infrared Sensor (Dry)
Carbon Dioxide (CO_2)	Non-dispersive Infrared Sensor (Dry)
Total Hydrocarbons (THCs)	Flame Ionisation Detector (Hot)
Nitrogen Oxide (NOx)	Chemiluminescene Detector (Dry)

In this experimental work, the Horiba MEXA-7100EGR is controlled digitally by the CADET V14 software. The initial stage is purge, sample and then measurement for every engine test condition.

3.3.2 Smoke Analysis (Smoke Meter AVL415S)

Smoke emissions are measured by using an AVL 415S smoke meter which provides results directly as a Filter Smoke Number (FSN) unit. The colour of the filter paper mainly depends on the soot concentration emitted by the engine. The value 0 is assigned to the clean filter paper and the completely black paper filter that is loaded with soot is assigned value 10. The effective length is standardized from ISO DP 10054 with 405 mm, a sampled volume of 0.33l and a loaded paper face of 8.15 cm² (Ø 32 mm). The

sampling time is approximately 30 seconds with 1.0l of a sampled volume. However, at higher soot concentrations (FSN > 6), the sampled volume must be reduced down to 0.33l. The smoke meter has a capability to take 5 measurements and then average.

3.4. Fuel Properties and Engine Oil

Two biodiesel-diesel blends Tallow Methyl Ester (TME10 and TME30) and ultra low sulphur diesel (ULSD) were used throughout the research work. All fuels are provided by Green Fuels and Shell Global Solutions UK and conform to EN590 and EN14214, the standard for ULSD and TME respectively. The fuel properties are shown in Table 3.9.

Table 3.9. Fuel properties [172-174]

	Test method	ULSD	TME
Cetane number[a]	ASTM D613	47	58.8
Density at 15°C (kg/m^3)[a]	ASTM D4052	843.51	877
KinematicViscosity at 40°C (cSt)[a]	ASTM D445	3.6	5.07
LHV (MJ/kg)[a]		42.7	39.8
Sulphur (% wt)[b]		0.29	0.18
C (% wt.)[b]		87.12	76.77
H (% wt.)[b]		12.88	12.88
O (% wt.)[b]		-	11.47

a [172]
b [137, 174]

In all the experimental study, biodiesel blended fuels are designated as TMEXX etc where XX represents the volumetric percentage of neat biodiesel contained in the blended mixture. For example, TME30 represents the volumetric blend of 30 percent TME with 70 percent ULSD.

The engine lubrication oil used throughout the research as recommended by the manufacturer for the engine is Castrol MAGNATEC 5W-30 A1. The initial oil capacity is 7.7l and for the next service oil capacity is 6.6l for both engines. The initial line fill is higher than usual since the oil needs to be circulated through all engine parts including the oil filter. The maximum dipstick indication is 6.4l and the minimum dipstick indication is 4.9l in both engine capacities. Both engines use the same amount of oil as shown in Table 3.10.

Table 3.10. : Engine oil capacity

Volume of Engine Oil	**2.7l Engine**	**3.0l Engine**
Initial line fill (l)	7.7	7.7
Service oil fill (l)	6.6	6.6
Maximum dipstick (l)	6.4	6.4
Minimum dipstick (l)	4.9	4.9

3.5 Engine Test Conditions

The engine test conditions are explained in each chapter separately. The results presented in the following chapters are the average of the measurements taken from three separate tests, with outlying points either removed or retested.

CHAPTER 4

COMBINED EFFECT OF FUEL INJECTION PRESSURE AND EGR ON THE ENGINE PERFORMANCE AND EMISSIONS

This chapter presents the measurable engine performance parameters and emissions of a diesel engine fuelled with ultra-low sulphur diesel (ULSD). The experiments are carried out on a fully instrumented 2.7l V6 Jaguar diesel engine, twin-turbocharged, water-cooled, variable geometry turbochargers, with cooled EGR and equipped with a common rail direct fuel injection system as given in Chapter 3. The details of the engine test conditions are described in the following section. In Sections 4.2 and 4.3 the effect of fuel injection pressure and EGR on the measurable engine performance parameters and emissions are discussed, respectively. The summary of the chapter is presented in Section 4.4.

4.1 Engine Test Conditions

The present study was carried out with a constant engine speed and three different engine loads as shown in Table 4.1. Five different levels of fuel injection pressure 300, 430, 500, 600, 700 bar, at three different engine loads (35.1, 70.2 and 140 Nm) were carried out in this experiment. The selected conditions (speed and loads) are chosen in order to investigate fuel injection pressure effect at low speed and moderate engine loads. The effect of the EGR mode on the engine performance and emissions is discussed in detail in Section 4.3.

The focus of the study is to investigate the effect of a variation in fuel injection pressures with split (pilot and main) injection, (with and without cooled EGR) on engine

performance and emissions. The fuel ratio between the pilot and main injection is approximately 10:90 by mass. The fuel injection pressure for both pilot and main injection are the same. The pilot injection was timed at -15.80 CAD and main injection was timed at 2.55 CAD.

Table 4.1. Engine test conditions

Engine Speed (rpm)	Engine Load (Nm)			Injection Pressure (bar)
1500	35.1 (10%)	70.2 (20%)	140.4 (40%)	300-700

The inlet fuel temperature (35 ± 1 °C), inlet air temperature (30 ± 1 °C) and relative humidity (45-50%) were kept constant and monitored throughout the tests. These parameters are significantly important as are influencing ignition delay and combustion behaviour, particularly when the engine operating with EGR. In Chapter 5, the same conditions used in order to study the effects of injection pressure and dwell period on the engine performance and emissions.

4.2 The Effects of Fuel Injection Pressures

The study is designed to investigate the effects of fuel injection pressure on a V6 diesel engine at a variation of engine loads operating without EGR. The engine test conditions were mentioned in section 4.1.

4.2.1 Engine Performance and Combustion Characteristics

Figure 4.1 shows the rate of heat release (ROHR) and in-cylinder pressure as a function of crank angle degree (CAD) at 1500 rpm, without EGR at five different fuel injection pressures (300, 430, 500, 600 and 700 bar). It can be clearly seen that the peak

in-cylinder pressure increased with the increase of the fuel injection pressure, as the start of the main combustion was advanced.

High fuel injection pressures enhancing fuel atomisation corresponding to small fuel droplets size, thus promoting a shorter duration of combustion and faster heat release rate [68]. In contrast, the lower fuel injection pressure produces lower peak in-cylinder pressure due to a reduction in the premixed combustion phase, a consequence of a poor rate of fuel evaporation at lower fuel injection pressure. In addition, the peak in-cylinder pressure mainly depends upon the initial combustion rate which is strongly influenced by the amount of fuel available to burn at this stage [36]. The ROHR diagram shows the combustion from lower fuel injection pressure consists of a shorter premixed phase and a longer diffusion-controlled combustion phase.

The different in a first peak (peak 1) in-cylinder pressure is very difficult to notice. However, it is clearly seen in the peak 2 of in-cylinder pressure where the highest fuel injection pressure of 700 bar produced the highest peak in-cylinder pressure. The second envelope of peak in-cylinder pressure appears due to the engine operating with split injection strategy. The peak 1 is appeared due to the pilot combustion and the peak 2 is due to the main combustion.

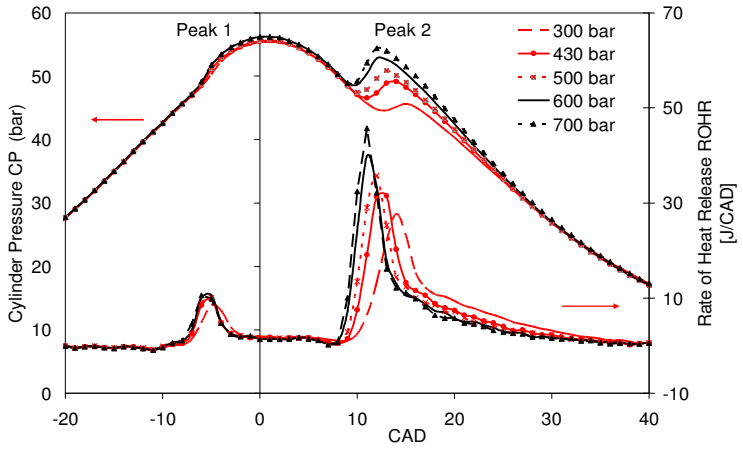

Figure 4.1. The heat release rate and in-cylinder pressure for a variation of fuel injection pressures at 1500 rpm, 35.1 Nm with EGR OFF.

Figures 4.2a and 4.2b show the values of peak in-cylinder pressure (peak 1 and peak 2) due to pilot combustion and main combustion, respectively. The values of peak 1 are increased by 2.3%, 14.0% and 15.0% with the increase of fuel injection pressure from 300 bar to 700 bar at 35.1 Nm, 70.2 Nm and 140.4 Nm respectively. Meanwhile, the values of peak 2 are increased by 19.0%, 18.3% and 23.7% with the increase of fuel injection pressure from 300 to 700 bar at 35.1 Nm, 70.2 Nm and 140.4 Nm respectively. The results showed that the higher fuel injection pressure is more important at high loads compared with lower load where Fuel-Air mixing is easier.

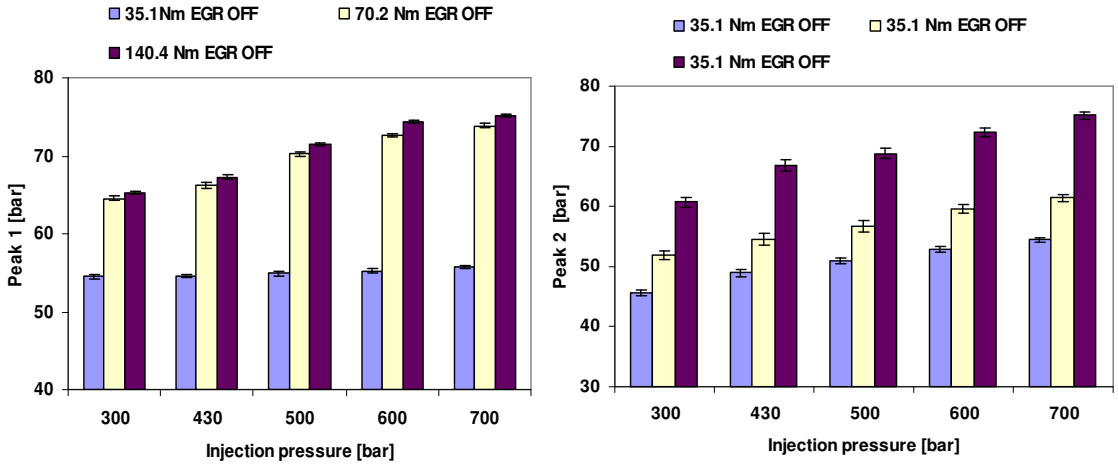

a) b)

Figure 4.2. a) Peak in-cylinder pressure 1(peak 1), b) peak in-cylinder pressure 2 (peak 2) from a variation of fuel injection pressures and three engine loads at 1500 rpm, error bars represent 95 percent confidence.

Figures 4.3a and 4.3b show the brake specific fuel consumption (BSFC) and engine thermal efficiency respectively for a variation of fuel injection pressures at three different engine loads. In all engine test conditions BSFC decreases as the fuel injection pressure increases due to advanced combustion (Figure 4.1), reduced ignition delay (Figure 4.4) and rapid combustion rate [64]. Ignition delay was calculated from the start of injection (SOI) of the main injection to the first point of a positive value of ROHR. In addition, based on the lower CO and THCs emissions from Figures 4.6 and 4.7 respectively, it can be concluded that the higher fuel injection pressure gave slightly improved fuel combustion efficiency. This is strongly believed to be due to the improved mixing process as compared to the lower fuel injection pressure. In fact, the higher fuel injection pressure leads to an improvement in the combustion process and a high power output is produced due to better fuel distribution and heat utilisation for almost all engine test conditions [64].

The engine thermal efficiency was increased as the main combustion advanced due to increased fuel injection pressure. This is due to less injected fuel to produce the equal power output by high fuel injection pressure. The results also showed that the higher load has higher efficiency due to higher combustion temperatures and lower heat losses.

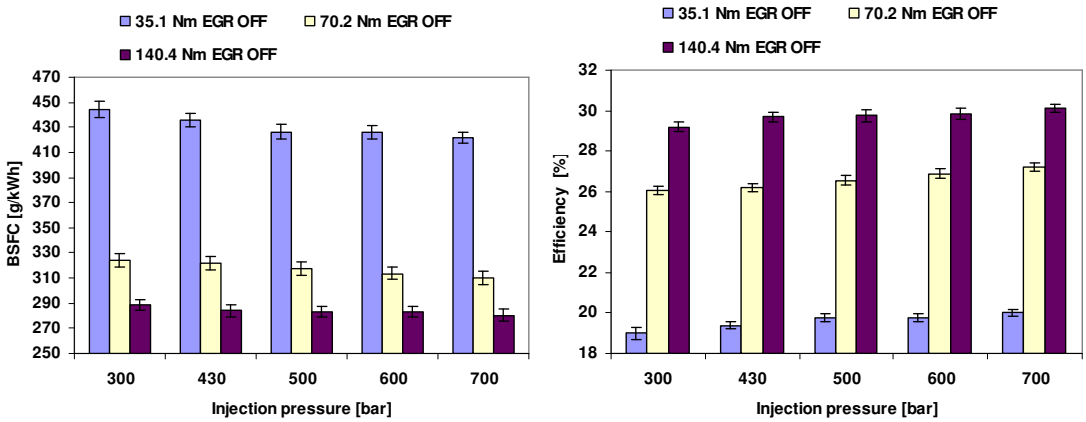

a) b)

Figure 4.3. a) Brake specific fuel consumption, b) engine thermal efficiency for a variation of fuel injection pressures and three engine loads at 1500 rpm, error bars represent 95 percent confidence.

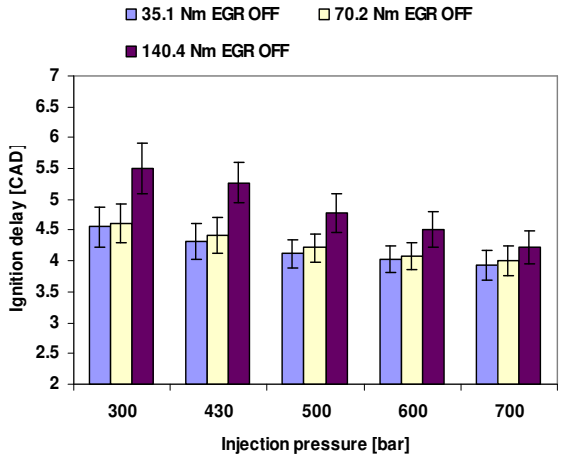

Figure 4.4. Ignition delay for a variation of fuel injection pressures and three engine loads at 1500 rpm, error bars represent 95 percent confidence.

4.2.2 Engine Emissions

Figure 4.5 shows the emissions of NO_x for a variation of fuel injection pressures and three different engine loads at 1500 rpm. The results showed that the NO_x emissions are increased with the increase of fuel injection pressure for all engine test conditions. The higher fuel injection pressure leads to higher levels of NO_x emissions as compared to the lowest fuel injection pressure. This is due to rapid combustion process as a result of the increased global in-cylinder temperatures due to advanced combustion [36, 64].

The smaller fuel droplets size, produced by the higher fuel injection pressure is strongly contributes to the higher flame temperature [2, 36, 142, 175]. Several factors that contribute to the fast combustion process in diesel engines are; fuel properties, fuel droplet size, penetration length, turbulence intensity, fuel evaporation, rate of combustion and ignition delay.

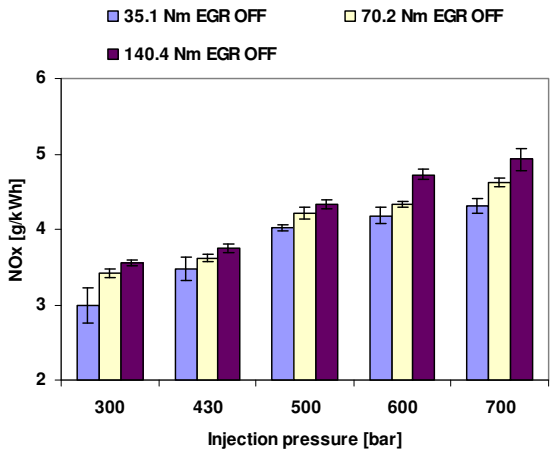

Figure 4.5. NO_x emissions for a variation of fuel injection pressures and three engine loads at 1500 rpm, error bars represent 95 percent confidence.

Figures 4.6 and 4.7 show the carbon monoxide (CO) and total hydrocarbons (THCs) emissions respectively for a variation of fuel injection pressures and three different

engine loads at 1500 rpm. The overall results show that both emissions decreased as the fuel injection pressure increases for almost all engine test conditions due to improved combustion efficiency. As explained earlier, higher in-cylinder pressure, high combustion temperatures, improved Air-Fuel mixing and fuel atomisation led to enhanced CO and THCs oxidation [69, 142].

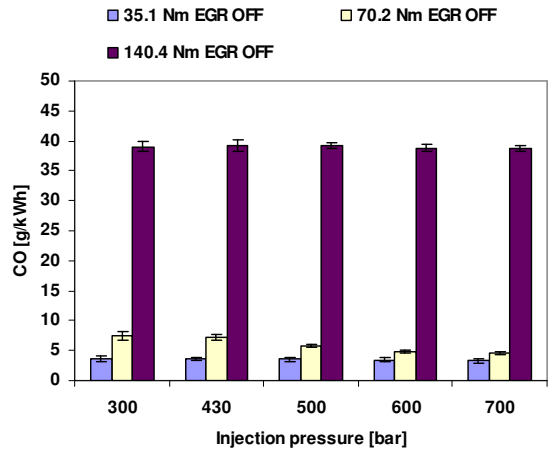

Figure 4.6. CO emissions for a variation of fuel injection pressures and three engine loads at 1500 rpm, error bars represent 95 percent confidence.

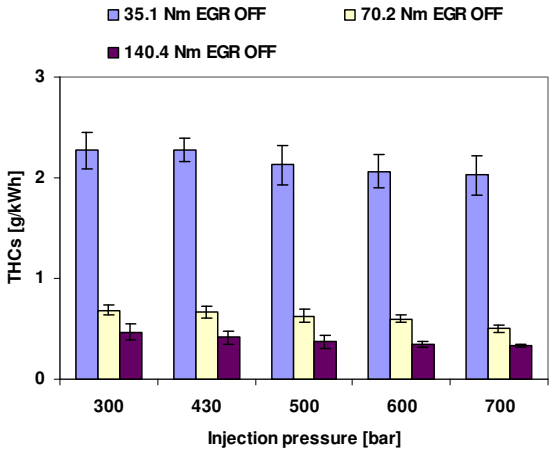

Figure 4.7. THCs emissions for a variation of fuel injection pressures and three engine loads at 1500 rpm, error bars represent 95 percent confidence.

Figure 4.8 shows the smoke levels for a variation of fuel injection pressures and three different engine loads at 1500 rpm. The smoke levels are decreased with the increase of fuel injection pressure. These results are consistent with other studies by Bhusnoor et al. [36] and Dhananjaya et al. [64] and suggest that the higher fuel injection pressure can be beneficial due to better fuel atomisation leading to improved combustion behaviour. This leads to a reduction of the rate of soot formation. In fact, the smoke emissions decrease as the fuel injection pressure increases due to an improved mixing process and less fuel-rich regions that can contribute to soot formation [84, 176].

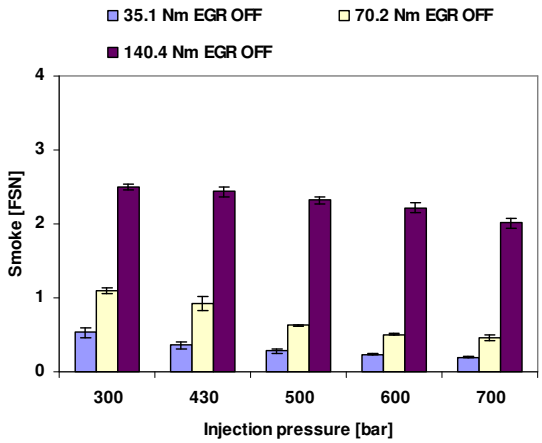

Figure 4.8. Smoke level for a variation of fuel injection pressures and three engine loads at 1500 rpm, error bars represent 95 percent confidence.

Figure 4.9 shows the NO_x-smoke trade-off emissions, for a variation of fuel injection pressures and three different engine loads at 1500 rpm, 35.1 Nm. The smoke levels appeared to be lower with high fuel injection pressure while the NO_x emissions increased dramatically at all engine loads. A low level of 0.533 FSN smoke and a high level of 2.992 g/kWh NO_x can be achieved at the fuel injection pressure of 700 bar when the engine is operating with the engine load of 35.1 Nm, without EGR. Therefore, the

simultaneous reductions in smoke and NO_x could be achieved when there is a combined strategy between high fuel injection pressure and EGR.

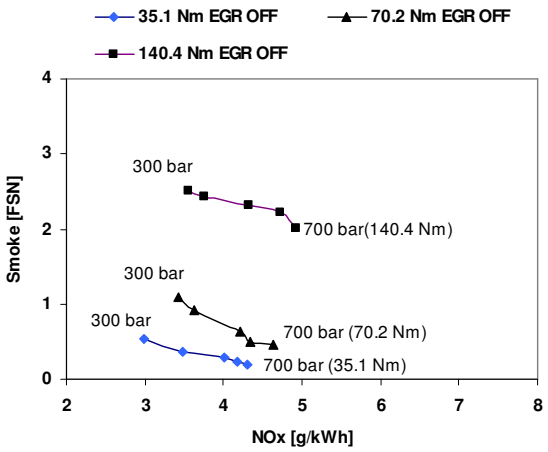

Figure 4.9. NO_x-Smoke trade-off emissions for a variation of fuel injection pressures and three engine loads at 1500 rpm.

4.3 Effects of Cooled Exhaust Gas Recirculation

In Section 4.2, the higher fuel injection pressure tends to produce a high level of NO_x emissions due to high combustion temperatures. Therefore, in this section, EGR is used to balance the higher level of NO_x emissions produced by higher fuel injection pressure and in an attempt to break the NO_x -Smoke trade-off. As it is well accepted, EGR is favourable for NO_x reduction and high fuel injection pressure is favourable for engine performance and emissions. The main objective of this study is to investigate the combined effects of cooled EGR and fuel injection pressure to the engine performance and emissions

Below are the summaries of engine test conditions for the effects of fuel injection pressure and exhaust gas recirculation on engine performance and emissions. The test conditions were carried out at 1500 rpm and 35.1 Nm at a variety of fuel injection

pressures (300 – 700 bar) with EGR OFF and EGR ON. In EGR ON mode, the EGR rates are changing in between (44.4 -45.79%) at a variation of fuel injection pressures as shown in Table 4.2. The EGR rate is controlled automatically by the engine management system (EMS), and is dependent on the engine test conditions. The detail about EGR's control was mentioned in Section 3.27.

Table 4.2. Engine test conditions (Various fuel injection pressures + EGR)

Injection Pressure (bar)	300	430	500	600	700
EGR ON (%)	44.4	44.7	46.31	45.75	45.79
EGR OFF (%)	0	0	0	0	0

4.3.1 Engine Performance and Combustion Characteristics

Figures 4.10a, 4.10b, 4.11a and 4.11b show that the peak pressures are increased as the engine operation changed from EGR ON to EGR OFF. It is clearly observed from the graph that the EGR ON delayed the start of combustion due to a lean mixture and thus resulted in a longer ignition delay. The EGR ON influenced the start of combustion and the combustion period through the longer ignition delay. The overall results show a good agreement with the study by Zheng et al. [177] that shows the ignition delay increases with the EGR. The use of cooled EGR produces lower peak in-cylinder pressure as compared to EGR OFF. This is due to a retarded combustion, a result of the reduced oxygen density and high heat capacity of the gas mixture [34, 68]. In addition, the reduction of fuel burnt in the premixed combustion phase can be considered as a strong factor in lowering in-cylinder peak pressure.

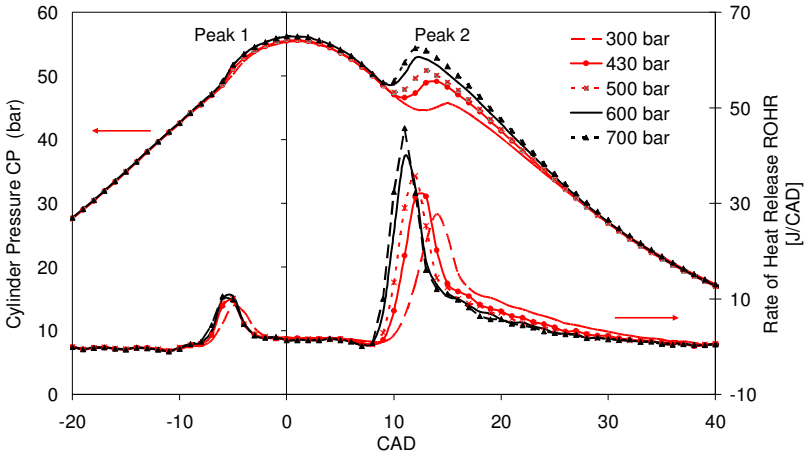

a)

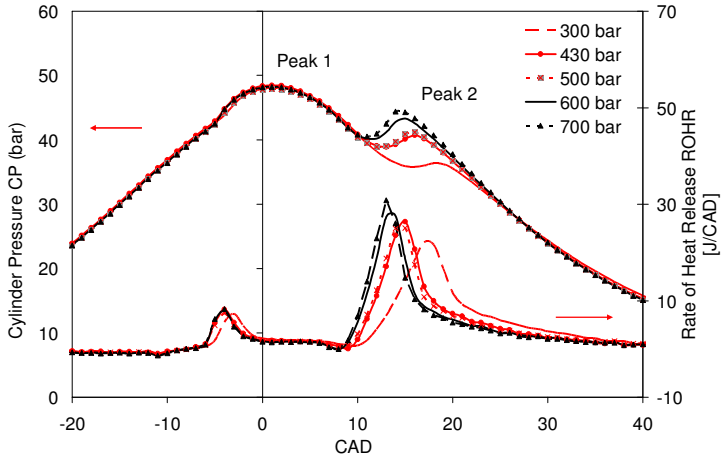

b)

Figure 4.10. a) ROHR and in-cylinder pressure profile for EGR OFF and b) ROHR and in-cylinder pressure profile for EGR ON at 1500 rpm, 35.1 Nm.

Figures 4.11a and 4.11b show the values of peak 1 and peak 2 for both EGR ON and EGR OFF respectively. The values of peak 1 are due to pilot combustion and peak 2 are due to main combustion. The values of peak 1 are increased by 4.8% and 2.3% with the increase of fuel injection pressure from 300 to 700 bar for EGR ON and EGR OFF respectively. Meanwhile, the values of peak 2 are increased by 22.5% and 19.1 % with the increase of fuel injection pressure from 300 to 700 bar for EGR ON and EGR OFF

respectively. These results showed that the higher improvement to the EGR ON rather than the EGR OFF with the increase of fuel injection pressure. This is because a poor combustion at lower fuel injection pressure with EGR ON as compared to EGR OFF due to less availability of oxygen in EGR ON. Therefore, the increased fuel injection pressure is more significant to the EGR ON.

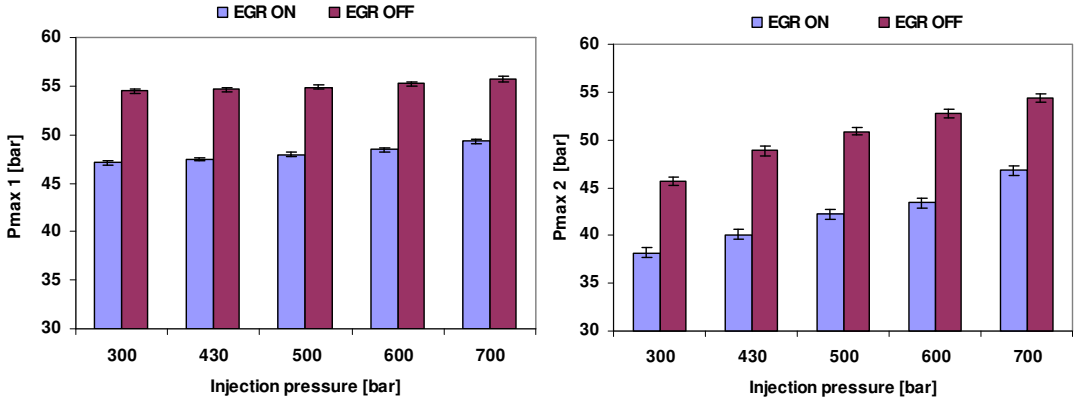

a) b)

Figure 4.11. a) Peak in-cylinder pressure 1 and b) Peak in-cylinder pressure 2 for a variation of fuel injection pressures at 1500 rpm, 35.1 Nm, error bars represent 95 percent confidence.

Figure 4.12 shows the main ignition delay for a variation of fuel injection pressures with EGR ON and EGR OFF at 1500 rpm, 35.1 Nm. The ignition delays are decreased by 4.8% and 13.6% with the increase of fuel injection pressure from 300 to 700 bar at EGR ON and EGR OFF respectively. The longer ignition delay with EGR ON is due to the dilution effect, chemical effect and thermal effect [89, 178-180].

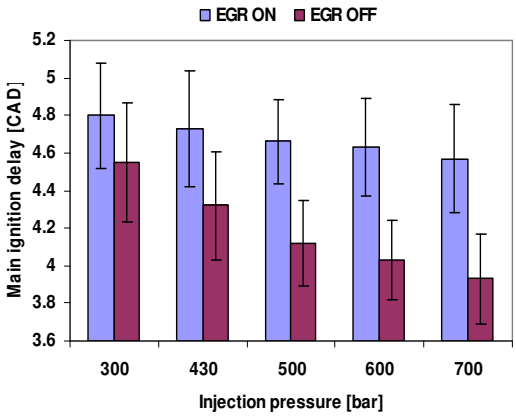

Figure 4.12. Main ignition delay for a variation of fuel injection pressures at 1500 rpm, 35.1 Nm, error bars represent 95 percent confidence.

Figures 4.13a and 4.13b show the brake specific fuel consumption and engine thermal efficiency respectively, for a variation of fuel injection pressures with EGR ON and EGR OFF at 1500 rpm, 35.1 Nm. The BSFC is decreased by 2.7% and 5.1% with the increase of fuel injection pressure from 300 to 700 bar for EGR ON and EGR OFF, respectively. The engine thermal efficiency is increased with the higher injection pressure in both cases EGR ON and EGR OFF. The values of engine thermal efficiency are increased from 18.5% to 20.0% and 19.0% to 20% with the increase of fuel injection pressure from 300 to 700 bar for EGR ON and EGR OFF, respectively. It showed that the effect of higher fuel injection pressure to the BSFC is better in EGR OFF as compared to EGR ON. The results also showed that the BSFC decreased when the engine is switched from EGR ON to EGR OFF. This is due to the higher availability of oxygen in the cylinder that is ready to mix with the injected fuel.

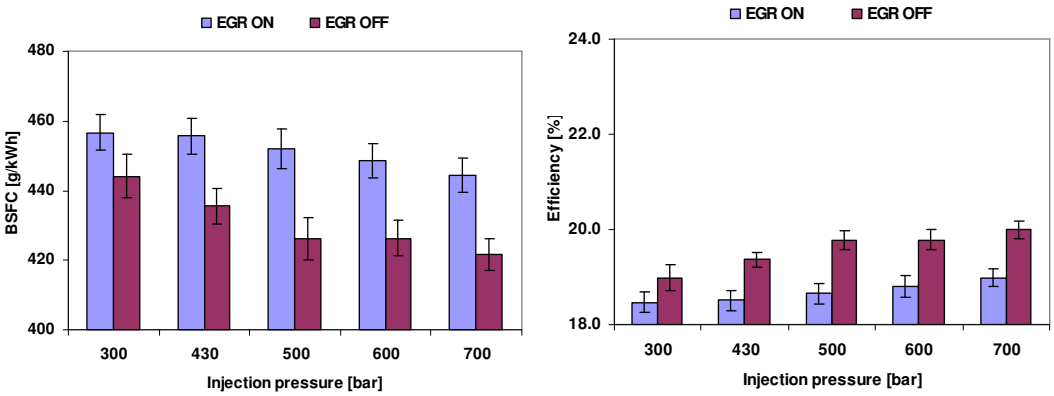

Figure 4.13. a) Brake specific fuel consumption (BSFC), b) Engine thermal efficiency for a variation of fuel injection pressures at 1500 rpm, 35.1 Nm, error bars represent 95 percent confidence.

4.3.2 Engine Emissions

Figure 4.14 shows the emissions of NO_x as a function of fuel injection pressure at 1500 rpm, 35.1 Nm with EGR ON and EGR OFF. The EGR was used to dilute the intake air resulting in longer ignition delay. This condition tends to reduce combustion temperatures that result in low NOx emissions as clearly seen from Figure 4.14.

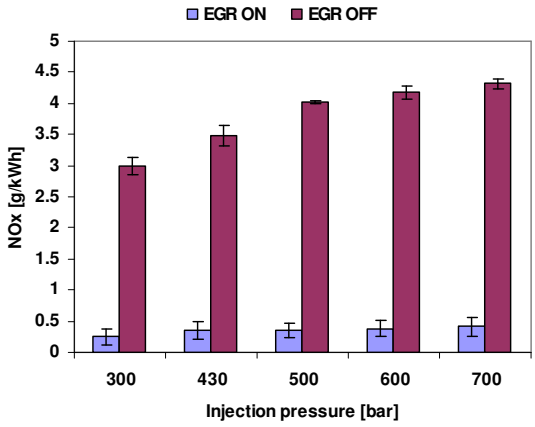

Figure 4.14. NOx emissions for a variation of fuel injection pressures at 1500 rpm, 35.1 Nm, error bars represent 95 percent confidence.

Figures 4.15 and 4.16 show the CO and THCs emissions respectively, for a variation of fuel injection pressures operating with EGR ON and EGR OFF at 1500 rpm, 35.1 Nm. The both emissions are decreased with the increase of fuel injection pressure from 300 to 700 bar for EGR ON and EGR OFF. The CO and THCs emissions are decreased when the engine operation is switched from EGR ON to the EGR OFF. This is due to less oxygen availability [49, 181] and a lower combustion temperature [182] with EGR ON that contributes to the higher CO and THCs emissions. The poor fuel distribution and less amounts of oxygen with EGR ON contributed to the higher CO and THCs emissions in the exhaust pipe as agreed by Sayin et al. [56]. Meanwhile, the lower THCs emissions with EGR OFF are due higher oxygen content resulting in a complete combustion.

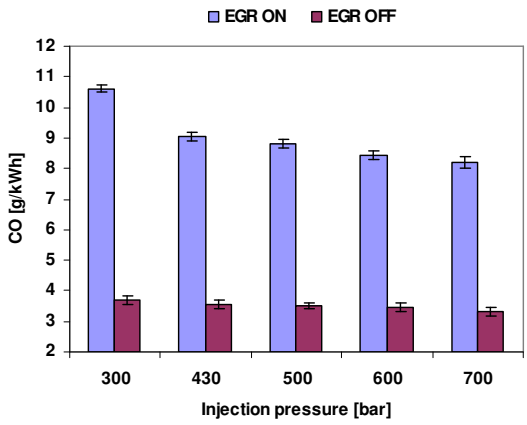

Figure 4.15. CO emissions for a variation of fuel injection pressures at 1500 rpm, 35.1 Nm, error bars represent 95 percent confidence.

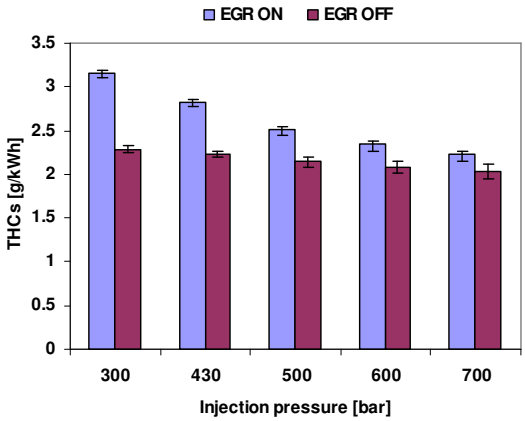

Figure 4.16. THCs emissions for a variation of fuel injection pressures at 1500 rpm, 35.1 Nm, error bars represent 95 percent confidence.

Figure 4.17 shows the smoke level for a variation of fuel injection pressures operating with EGR ON and EGR OFF at 1500 rpm, 35.1 Nm. The smoke levels are decreased by 74.6% and 63.4% with the increase of fuel injection pressure from 300 to 700 bar for EGR ON and EGR OFF respectively. As expected, the EGR ON has higher smoke level as compared to EGR OFF. This is due to high oxygen availability in EGR OFF contributes to complete mixing process resulting in low smoke level. The difference of smoke level between EGR ON and EGR OFF becomes smaller when the engine operates with high fuel injection pressure. Therefore, the higher fuel injection pressure has a promising result in smoke level even with EGR ON.

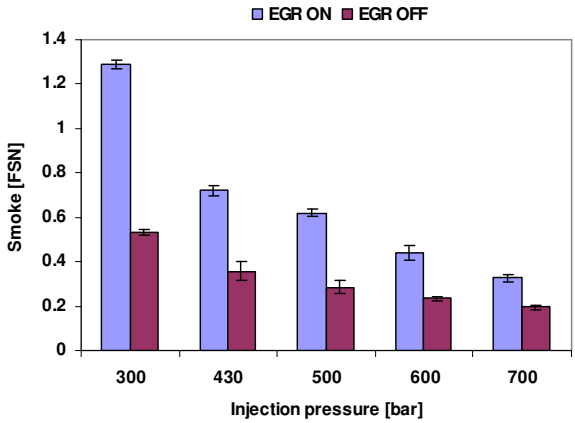

Figure 4.17. Smoke level for a variation of fuel injection pressures with EGR ON and EGR OFF, error bars represent 95 percent confidence.

Figure 4.18 shows the NO_x-smoke trade-off emissions, for a variation of fuel injection pressures operating with EGR ON and EGR OFF at 1500 rpm, 35.1 Nm. The smoke levels appeared to be higher with EGR ON while the NOx emissions decreased dramatically. However, there was a considerable decrease in smoke with the increase of fuel injection pressure from 300 to 700 bar for both EGR ON and EGR OFF. Very low levels of smoke and NO_x can be achieved at the fuel injection pressure of 700 bar when the engine is operating with EGR. Under the same fuel injection pressure, running without EGR results in higher NO_x emissions (9 times) while achieving a lower smoke number (41%). Therefore, the simultaneous reductions in smoke and NO_x could be achieved when the engine is operating with high fuel injection pressure and EGR ON.

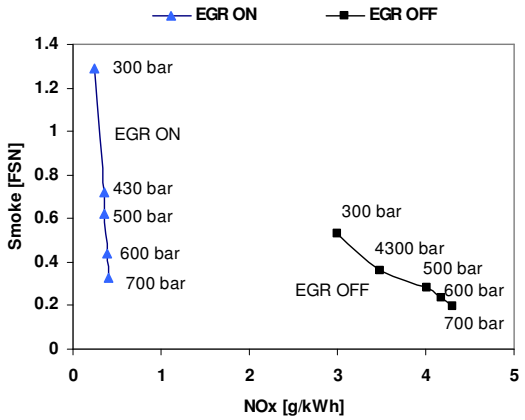

Figure 4.18. NO_x-Smoke trade-off emissions for a variation of fuel injection pressures with EGR ON and EGR OFF.

4.4 Summary

Experimental work was carried out to investigate the effect of a variation in fuel injection pressures with split (pilot and main) injection, (with and without cooled EGR) on engine performance and emissions of a modern 2.7l V6 diesel engine. The results clearly showed that increasing the fuel injection pressure from 300 to 700 bar resulted in a significant improvement in engine performance and emissions (THCs, CO and smoke) for all engine test conditions. The engine thermal efficiencies are increased from 19.0 to 20.0%, 26.1 to 27.2% and 29.2 to 30.1%, BSFC is decreased by 4.4%, 4.2% and 3.0%, smoke levels are decreased by 63.4%, 57.8% and 19.6% and NO_x emissions are increased by 44.0%, 35.0% and 37.0% with the increase of fuel injection pressure from 300 to 700 bar at 35.1 Nm, 70.2 Nm and 140.4 Nm respectively. The effect of higher fuel injection pressure is more important at the higher engine load compared with the lower loads. This is due to higher injected fuel at higher engine load that requires a longer time for a mixing process. The smaller fuel droplet size that can be produced by higher fuel injection pressure is significantly important in this case to form a complete mixing process.

The combined effect of fuel injection pressure and EGR study showed that effect of fuel injection pressure is more important in the case of EGR ON compared with EGR OFF due to higher availability of oxygen in the charge air in the EGR OFF mode. This is clearly observed from Figures 4.15, 4.16 and 4.17 that the emissions of CO, THCs and smoke were converging between EGR ON and EGR OFF at higher fuel injection pressure. In the case of less oxygen availability, the higher fuel injection pressure plays an important role in creating a better mixture formation resulting in a cleaner combustion. The smoke level, CO and THCs are decreased by 74.6%, 22.7% and 29.4% respectively with the increase of fuel injection pressure from 300 to 700 bar when engine operating with EGR ON at 1500 rpm, 35.1 Nm. Meanwhile, the smoke level, CO and THCs are decreased by 63.4%, 10.2% and 11.0% with the increase of fuel injection pressure from 300 to 700 bar when the engine is operating with EGR OFF at the same engine test condition. The BSFC is decreased by 2.7% and 5.1%, thermal efficiencies are increased from 18.5 to 19.0% and 19.0 to 20.0%, and NO_x emissions are increased by 65.0% and 44.0% with the increase of fuel injection pressure from 300 to 700 bar for EGR ON and EGR OFF respectively. The NO_x-smoke trade-off could be improved when the engine is operating with high fuel injection pressure and EGR ON.

CHAPTER 5

COMBINED EFFECT OF FUEL INJECTION PRESSURE, DWELL PERIOD (INTERVAL BETWEEN PILOT AND MAIN) AND EGR ON THE ENGINE PERFORMANCE AND EMISSIONS

This chapter presents experimental results for a diesel engine operating with ULSD at short and long dwell period (interval between pilot and main) with a variation of fuel injection pressures. The study is designed to determine the combined effects of dwell period (5 CAD and 40 CAD), fuel injection pressure and EGR modes on a modern 2.7l V6 diesel engine. The aim of this study is to induce a better mixture formation by tailoring the dwell period between pilot and main injection at a variation of fuel injection pressures. It is thought that there is potential in this method as it is known that only 80% of the intake air is effectively used in the combustion process. This is due in part to an insufficient reaction time between fuel and compressed air to form a combustible mixture [36]. The details of engine test conditions are described in Section 5.1. Sections 5.2 and 5.3 discuss the details of the effect of dwell period and engine speed on the measured engine performance and emissions respectively. The overall results are summarised in Section 5.4.

5.1 Engine Test Conditions

The present work involves with two different engine speeds at a constant engine load of 35.1 Nm. The details about the engine setting parameters were described in Chapter 3. The dwell period, EGR modes and fuel injection pressures are changed by using the INCA V5.3 software. The dwell period is changed from 5 (short dwell) to 40

CAD (long dwell) at a variation of fuel injection pressures (300 – 800 bar) in parallel with EGR modes (EGR ON and EGR OFF). The fuel injection pressure for the pilot and main injection are the same. The fuel split between the pilot and main are approximately 10:90 by mass as explained in Chapter 4. The inlet fuel temperature (35 ± 1 °C), inlet air temperature (30 ± 1 °C) and relative humidity (45-50%) were kept constant and monitored throughout the tests.

The experiment was carried out with a fixed start of main injection. The main injections are timed at 2.55 CAD and 0.70 CAD for 1500 rpm and 2250 rpm respectively. Therefore, the start of pilot injection is changed in order to make 5 CAD (later pilot injection) and 40 CAD (advanced pilot injection) of dwell period for both 1500 rpm and 2250 rpm. In the case of 1500 rpm, the SOI for the pilot are -2.45 CAD and -37.45 CAD for short dwell and long dwell, respectively. Meanwhile, in the case of 2250 rpm, the SOI for the pilot are -4.30 CAD and -39.30 CAD for short dwell and long dwell, respectively. The details about EGR rates are displayed in Tables 5.1 and 5.2 for both 1500 rpm and 2250 rpm respectively.

Table 5.1. EGR rates at1500 rpm, 35.1Nm

Fuel injection pressure (bar)	300	430	500	600	700	800
EGR OFF (%) - Short dwell	0	0	0	0	0	0
EGR OFF (%) - Long dwell	0	0	0	0	0	0
EGR ON (%) - Short dwell	51.89	51.65	52.68	52.36	49.52	49.57
EGR ON (%) - Long dwell	51.37	51.11	51.4	51.14	49.8	49.73

Table 5.2. EGR rates at 2250 rpm, 35.1Nm

Fuel injection pressure (bar)	300	430	500	600	700	800
EGR OFF (%) –Short dwell	0	0	0	0	0	0
EGR OFF (%)- Long dwell	0	0	0	0	0	0
EGR ON (%)-Short dwell	33.01	34.13	33.61	33.18	32.58	33.92
EGR ON (%)-Long dwell	32.7	32.14	31.92	31.56	31.28	31.5

5.2 The Effects of Dwell Period

Previous studies have reported that the ignition delay period depends on the quality of the combustible mixture, air temperature and the size of fuel droplets [61, 70]. As is well accepted, the timing of start of injection (SOI) for both (pilot and main) is an important parameter to control the mixing process. Early SOI leads to a homogenous charge combustion that leads to a low combustion temperatures. Meanwhile, late SOI leads to poor mixing process resulting in incomplete combustion. Therefore, the effect of dwell period (between pilot and main) is significantly important to the mixture formation resulting in lower fuel consumption and engine emissions. The exhaust gas recirculation (EGR) is an effective method of NO_x control [155, 183, 184], therefore the dwell period is also a function of to exhaust gas recirculation (EGR).

5.2.1 Engine Performance and Combustion Characteristics

Figures 5.1a and 5.1b show the rate of heat release (ROHR) and the in-cylinder pressure as a function of crank angle degree (CAD) for a variation of fuel injection pressures and dwell periods at 1500 rpm, 35.1 Nm EGR ON and EGR OFF respectively. It can be clearly seen from both figures that the peak in-cylinder pressure increases as the fuel injection pressure increases for both dwell periods. The longer dwell period of 40

CAD produced the highest peak in-cylinder pressure from all engine test conditions, due to better fuel mixing process corresponding to long ignition delay, thus promoting a complete combustion. In contrast, the shorter dwell period produces lower in-cylinder pressure due to a reduction in the premixed combustion phase, a consequence of a poor mixing process.

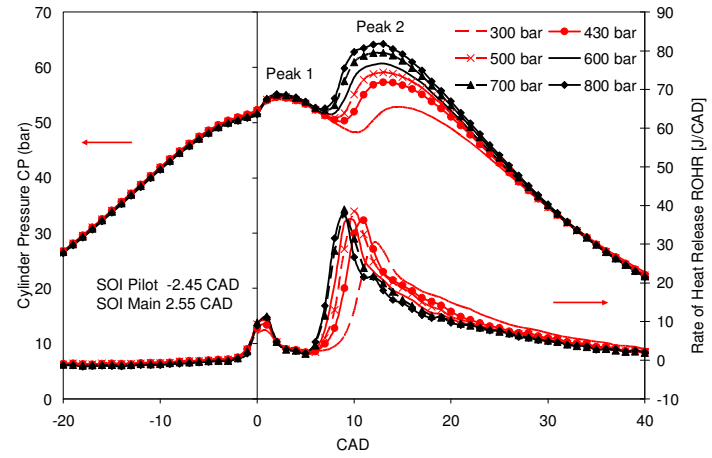

a)

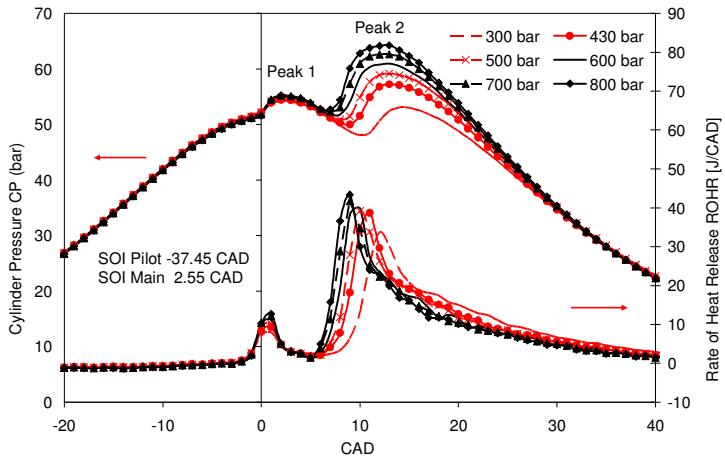

b)

Figure 5.1 The rate of heat release and in-cylinder pressure for a variation of fuel injection pressures at 1500 rpm, 35.1 Nm EGR OFF. a) Short dwell , and b) Long dwell.

Figures 5.2a and 5.2b show the peak in-cylinder pressure for a variation of fuel injection pressures and two dwell periods at 1500 rpm, 35.1 Nm for both EGR ON and EGR OFF respectively. The results show that the long dwell period produces a higher peak in-cylinder pressure when compared to the short dwell period for both EGR ON and EGR OFF. This is attributed to the longer residence time of the pilot fuel. Consequently more fuel is mixed with air and in turn, more of the fuel is burnt during premixed combustion. In contrast, the short dwell provides a limited residence time for the pilot fuel to mix with air especially at lower fuel injection pressure and EGR ON. In this study, the difference in the first peak in-cylinder pressure is very difficult to notice (Figures 5.1a and 5.1b). However, it is clearly seen in the second envelope of peak (Peak 2) in-cylinder pressure where the longer dwell period of 40 CAD produced the highest peak in-cylinder pressure.

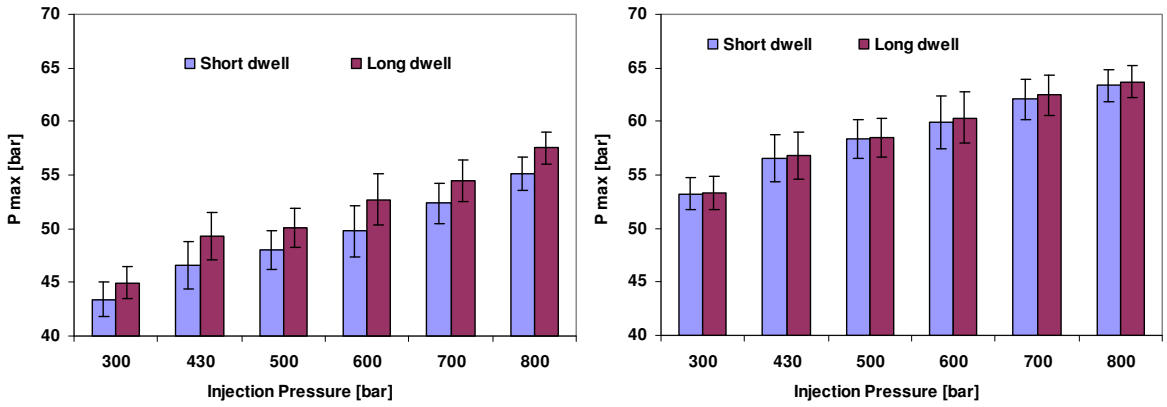

a) b)

Figure 5.2. Peak in-cylinder pressure (Peak 1) for a variation of fuel injection pressures and two dwell periods at1500 rpm, 35.1 Nm a) EGR ON, b) EGR OFF, error bars represent 95 percent confidence.

Figures 5.3a and 5.3b show the brake specific fuel consumption (BSFC) for a variation of fuel injection pressure and two dwell periods at 1500 rpm, 35.1 Nm for both EGR ON and EGR OFF respectively. The results show that the brake specific fuel consumption (BSFC) decreases with the increase of dwell period due to an improved mixing process. In addition, based on the lower CO (Figures 5.7a and 5.7b) and THCs (Figures 5.8a and 5.8b) emissions, it can be concluded that the longer dwell period gave slightly improved fuel combustion. This is strongly believed to be due to the improved mixing process as compared with the lower dwell period. In fact, the longer dwell period leads to an improvement in the combustion process and a high power output is produced due to the better fuel mixing process for almost all engine test conditions. As a result, energy release takes place closer to TDC, which increases the thermodynamic efficiency and thus reduces BSFC [61]. The shorter dwell period provides a limited time for fuel to entrain with the air. As previously mentioned, this is thought to be due to the poorer mixing process of the short dwell period which relates to the residence time of the fuel to mix with air in the combustion chamber. The overall results show that the long dwell period required less fuel as compared to the short dwell period for both EGR ON and OFF.

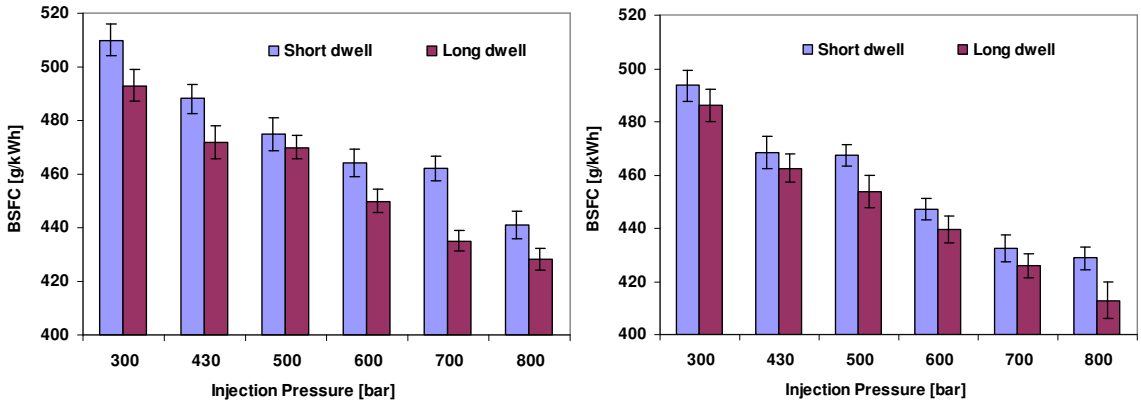

Figure 5.3. Brake specific fuel consumption (BSFC) for a variation of fuel injection pressures and two dwell periods at 1500 rpm, 35.1 Nm a) EGR ON, b) EGR OFF, error bars represent 95 percent confidence.

It is clearly observed from Figures 5.4a and 5.4b that the pilot ignition delay increased with the increase of dwell period for both EGR ON and EGR OFF, respectively. The results also show that a small variation of pilot ignition delay versus fuel injection pressure for both EGR ON and EGR OFF. Therefore, the effect of dwell period on the pilot ignition delay is more dominant than that of the EGR. The long dwell leads to the longer pilot ignition delay due to low local temperatures at that time (earlier in the compression stroke). The effect of fuel injection pressure is more significant at a condition of long dwell period with EGR ON. It seems possible that these results are due to less oxygen availability with EGR ON that required a small fuel droplet size to enhance the mixing process. In the case of EGR ON, the dwell period plays a major role in producing a better mixture due to the decreased availability of oxygen in the cylinder. Hence, it could be hypothesised that the long dwell period enhanced the combustion as the oxygen deficiency caused by EGR operation increased the dominance of the mixing process for

complete combustion. In the case of EGR OFF, the results show that the ignition delay is less sensitive to the dwell period due to higher oxygen availability.

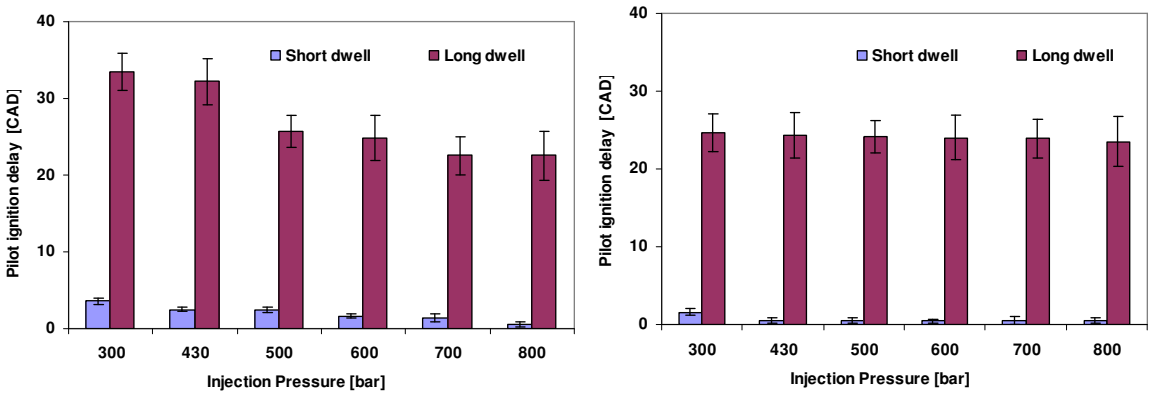

a) b)

Figure 5.4. Pilot ignition delay for a variation of fuel injection pressures and two dwell periods at 1500 rpm, 35.1 Nm a) EGR ON, b) EGR OFF, error bars represent 95 percent confidence.

Figures 5.5a and 5.5b show the engine thermal efficiency for a variation of fuel injection pressures and dwell periods at 1500 rpm, 35.1 Nm EGR ON and EGR OFF, respectively. The longer dwell period produces higher thermal efficiency than the short dwell period. The higher thermal efficiency indicates less fuel is consumed to produce the same required power output. The thermal efficiency increased with the increase of dwell period due to the complete mixing process.

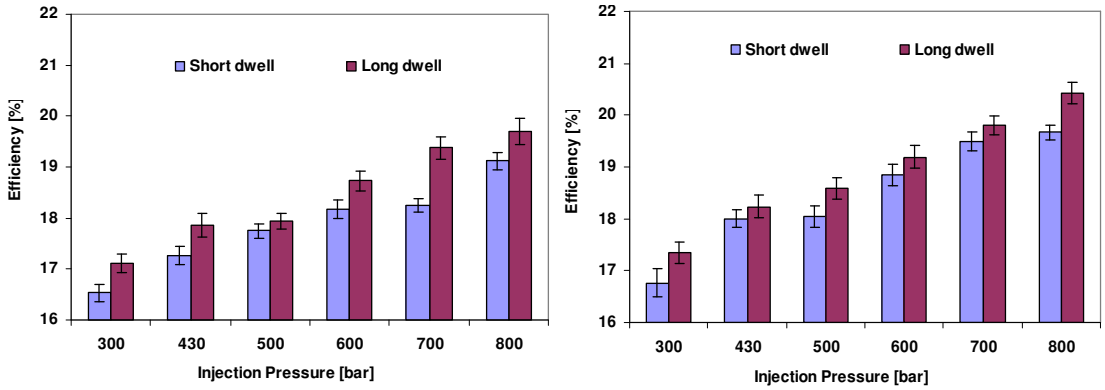

Figure 5.5. Engine thermal efficiency for a variation of fuel injection pressures and two dwell periods at 1500 rpm, 35.1 Nm a) EGR ON, b) EGR OFF, error bars represent 95 percent confidence.

5.2.2 Engine Emissions

As is seen from the Figures 5.6a and 5.6b, the emissions of NO_x slightly increased with the increase of dwell period for both EGR ON and EGR OFF respectively. This is due to longer dwell tends to introduce the higher combustion temperatures that promote NO_x formation. The results show a good agreement with many authors, that the formation of NO_x is highly influenced by the higher combustion temperatures [140, 141]. Meanwhile, the shorter dwell tends to produce lower combustion temperatures that lead to the lower level of NO_x emissions [49, 83, 181].

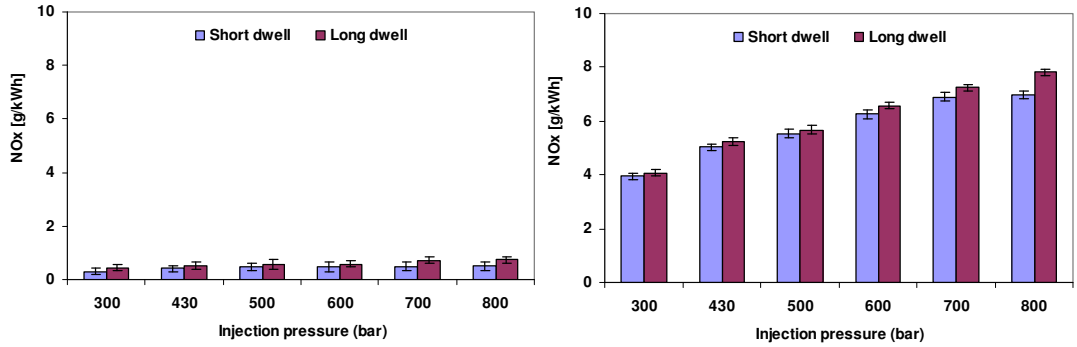

Figure 5.6. NO_x emissions for a variation of fuel injection pressures and two dwell periods at 1500 rpm, 35.1 Nm a) EGR ON, b) EGR OFF, error bars represent 95 percent confidence.

Figures 5.7a and 5.7b show the carbon monoxide emissions for a variation of fuel injection pressures and two dwell periods at 1500 rpm, 35.1 Nm EGR ON and EGR OFF respectively. As expected, CO levels are decreased when the engine is operating without EGR. The higher CO levels with EGR are due to the reduced combustion temperatures through dilution and decreased oxygen availability [34, 68, 156]. In fact, CO emissions are strongly influenced by mixing process and the Air-Fuel ratio [36]. It is observed that the CO emissions are decreased for longer dwell across the range of fuel injection pressure especially with EGR OFF. The longer dwell period leads to a complete mixing process that is favourable for CO emissions reduction. Therefore, the longer dwell produced a complete combustion resulting in low CO emissions. The overall results show that the CO emissions decrease as dwell period increases for almost all engine test conditions due to a more complete combustion at the longer dwell period and therefore, complete oxidation of CO to CO_2.

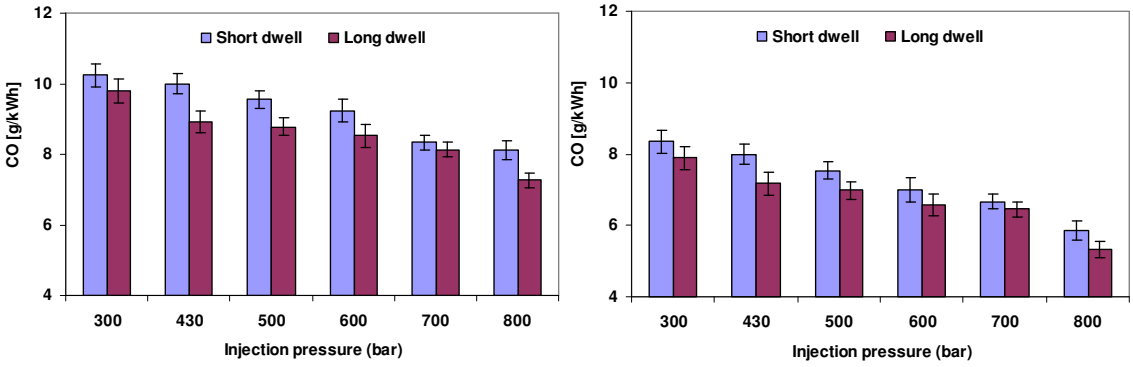

Figure 5.7. CO emissions for a variation of fuel injection pressures and two dwell periods at 1500 rpm, 35.1 Nm a) EGR ON, b) EGR OFF, error bars represent 95 percent confidence.

Figures 5.8a and 5.8b show the total hydrocarbons (THCs) emissions for a variation of fuel injection pressures and two dwell periods at 1500 rpm, 35.1 Nm EGR ON and EGR OFF respectively. The THCs emissions are emitted by the engine as a result of incomplete combustion, due in part to heavier hydrocarbons in diesel fuel [64]. It is clearly seen from Figures 5.8a and 5.8b that the THCs emissions decrease as the dwell period increases, due to more complete vaporisation process to form a more combustible mixture. Ideally, the fuel should be atomised, vaporized and mixed with air before it reaches a self-ignition temperature and the combustion process is initiated. The mixing process is highly dependent on the interaction time between fuel and air. As would be expected, the longer dwell period provides more time and therefore, improved mixing process. These results are consistent with Abd-Alla et al. [57] who found the long dwell promoted higher combustion temperatures thus lowering the THCs emissions. The reason for the low THCs with longer dwell period is may be due mainly to improved mixing, but it is thought that

perhaps higher turbulence and high combustion temperature also contribute to the more complete combustion at longer dwell [70].

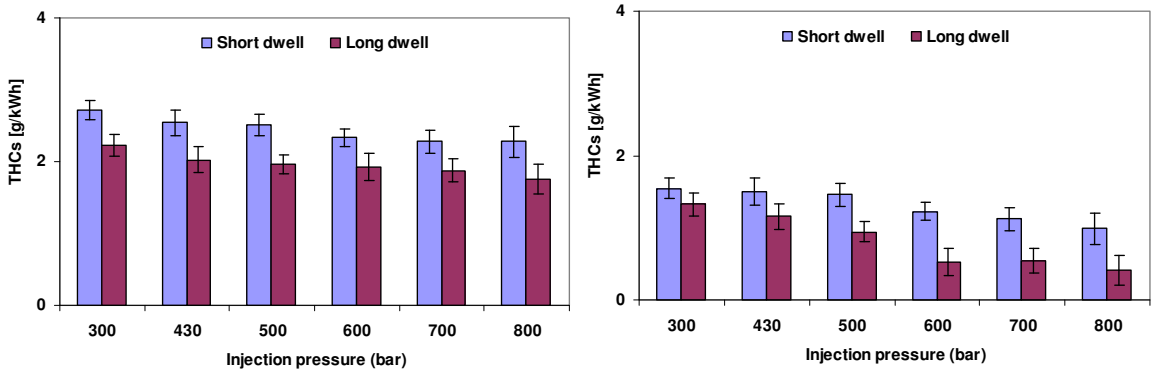

a) b)

Figure 5.8. THCs emissions for a variation of fuel injection pressures and two dwell periods at 1500 rpm, 35.1 Nm a) EGR ON, b) EGR OFF, error bars represent 95 percent confidence.

Figures 5.9a and 5.9b show the smoke level for a variation of fuel injection pressures and two dwell periods at 1500 rpm, 35.1 Nm EGR ON and EGR OFF respectively. The smoke level is decreased with the increase of dwell period for both EGR ON and EGR OFF particularly for low fuel injection pressure with EGR ON. The finding suggests that the longer dwell period can be beneficial for the smoke reduction due to better fuel mixing leading to improved combustion behaviour as suggested by many studies [36, 61, 105, 185].

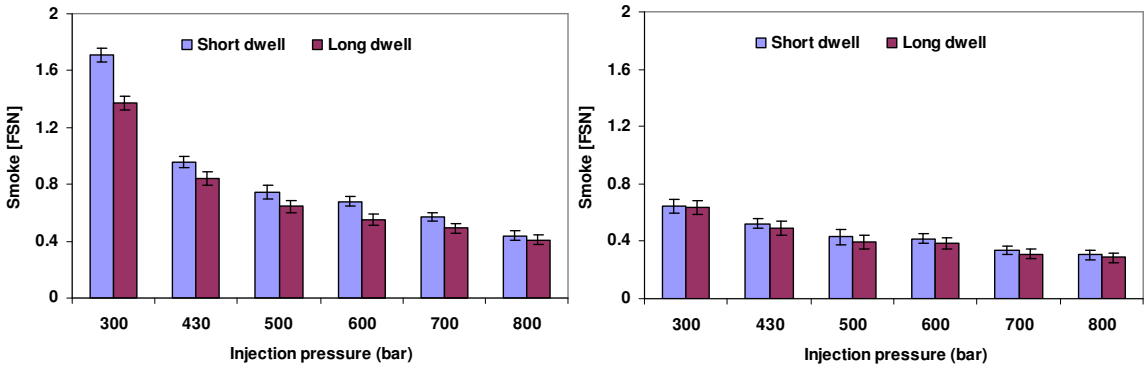

a) b)

Figure 5.9. Smoke for a variation of fuel injection pressures and two dwell periods at 1500 rpm, 35.1 Nm. a) EGR ON, b) EGR OFF, error bars represent 95 percent confidence.

Figures 5.10a and 15.10b show the NO_x-smoke trade-off emissions, for a variation of fuel injection pressures and two dwell periods at 1500 rpm, 35.1 Nm EGR ON and EGR OFF respectively. The smoke levels appeared to be lower and the NO_x emissions appeared to be higher with the increase of the injection pressure from 300 to 800 bar for all engine test conditions. Low levels of smoke and NO_x can be achieved at long dwell period when the engine is operating at the fuel injection pressure of 800 bar and EGR ON. Under the same engine conditions, dwell period and fuel injection pressure, running without EGR results in higher NO_x (approximately 9 times) while achieving a lower smoke number (41%). Therefore, the simultaneous reductions in smoke and NO_x could be achieved when the engine is operating with EGR ON, high fuel injection pressure and long dwell period.

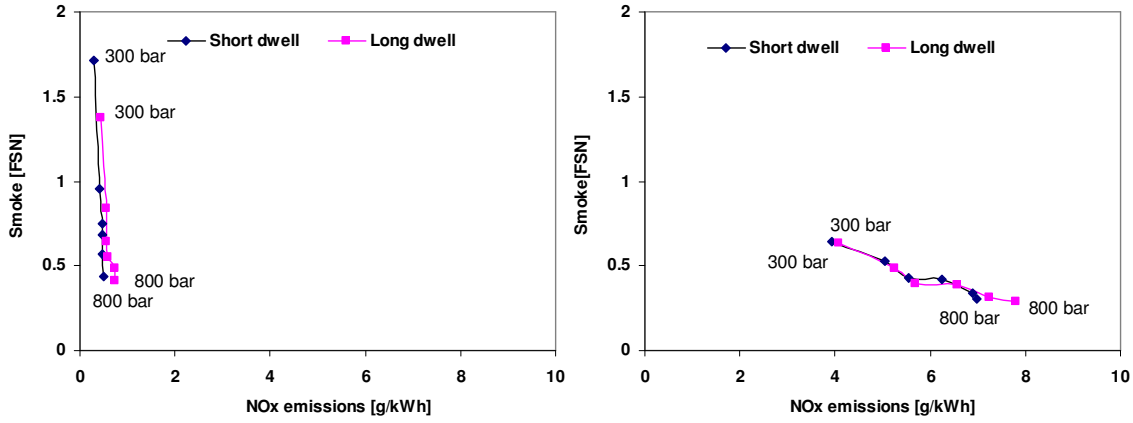

a) b)

Figure 5.10. NO_x-smoke trade-off emissions for a variation of fuel injection pressures and two dwell periods at 1500 rpm, 35.1 Nm. a) EGR ON, b) EGR OFF.

5.3 Effects of Engine Speed

In section 5.2, the overall results showed that EGR ON is favourable for NO_x reduction even when the engine is operating with high fuel injection pressure. Therefore, in this chapter the author would like to investigate the effect of dwell period with EGR ON at different engine speeds (1500 rpm and 2250 rpm) and one constant load (35.1Nm).

5.3.1 Engine Performance and Combustion Characteristics

Figures 5.11a and 5.11b show the in-cylinder pressure and rate of heat release resulting for a variation of fuel injection pressures and two dwell periods at 2250 rpm, 35.1 Nm. It is noticeable that the rate of heat release is shifted forwards to the early of expansion stroke with the longer dwell period. It is clearly seen from Figures 15.11a and 15.11b that less energy is released with the short dwell period (the area under the curve of the ROHR) suggesting that only a proportion of the fuel has been burnt and indicates poor mixing. This suggestion is reinforced on inspection of Figure 5.12 which details about the

brake specific fuel consumption (BSFC) as fuel consumption increases with the short dwell period.

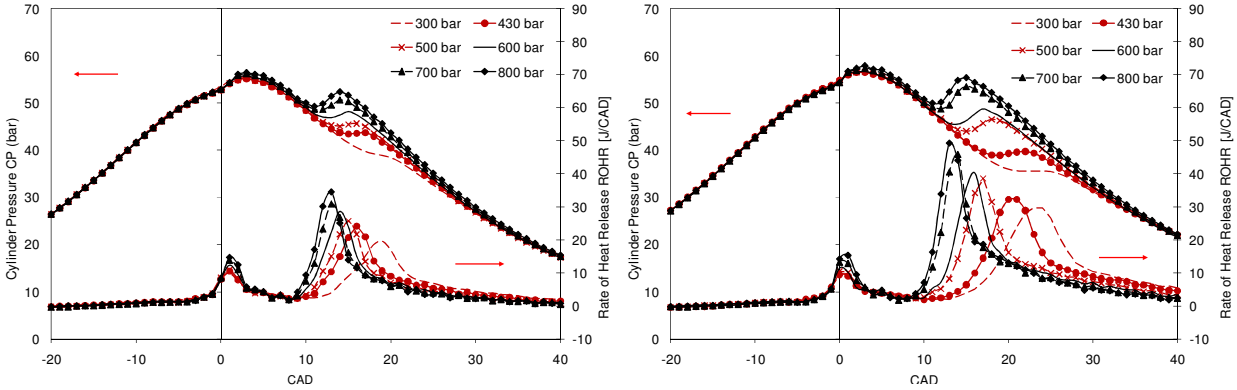

Figure 5.11. Cylinder pressure and rate of heat release for a variation of fuel injection pressures at 2250 rpm, 35.1 Nm a) short dwell, b) long dwell.

Figures 5.12a and 5.12b show the brake specific fuel consumption for a variation of fuel injection pressures and two dwell periods at 1500 rpm and 2250 rpm, respectively. The BSFC is lower at higher engine speed as compared with lower engine speed. The results are in good agreement with An et al. [2] who also found the improvement in specific fuel consumption at higher engine speed. This is due to high air motion and turbulence that is favourable in the Fuel-Air mixing and evaporation process. Therefore, the higher engine speed tends to create a better mixing process thus consuming less fuel to produce the same required power output. The higher engine speed also can provides higher combustion temperatures that lead to the complete combustion and lower heat losses. In both cases of engine speed, the results showed that the long dwell period requires less fuel as compared with the short dwell period in all fuel injection pressures.

This is particularly at higher speed as the difference at dwell period between 5 and 40 CAD is more important.

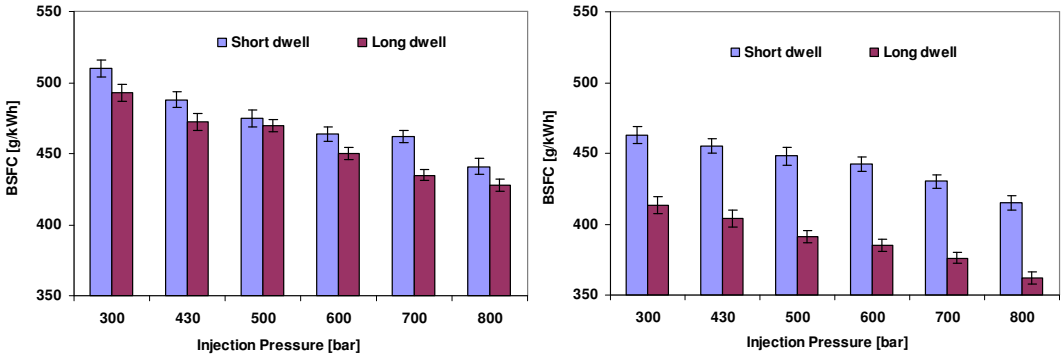

a) b)

Figure 5.12. Brake specific fuel consumption (BSFC) for a variation of fuel injection pressures and two dwell periods at, a) 1500 rpm, b) 2250 rpm, error bars represent 95 percent confidence.

Figures 5.13a and 5.13b show the thermal efficiency from a variation of fuel injection pressures and two dwell periods at 1500 rpm and 2250 rpm, respectively. The results show that the thermal efficiency increases as the engine speed increases. This is due to less heat lost to the cylinder wall during high engine speed operation. The volumetric efficiency also increases as the engine speed increases that resulting in the higher thermal efficiency due to complete combustion process.

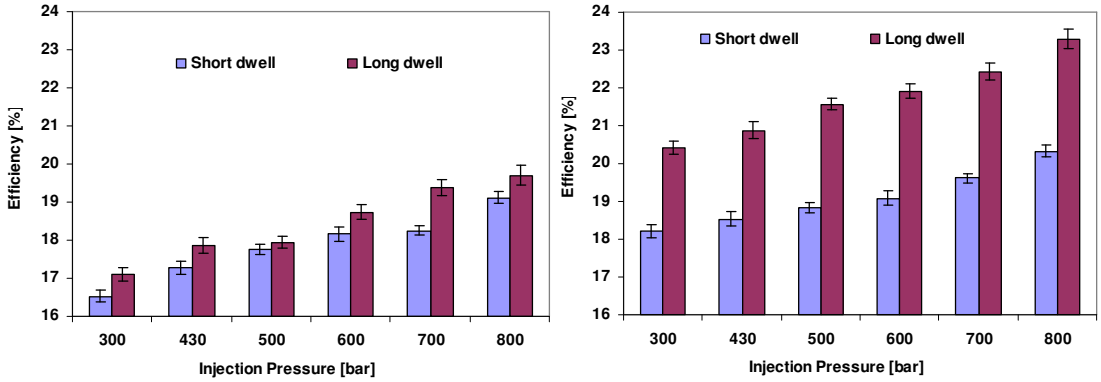

a) b)

Figure 5.13. Engine thermal efficiency for a variation of fuel injection pressures and two dwell periods at, a) 1500 rpm, b) 2250 rpm, error bars represent 95 percent confidence.

Figures 5.14a and 5.14b show the in-cylinder peak pressure for a variation of fuel injection pressures and two dwell periods at 1500 rpm and 2250 rpm, respectively. The results show that the peak pressure is less influenced by the fuel injection pressure when engine operating at higher engine speed. However, the dwell period has a significant influence on the peak pressure in both engine speeds. The effect of fuel injection pressure is less significant at higher engine speed due to high air turbulence motion that is favourable for the mixing process even at lower injection pressure.

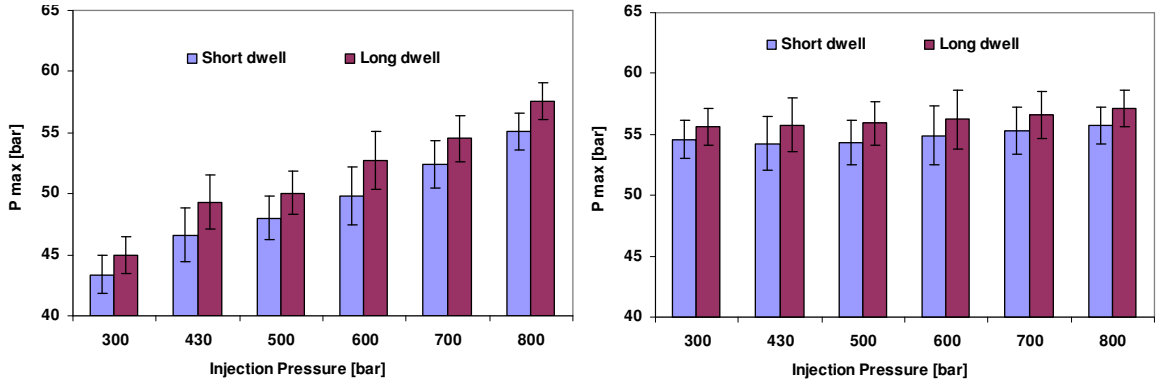

a) b)

Figure 5.14. In-cylinder peak pressure (P max) for a variation of fuel injection pressures and two dwell periods at, a) 1500 rpm, b) 2250 rpm, error bars represent 95 percent confidence.

5.3.2 Engine Emissions

Figures 5.15a and 5.15b show the NO_x emissions for a variation of fuel injection pressures and two dwell periods at 1500 rpm and 2250 rpm, respectively. As expected, the NO_x formation is higher at high engine speed as compared with low engine speed due to high combustion temperatures. The NO_x emissions increased with the increase of engine speed due to a large amount of fuel being injected during the ignition delay. The air flow also increases with the increase of engine speed. This condition is favourable to the fuel-compressed air mixing process that leads to a leaner mixture (fewer localised fuel rich regions) and complete combustion resulting in a higher level of NO_x emissions. The higher combustion temperatures at high engine speed also contribute to the improved fuel evaporation rate resulting in well mixed Fuel-Air charge.

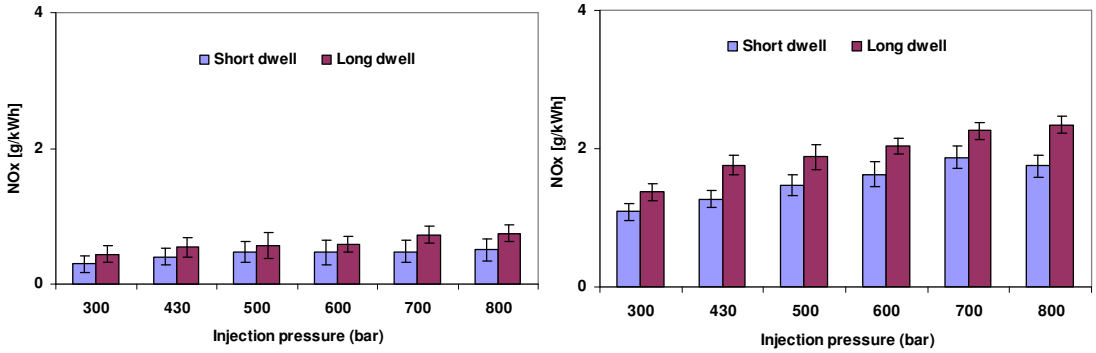

a) b)

Figure 5.15. NO_x emissions for a variation of fuel injection pressures and two dwell periods at, a) 1500 rpm, b) 2250 rpm, error bars represent 95 percent confidence.

Figures 5.16a and 5.16b show the THCs emissions for a variation of fuel injection pressures and two dwell periods at 1500 rpm and 2250 rpm, respectively. The results show that the level of THCs is decreased at high engine speed as compared with low engine speed. Similar results are obtained by Sinha and Agarwal [127]. It seems possible that these results are due to increased oxygen availability forming an improved mixture resulting in a more complete combustion [70]. On the other hand, the lower engine speed conceivably leads to the poor mixing process and low combustion temperatures resulting in higher THCs emissions level.

The reduction of THCs emissions at high engine speeds is related to the improved mixing process. At the same time, the air flow is increased with the increase of engine speed or turbulence. This enhances the fuel atomisation and evaporation to form a homogeneous mixture [151].

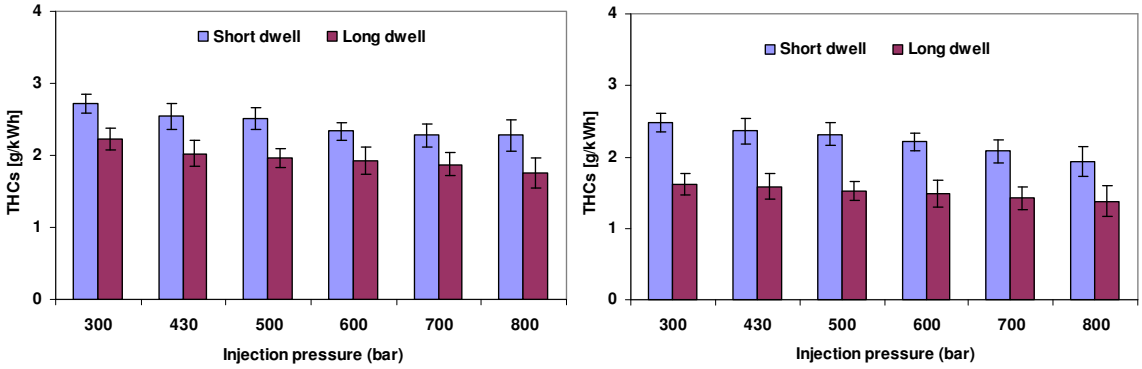

a) b)

Figure 5.16. THCs emissions for a variation of fuel injection pressures and two dwell periods at, a) 1500 rpm, b) 2250 rpm, error bars represent 95 percent confidence.

Figures 5.17a and 5.17b show the CO emissions for a variation of fuel injection pressures and two dwell periods at 1500 rpm and 2250 rpm, respectively. The results show that the CO emissions decrease as engine speed increases for both dwell periods. The higher engine speed increases the volumetric efficiency, boosting turbulence and resulting in complete combustion and high cylinder temperatures. The higher combustion temperatures lead to lower carbon monoxide emissions [56, 181, 186]. The higher CO emissions at low engine speed are due to low combustion temperatures that prevent the further oxidation of CO to CO_2 [187].

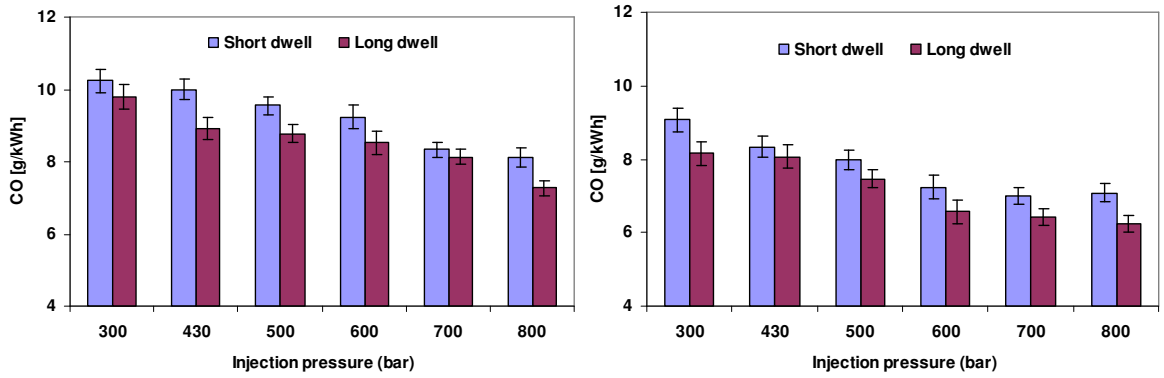

a) b)

Figure 5.17. CO emissions for a variation of fuel injection pressures and two dwell periods at, a) 1500 rpm, b) 2250 rpm, error bars represent 95 percent confidence.

Figures 5.18a and 5.18b show the smoke level for a variation of fuel injection pressures and two dwell periods at 1500 rpm and 2250 rpm, respectively. It is clearly observed from both figures that the higher engine speed produces higher levels of smoke emissions, probably due to the higher quantity of injected fuel. This leads to a reduction of the rate of soot oxidation. However, the smoke emissions are decreased with the increase of the dwell period (earlier pilot fuel injection) due to an improved mixing process and fewer fuel-rich regions that can contribute to soot formation. The effect of the dwell period on smoke emissions is more significant when the engine operates at higher speed. This is as expected and is explained by the increased quality of mixing achieved with a longer dwell period. In this case, the smoke level reduces due to better fuel atomisation leading to improved combustion behaviour. In contrast, the shorter dwell period tends to produce higher levels of smoke due to less time being available for the fuel to mix with air; this leads to less complete combustion.

A late combustion process can bring benefits the soot oxidation, resulting in low emission levels due to higher temperatures extending the combustion into the expansion

stroke. The current findings suggest that the long dwell period can be considered beneficial for smoke reduction particularly at higher engine speed. This might have potential for an optimised injection strategy incorporating higher EGR rates (e.g. >60% EGR) to reduce both smoke and NO_x emissions simultaneously.

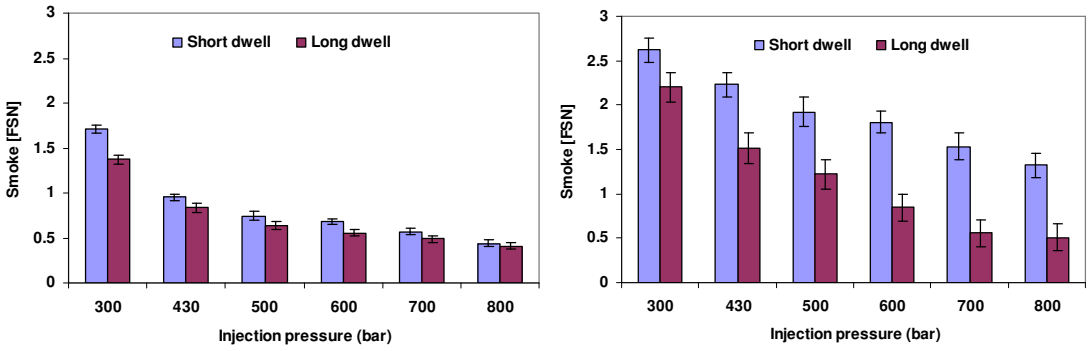

a) b)

Figure 5.18. Smoke level for a variation of fuel injection pressures and two dwell periods at, a) 1500 rpm, b) 2250 rpm, error bars represent 95 percent confidence.

Figures 5.19a and 5.19b show the NO_x-smoke trade-off emissions, for a variation of fuel injection pressures and two dwell periods at 1500 rpm and 2250 rpm, respectively. The smoke levels appeared to be lower and the NO_x emissions appeared to be higher with the increase of the injection pressure from 300 to 800 bar for both dwell periods. Low levels of smoke and NO_x can be achieved at long dwell periods when the engine is operating at a fuel injection pressure of 800 bar and a engine speed of 1500 rpm. Under the same fuel injection pressure and dwell period, running at 2250 rpm results in higher NO_x (approximately 2 times) while achieving a similar smoke number. Therefore, a different engine test condition (i.e. engine speed) required a different injection strategy to control NO_x-smoke trade-off emissions.

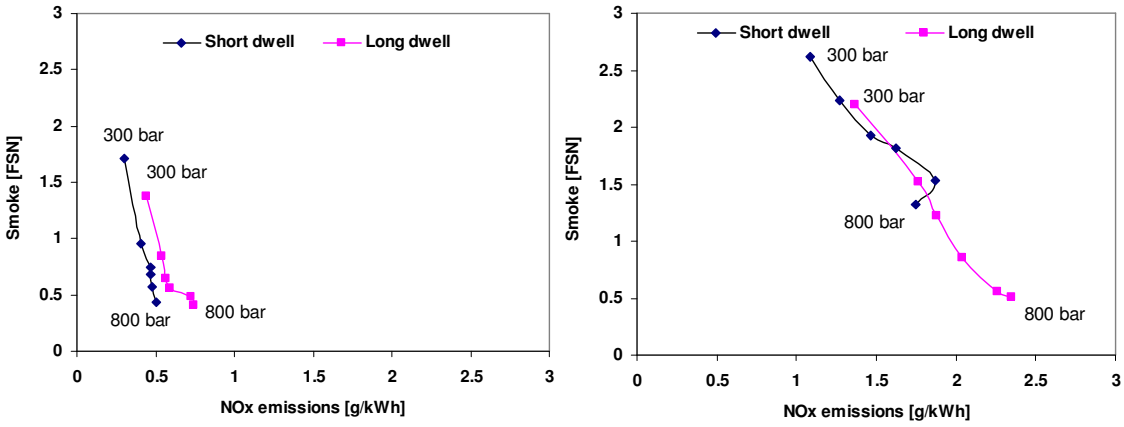

a) b)

Figure 5.19. NO_x-smoke trade-off emissions for a variation of fuel injection pressures and two dwell periods at, a) 1500 rpm, b) 2250 rpm.

5.4 Summary

Experimental work was carried out to evaluate the combined effect of fuel injection pressure, dwell period and EGR modes on the engine performance and emissions of a modern 2.7l V6 diesel engine. This study shows that the long dwell produces higher peak in-cylinder pressure and better fuel economy as compared with the short dwell for both EGR ON and EGR OFF. In the case of EGR ON (49-52% EGR) at 1500 rpm, 35.1 Nm, by increasing the fuel injection pressure from 300 to 800 bar, engine thermal efficiency increased from 16.5 to 19.1% and 17.1 to 19.7%, BSFC decreased by 13.5% and 13.2%, smoke level decreased by 74.3% and 70.1% and NO_x emissions increased by 69.6% and 68.0%, respectively for a short (5CAD) and a long (40CAD) dwell period. Meanwhile, when the engine is operating without EGR at the same engine load condition, the engine thermal efficiency increased from 16.8 to 19.7% and 17.3 to 20.4%, BSFC decreased by 14.8% and 15.1%, smoke level decreased by 52.6% and 55.0% and NOx emissions

increased by 77.5% and 91.8% with the increase of injection pressure from 300 to 800 bar for a short (5 CAD) and a long (40 CAD) dwell period respectively. The long dwell provides a longer residence time for the pilot fuel to mix, resulting in more fuel ready to burn during premixed combustion phase, thus resulting in higher in-cylinder pressure due to the combustion of the pilot injection. It is also shown that the longer dwell produced higher exhaust temperature as compared with the shorter dwell. The long dwell shows better engine emissions except for NO_x emissions. The longer dwell period improved the mixing process particularly when the engine operated with EGR ON.

In the study of the effects of engine speed the results clearly showed that increasing the engine speed resulted in a significant improvement in engine performance and emissions for almost all engine test conditions. In the case of 1500 rpm, the BSFC is decreased with the increase of fuel injection pressure from 300 to 800 bar by 13.5% and 13.2%, engine thermal efficiencies are increased from 16.5 to 19.1% and 17.1 to 19.7%, smoke levels are decreased by 74.3% and 70.1% and NO_x emissions are increased by 69.6% and 68.0% at short and long dwell period respectively. Meanwhile, at 2250 rpm, the BSFC is decreased with the increase of fuel injection pressure from 300 to 800 bar by 10.4% and 12.4%, thermal efficiency increased from 18.2 to 20.3% and 20.4 to 23.2%, smoke levels are decreased by 49.6% and 67.7% and NOx emissions are increased by 61.0% and 71.1% at short and long dwell period respectively. It can therefore be concluded that the higher engine speed operating with the longer dwell period can be considered to provide an enhanced fuel-air mixing process, resulting in lower exhaust emissions and fuel consumption.

In the above cases, the emissions of NO_x are higher with the increase of dwell period and engine speed but improving with EGR ON. Meanwhile, smoke level is higher

with the increase of engine speed and EGR ON but improving with the longer dwell period and high injection pressure. Therefore, the combination of higher fuel injection pressure, longer dwell and EGR ON might have potential for a simultaneous reduction of both smoke and NO_x emissions.

CHAPTER 6

COMBINED EFFECTS OF PILOT FUEL QUANTITY, FUEL INJECTION PRESSURE AND DWELL TIMING ON THE ENGINE PERFORMANCE AND EMISSIONS

This chapter presents a study on the influence of the pilot fuel quantity, fuel injection pressure and pilot fuel injection timing on the engine performance and emissions. All test conditions were carried out with the engine operation on ULSD fuel and EGR ON since the previous results from Chapters 4 and 5 showed that EGR ON is effective for the NO_x reduction in any combustion strategy. The summary of the chapter is presented in Section 6.3.

6.1 The Combined Effects of Pilot Fuel Quantity and Fuel Injection Pressure

In this study, the objective is to introduce a better air/fuel mixing process through a variation of pilot fuel quantities at low and high fuel injection pressures. Optimum combustion phasing and improved mixing process while EGR is employed can lead to lower combustion temperatures and improved smoke and NOx emissions.

The tests are carried out at five different pilot fuel quantities 0.8, 1.5, 2.0, 2.5 and 3.0 mg/stroke with a fixed dwell period (5 CAD) between pilot and main injection timing at two different fuel injection pressures 250 bar and 800 bar. In this case, the pilot fuel quantity was changed from 0.8 to 3.0 mg/stroke, while the main fuel quantity was controlled by the EMS in order to meet the required power output. The start of injection (SOI) of pilot fuel was timed at -2.43 CAD and the SOI of main fuel was timed at 2.57. The fuel injection pressures are similar for both pilot and main injection. The selected

engine speed and load are 1500 rpm and 30 Nm respectively. The injection timing (pilot and main), engine speed and load were all kept constant throughout the experiment. The EGR rates for each condition are shown in Table 6.1. The inlet fuel temperature (35 ± 1 °C), inlet air temperature (30 ± 1 °C) and relative humidity (45-50%) were kept constant and monitored throughout the tests.

Table 6.1. EGR rates at different fuel injection pressures

Pilot fuel quantity (mg/stroke)	0.8	1.5	2.0	2.5	3.0
250 bar - EGR ON (%)	42.26	41.99	40.81	37.28	39.06
800 bar- EGR ON (%)	39.62	40.69	41.13	40.61	41.79

6.1.1 Engine Performance and Combustion Characteristics

Figures 6.1a and 6.1b show the in-cylinder pressure and Figure 6.1c and 6.1d show the rate of heat release (ROHR) as a function of crank angle degree (CAD) for the different pilot fuel quantities at 250 bar and 800 bar fuel injection pressures. Increased pilot fuel quantity advances the combustion, leading to higher in-cylinder peak pressure and rates of the pressure rise for both fuel injection pressures (Figures 6.1a and 6.1b).

The influence of the pilot fuel quantity is less sensitive at higher fuel injection pressure due to the fast evaporation process resulting in good mixture quality. The fuel evaporation rate can be seen from the rate of heat release (Figures 6.1c and 6.1d). The lower fuel injection pressure shows a slower combustion process as compared with the higher fuel injection pressure. The longer ignition delay also related to the low local temperatures and pressures. The rate of evaporation is higher with the higher fuel injection pressure. The ROHR curve dropped to the negative values as the main fuel injection evaporated. In the case of 250 bar, the ROHR curve dropped to almost zero value during

evaporation. This is strongly believed to be due to the small amount of heat absorbed from pilot combustion to evaporate the main fuel injection. This is the reason why the ROHR from pilot fuel injection in both cases almost disappears.

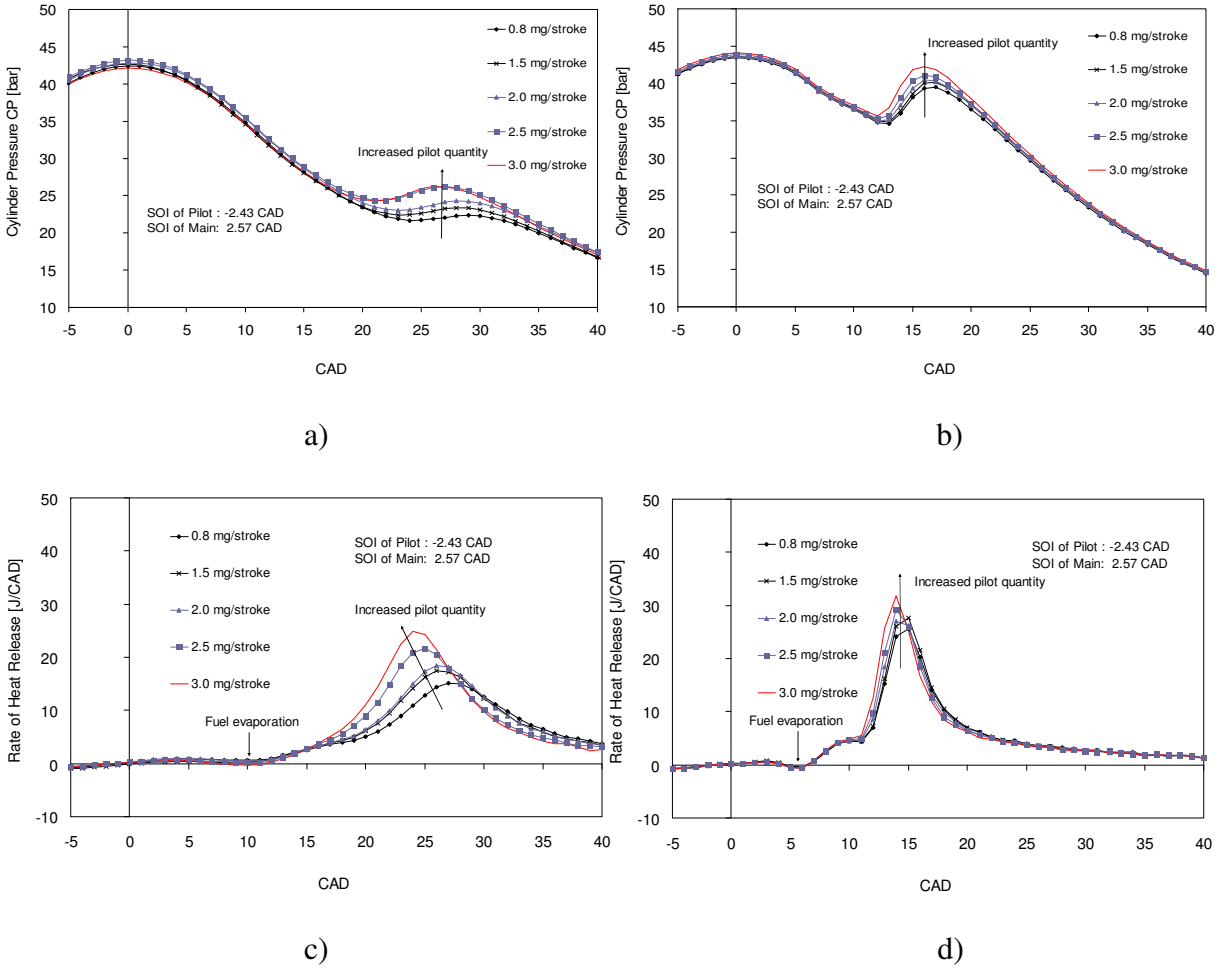

Figure 6.1. The in-cylinder pressure and rate of heat release as a function of crank angle degree (CAD) for a variation of pilot fuel quantities a) In-cylinder pressure 250 bar, b) In-cylinder pressure 800 bar, c) ROHR 250 bar and d) ROHR 800 bar.

In all engine test conditions the BSFC increases as the pilot fuel quantity increases due to the poor mixing process as shown in Figure 6.2. The dwell period is 5 CAD (short period), therefore the pilot fuel has a limited time to combust before the main fuel injection

takes place. In the case of low fuel injection pressure, the higher BSFC is due to the poor mixing process resulting in longer main ignition delay and slower combustion. The slower combustion from the lower fuel injection pressure leads to the pressure rise at the middle of the expansion stroke. This leads to high fuel consumption due to loss of the work available and fuel impingement [77]. In fact, the lowest fuel consumption can be achieved if all the injected fuel burned quickly near to TDC [68]. While in the case of high fuel injection pressure, the main ignition delay is shorter and the evaporation rate is fast. Therefore, the heat absorbed by the main injection was delayed in the pilot combustion and both fuels combusted together resulting in rapid and higher combustion temperatures.

The overall results show that the lower pilot fuel quantity with the higher fuel injection pressure leads to the improved fuel economy. These combinations tend to produce higher power output due to better fuel distribution and heat utilisation as agreed by Dhananjaya et al. [64]. The pilot fuel injection contributes to the shorter main ignition delay [8, 72]. As a result, more complete combustion leads to lower fuel consumption.

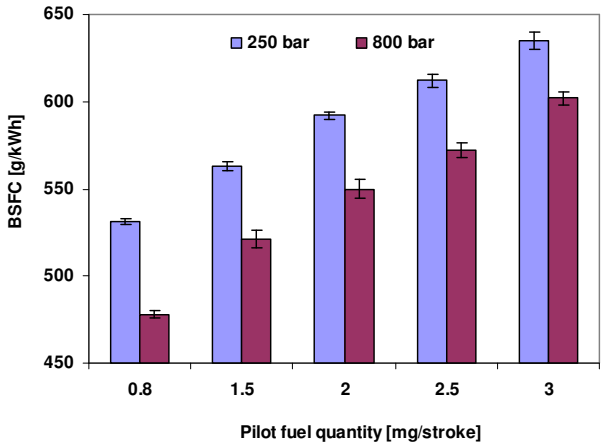

Figure 6.2. Brake specific fuel consumption (BSFC) as a function of pilot fuel quantity for different fuel injection pressures (250 bar and 800 bar), error bars represent 95 percent confidence.

The engine thermal efficiency is decreased with the increase of pilot fuel quantity in both cases of low and high fuel injection pressures (Figure 6.3). This is related to the incomplete combustion from the higher pilot fuel quantity at short dwell period.

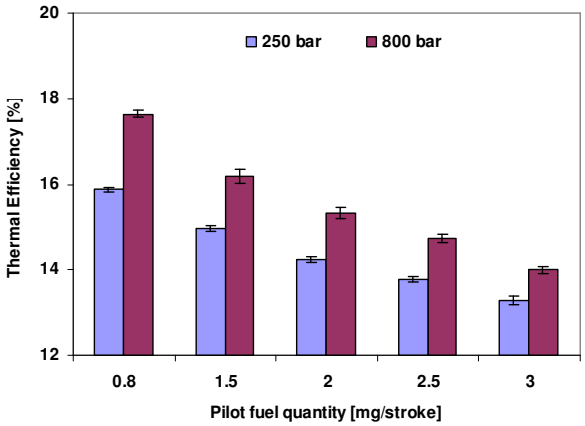

Figure 6.3. Engine thermal efficiency as a function of pilot fuel quantity at different fuel injection pressures (250 bar and 800 bar), error bars represent 95 percent confidence.

6.1.2 Engine Emissions

The results from Figure 6.4 show that the NO_x emissions were initially decreased but as the pilot fuel quantity was further increased the NO_x emissions were sharply rose for both fuel injection pressures. The higher pilot fuel quantity increases the in-cylinder pressure and rapid combustion resulting in higher NO_x formation [2, 36, 74, 142, 175]. Meanwhile, the longer dwell period between the two injections allows combustion to occur at different times resulting in lower NO_x emissions [78, 98, 188, 189]. A study by Montgomery and Reitz [77] shows that the emissions of NO_x can be controlled by limiting the amount of fuel burnt in the premixed combustion phase.

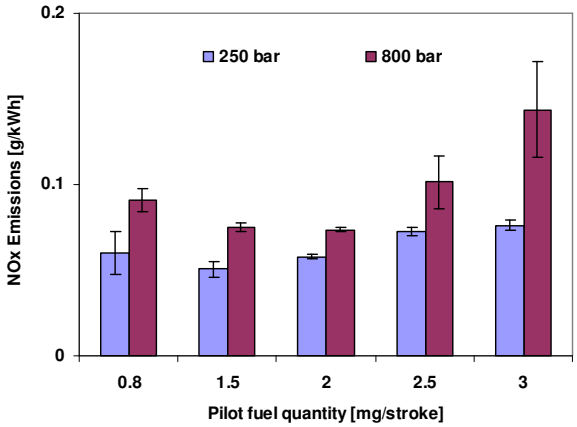

Figure 6.4. NO_x emissions as a function of pilot fuel quantity at different fuel injection pressures (250 bar and 800 bar), error bars represent 95 percent confidence.

Figure 6.5 depicts the behaviour of carbon monoxide (CO) emissions for a variation of pilot fuel quantities at different fuel injection pressures. In the lower fuel injection pressure, increasing pilot fuel quantity from 0.8 to 1.5 mg/stroke increases the CO emissions, and the CO emissions start rising again as the pilot fuel quantity is further increased from 2.5 to 3.0 mg/stroke. In between, the CO emissions are decreased with the increase of pilot fuel quantity from 1.5 to 2.5 mg/stroke. In the case of high fuel injection pressure, the CO emissions are decreased with the increase of pilot fuel quantity from 0.8 to 2.5 mg/stroke. However, the CO emissions are increased with the further increased of pilot fuel quantity from 2.5 to 3.0 mg/stroke. The 2.5 mg/stroke of pilot fuel quantity with the higher fuel injection pressure produced the lowest CO emissions due to the better mixing process. This is due to more complete combustion at the higher fuel injection pressure resulting in high oxidation rate of CO to CO_2 since the CO emissions are greatly dependent on the Fuel-Air ratio [36].

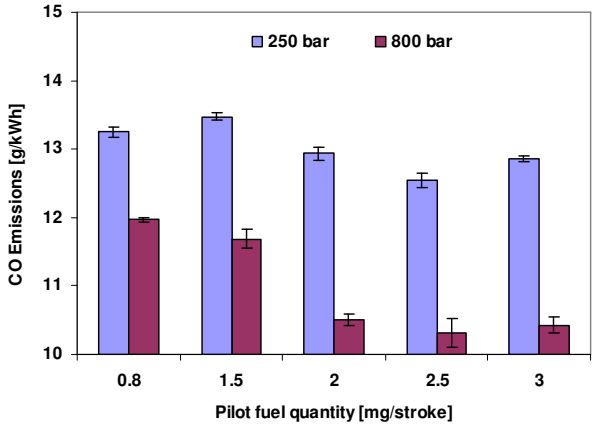

Figure 6.5. CO emissions as a function of pilot fuel quantity at different fuel injection pressures (250 bar and 800 bar), error bars represent 95 percent confidence.

Figure 6.6 shows the total hydrocarbons (THCs) emissions from the engine operating with different pilot fuel quantities. The THCs emissions are increased by 12.2 % and 27.3 % with the increase of pilot fuel quantity from 0.8 to 3.0 mg/stroke at 250 bar and 800 bar of fuel injection pressure, respectively. The high THCs are also related to the slow oxidation of the fuel adhered on the walls [85]. The effects on increased THCs emissions have been reported by other researchers [147, 148] and are due to the lean or rich mixture regions and low combustion temperatures. The higher fuel injection pressure produced improved spray atomisation to initiate and enhance the initial combustion resulting in a rapid rise in the cylinder pressure thus producing less THCs emissions [69, 142]. The poor fuel distribution at higher pilot fuel quantity contributed to the higher THCs emissions in the exhaust pipe [56]. Therefore, the injection strategy with the smaller pilot fuel quantity and higher fuel injection pressure improved the THCs emissions. In fact, the appropriate combination of pilot fuel quantity with a dwell period is an important parameter that needs to be controlled in order to mitigate THCs emissions.

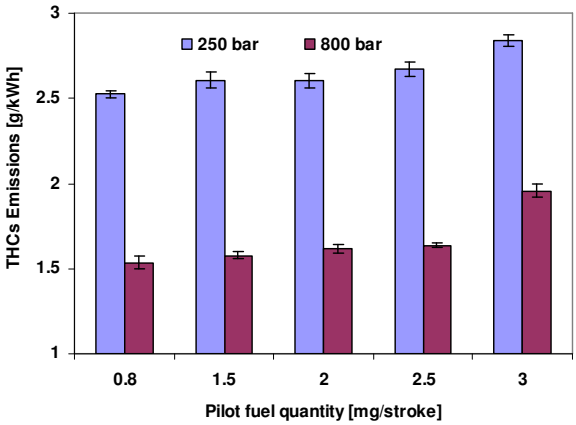

Figure 6.6. THCs emissions as a function of pilot fuel quantity at different fuel injection pressures (250 bar and 800 bar), error bars represent 95 percent confidence.

The variation of smoke is relative to the variation of the pilot fuel quantities as shown in Figure 6.7. The smoke levels are increased by 24.4% and 25.2% with the increase of pilot fuel quantity from 0.8 to 3.0 mg/stroke at 250 bar and 800 bar of fuel injection pressure, respectively. The increased pilot fuel quantity from 0.8 to 3.0 mg/stroke resulted in increased smoke levels is agreement with results reported by Carlucci et al. [73] and Badami et al.[190]. The higher pilot fuel quantity results in high soot formation which are not oxidised during the main combustion [84, 176]. The higher fuel injection pressure reduces the smoke level as fuel atomisation and the mixing process are improved. The higher combustion temperatures from the complete combustion are favourable for soot oxidation [97]. These findings suggest that the lower pilot fuel quantity with higher fuel injection pressure can be considered as a smoke reduction with a short dwell period. Alternatively, the research work by Horibe et al. [98] found that the fuel injection timing should be matched with the fuel injection quantity for cleaner combustion and lower emissions. The higher pilot fuel quantity can reduce the smoke level if the engine operates with the higher boost pressure [77].

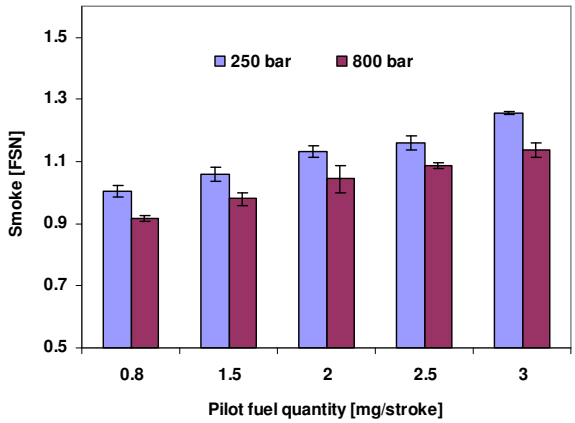

Figure 6.7. Smoke level as a function of pilot fuel quantity at different fuel injection pressures (250 bar and 800 bar), error bars represent 95 percent confidence.

Figure 6.8 shows the NO_x-smoke trade-off emissions, for a variation of pilot fuel quantities and two different fuel injection pressures. The smoke levels and NO_x emissions appeared to be higher with the increase of the pilot fuel quantity for both fuel injection pressures. Low levels of smoke and NO_x can be achieved at the pilot fuel quantity of 0.8 mg/stroke when the engine is operating with the fuel injection pressure of 800 bar. Under the same pilot fuel quantity, running with the fuel injection pressure of 250 bar results in slightly higher smoke (8.8%) and lower NO_x (90%). Therefore, the simultaneous reductions in smoke and NO_x could be achieved when the engine is operating with low pilot fuel quantity and high fuel injection pressure.

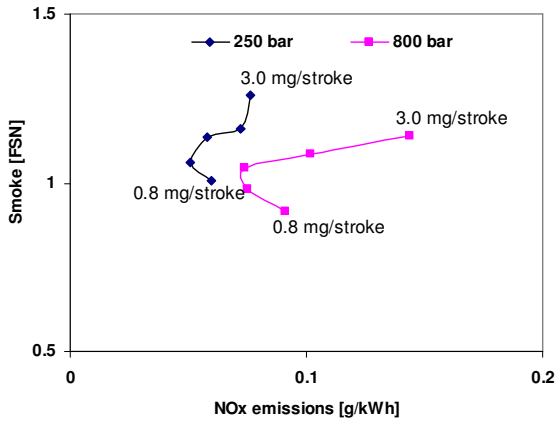

Figure 6.8. NO_x-smoke trade-off emissions for a variation of pilot fuel quantities with two different fuel injection pressures.

6.2 Effects of Pilot Fuel Injection Timing

In the present study, the variations of pilot fuel injection timings are carried out in order to investigate their effects on the main combustion behaviour and emissions. The pilot fuel injection has potential to control the pressure rise during the main combustion through a shorter main ignition delay. This experiment is carried out at a constant fuel injection pressure of 520 bar for both pilot and main fuel injections. The experimental works used a small amount of pilot fuel quantity due to the large amount of pilot tending to increase the NOx emissions due to a higher rate of heat release [74]. The fuel ratio between the pilot and main injection is approximately 10:90 by mass.

These experiments consists of three different regions of pilot fuel injection timing (early, middle and late) at two different engine loads (30 Nm, 55 Nm) operating with a constant engine speed of 2000 rpm with EGR ON. The start of main fuel injection was timed at 1.4 CAD throughout all the test conditions. The EGR rates for each engine condition are displayed in Table 6.2.

Table 6.2. The EGR rates at a variation of SOI of pilot fuel injection for both engine loads

SOI of pilot (CAD)	30 Nm - EGR Rates (%)	55 Nm – EGR Rates (%)
-9	45.48	33.95
-12	46.68	34.20
-15	44.20	36.5
-19	49.14	38.59
-21	49.81	38.52
-24	48.15	38.71
-27	48.44	37.68
-30	48.03	37.15

6.2.1 Engine Performance and Combustion Characteristics

Advancing pilot fuel injection timing while maintaining constant timing of the main fuel injection increases the peak in-cylinder pressure for both engine loads (Figure 6.9). Advancing pilot fuel injection produces a longer pilot ignition delay resulting in an intermediate main ignition delay. A shorter ignition delay for main injection provides a suitable time for fuel and air mixed to form a combustible mixture [191]. Early pilot fuel injection timing (-30 CAD) produces higher peak in-cylinder pressure. Retarding pilot fuel injection timing from -30 to -27, -24 and -21 CAD reduces the in-cylinder peak pressure, before the peak pressure starts rising again as the pilot fuel injection timing was further retarded to -19, -15, -12 and -9 CAD. The latter of pilot fuel injection (-9 CAD) produces similar results. However, the middle pilot fuel injection timing (-19 CAD) produces lower peak in-cylinder pressure due to poor combustion related to the main ignition delay. The middle pilot fuel injection timing generates longer main ignition delay that contributes to the over lean mixture. The lowest in-cylinder pressure is achieved approximately at -19 CAD for both engine loads. This value indicates that the mixture was burned incompletely due to over lean mixture and late start of combustion (SOC).

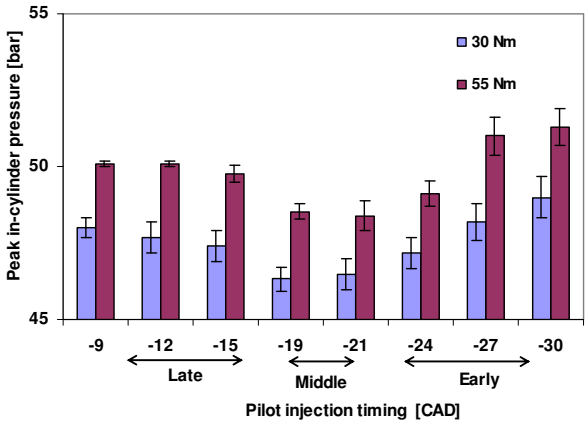

Figure 6.9. The variation of peak in-cylinder pressure as a function of pilot fuel injection timings (-9 to -30 CAD) at two different engine loads (30 Nm and 55 Nm) and constant engine speed 2000 rpm, error bars represent 95 percent confidence.

Figure 6.10 presents the in-cylinder pressure values at 1.4 CAD at a variation of pilot fuel injection timings. The purpose here is to look at the pressure and temperatures during the start of main injection timing. As mentioned earlier, the start of main injection was timed at 1.4 CAD throughout all the test conditions. The pressures and temperatures are greatly influential on the ignition delay [12]. The results show that the early pilot fuel injection produces slightly lower pressure as compared to the late injection. The late pilot fuel injection produces highest pressure at 1.4 CAD in both cases 30 and 55 Nm. This is strongly believed to be due to high pressure rise by late pilot fuel injection as a consequence of a short pilot ignition delay. The shorter ignition delay leads to produce a high pressure rise at early expansion stroke resulting in higher in-cylinder peak pressure [192]. Therefore, the late pilot fuel injection has a potential to reduce the main ignition delay. Whereas, the middle of the pilot fuel injection has a potential to extend the main injection delay due to low local temperatures.

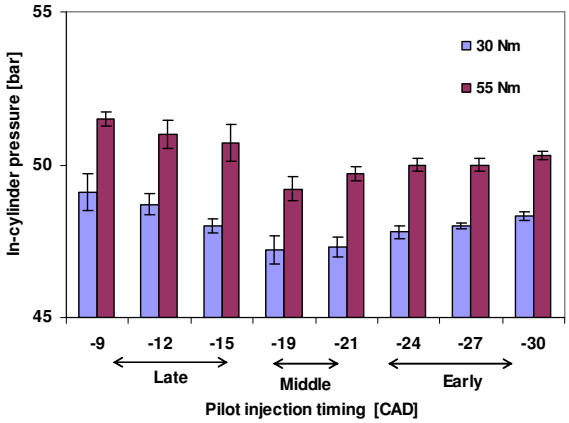

Figure 6.10. The variation of in-cylinder pressure at 1.4 CAD as a function of pilot fuel injection timings (-9 to -30 CAD) at two different engine loads (30 Nm and 55 Nm) and constant engine speed 2000 rpm, error bars represent 95 percent confidence.

Figure 6.11 presents the main ignition delay behaviours at a range of pilot fuel injection timings. The delay period is noted to be influenced by the engine load and the local temperature. The longer ignition delay tends to produce a slower combustion that gives a reduction in peak in-cylinder pressure [193] and is better for NO_x emissions. However, in other conditions the longer ignition delay induced a higher pressure rise resulting in high NO_x emissions and engine knocking due to more fuel burnt at the same time. The intermediate ignition delay gives a positive influence to the combustion behaviour in both cases premixed and diffusion flame combustion. The results showed that the shorter main ignition delay from the early and late of pilot fuel injection timing is consistent with the findings by Nwafor et al. [193].

The longer ignition delay is a consequence of the poor fuel evaporation due to large fuel droplet size and low local temperatures [194]. The late pilot fuel injection timing produced higher in-cylinder pressure thus producing a shorter main ignition delay. Whereas, the middle pilot fuel injection generated lower in-cylinder pressure and produced

longer main ignition delay. It is clearly seen that the early pilot fuel injection produces intermediate main ignition delay. This is due to the early pilot fuel injection producing less in-cylinder pressure at the start of main fuel injection as compared to the late pilot fuel injection.

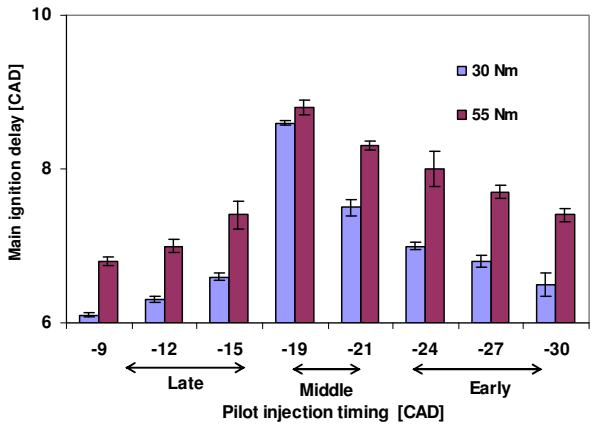

Figure 6.11. The variation main ignition delay as a function of pilot fuel injection timings (-9 to -30 CAD) at two different engine loads (30 Nm and 55 Nm) and constant engine speed 2000 rpm, error bars represent 95 percent confidence.

Figure 6.12 shows that the brake specific fuel consumption is improved by late (-9, -12 and -15 CAD) and early pilot (-24, -27, -30 CAD) injection timing when compared to middle, at both engine loads. This is due to a more combustion with early and late pilot fuel injection timing. The middle pilot fuel injection timing consumed higher fuel due to longer main ignition delay. The long ignition tends to produce incomplete combustion due to over lean. The injected fuel probably was stuck onto the cylinder wall before the combustion occurred. The early pilot fuel injection timing is better for the brake specific fuel consumption due to enough reaction time between fuel-air to produce a complete combustion. However, this is depending on the pilot fuel quantity.

The middle pilot fuel injection timing (-19 CAD) resulted in longer main ignition delay that led to the higher brake specific fuel consumption. The long ignition delay resulted in the slower combustion process. This led to the pressure rise after TDC resulting in high fuel consumption and loss of useful work [77]. The longer ignition delay allows a higher wall wetting by fuel and thus increases the amount of fuel consumption. In the case of late and early pilot fuel injection, the difference of BSFC is not significant.

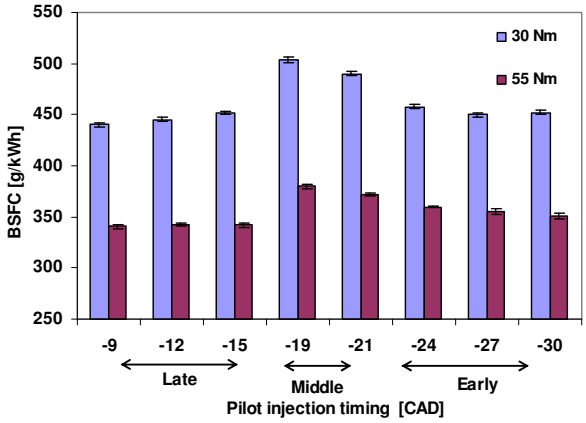

Figure 6.12. The variation brake specific fuel consumption (BSFC) as a function of pilot fuel injection timings (-9 to -30 CAD) at two different engine loads (30 Nm and 55 Nm) and constant engine speed 2000 rpm, error bars represent 95 percent confidence.

6.2.2 Engine Emissions

The NO_x emissions are mainly influenced by the peak in-cylinder pressure and high combustion temperatures. It can clearly be seen from Figure 6.13 that the NO_x concentration increases monotonically with early and late pilot fuel injection timing. The early pilot fuel injection timing tends to produce intermediate main ignition delay resulting in a complete combustion process due to long residence time for the reaction of Fuel-Air [195]. As a result, the early pilot fuel injection timing produces the higher in-cylinder

pressures leading to the higher temperatures and NO_x emissions [186, 196]. The middle pilot fuel injection produces the longest main ignition delay that leads to the slower combustion and low NO_x emissions [197].

Therefore, NO_x reduction generally can be controlled through the reduction of peak in-cylinder pressure by the air temperature and combustion duration [74]. The overall results show that the NO_x emissions increased with the early and late pilot fuel injection but decreased with the middle pilot fuel injection timing in both engine loads.

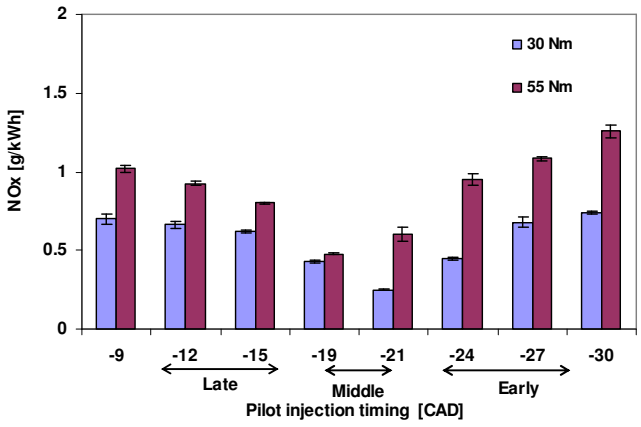

Figure 6.13. NO_x emissions as a function of pilot fuel injection timings (-9 to -30 CAD) at two different engine loads (30 Nm and 55 Nm) and constant engine speed 2000 rpm, error bars represent 95 percent confidence.

Figures 6.14 and 6.15 depict the effects of the variation of pilot fuel injection timings on THCs and CO emissions, respectively. The both emissions will be increased by several factors such as quenched flame, lean combustion, cold starting, and poor mixture preparation [193]. The results show that the early pilot fuel injection timing resulted in lower THCs and CO emissions as compared with late and middle pilot injection timing. This is due to the intermediate main ignition delay resulting in a complete combustion.

The shorter ignition delay leads to less fuel adhering to the combustion chamber walls resulting in more homogeneous mixture that produces less total unburned hydrocarbons THCs [70]. The early pilot fuel injection timing increased the wall wetting resulting in higher THCs emissions [39, 188, 195]. However, it does not affect the whole THCs emissions due to only less than 20 percent (pilot fuel quantity) of total injected fuel. It is clearly seen from Figures 6.14 and 6.15 show that the middle pilot fuel injection timing produces a higher level of THCs and CO emissions. The comparatively longer main ignition delay from the middle of pilot fuel injection timing resulted in higher fuel impingement contributing to the higher THCs and CO emissions. It is interesting to note that the CO emissions remained approximately constant with a variation of pilot fuel injection timing at 55 Nm of engine load. At higher combustion temperatures, the CO emissions decrease due to complete combustion resulting in higher cylinder temperature and an increasing oxidation process between carbon and oxygen molecules [186, 196].

The results show that the higher emissions at 30 Nm can be improved significantly by advancing the pilot fuel injection timing. This is due to early and late pilot injection timing introducing a comparatively shorter main ignition delay as compared with the middle pilot fuel injection timing. Therefore, the early pilot fuel injection timing is applicable to control the main ignition delay thus producing lower THCs and CO emissions.

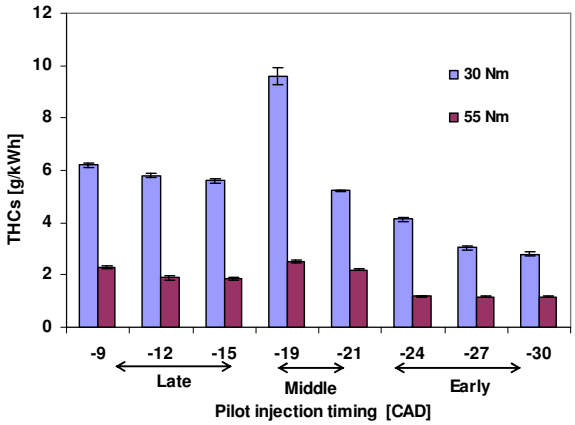

Figure 6.14. THCs emissions as a function of pilot fuel injection timings (-9 to -30 CAD) at two different engine loads (30 Nm and 55 Nm) and constant engine speed 2000 rpm, error bars represent 95 percent confidence.

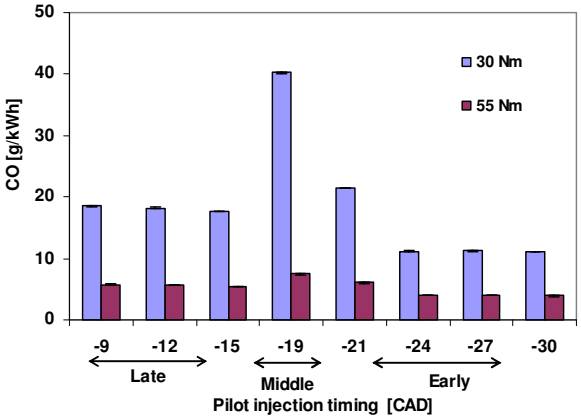

Figure 6.15. CO emissions as a function of pilot fuel injection timings (-9 to -30 CAD) at two different engine loads (30 Nm and 55 Nm) and constant engine speed 2000 rpm, error bars represent 95 percent confidence.

The effect of pilot fuel injection timing on the smoke level (FSN) is shown in Figure 6.16. The amount of smoke formation is strongly related to the fraction of diffusive combustion phase [198]. Smoke formation occurs at extremely local air deficiency. It increases as the Air-Fuel ratio decreases. The higher fraction of diffusive combustion

phase will result in an increase in the smoke formation. The presented results are in good agreement with Okude et al. [58] which showed that the smoke decreased as the pilot fuel injection timing is advanced. This is strongly believed to be due to an improvement in mixture formation with an early pilot fuel injection. This resulted in complete combustion due to a better mixing process. The early pilot fuel injection timing produces an intermediate main ignition delay that results in complete combustion. The formation of smoke is higher at a high engine load due to more fuel being injected resulting in higher smoke formation. The most obvious finding to emerge from this study is that the early pilot fuel injection timing is better for smoke reduction.

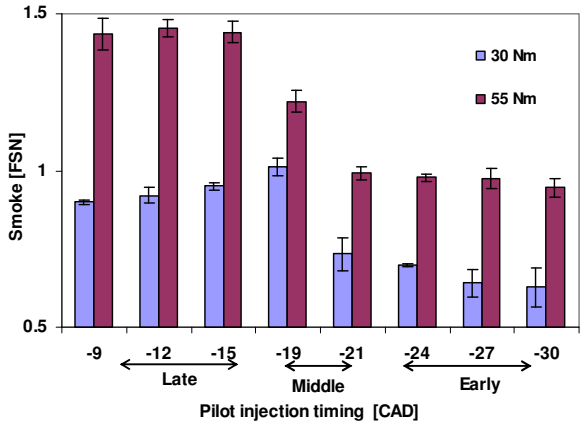

Figure 6.16. Smoke level (FSN) as a function of pilot fuel injection timings (-9 to -30 CAD) at two different engine loads (30 Nm and 55 Nm) and constant engine speed 2000 rpm, error bars represent 95 percent confidence.

Figure 6.17 shows the NO_x-smoke trade-off emissions, for a variation of pilot injection timings and two different engine loads. The smoke levels and NO_x emissions appeared to be lower with -21 and -19 CAD of pilot injection timing for the engine loads of 30 Nm and 55 Nm, respectively. Low levels smoke and NO_x can be achieved at the

pilot injection timing of -21 for the engine load of 30 Nm. Under the same pilot injection timing, running at the engine load of 55 Nm results in higher smoke (35%) and higher NO_x emissions (1.4 times). Therefore, the simultaneous reductions in smoke and NO_x could be achieved when the engine is operating at the right pilot injection timing i.e the pilot injection timing of -21 CAD is suitable for the engine is operating at low load (30 Nm) and low speed (2000 rpm).

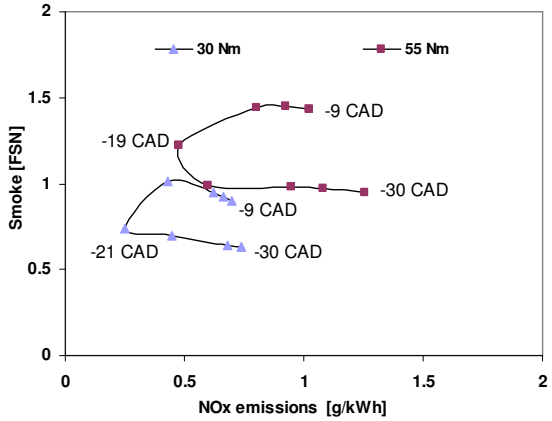

Figure 6.17. NO_x-smoke trade-off emissions for a variation of pilot fuel injection timings (-9 to -30 CAD) and two different engine loads (30Nm and 55 Nm).

6.3 Summary

Experimental work was carried out to evaluate the effect of pilot fuel quantity and pilot fuel injection timing on the engine performance and emissions of a modern 2.7l V6 diesel engine. The results clearly showed that increasing the pilot fuel quantity from 0.8 to 3.0 mg/stroke resulted in a significant deterioration in fuel consumption and engine emissions for almost all engine test conditions. The engine thermal efficiencies are decreased from 15.9 to 13.3% and 17.6 to 14.0%, BSFC is increased by 19.6% and 25.9%, smoke levels are increased by 24.4% and 25.2% and NO_x emissions are increased by

26.7% and 60.0% with the increase of pilot fuel quantity from 0.8 to 3.0 mg/stroke at low and high fuel injection pressure respectively. It can therefore be concluded that the smaller pilot fuel quantity with the higher fuel injection pressure can be considered as an enhanced strategy in order to control exhaust emissions and engine performance simultaneously. The simultaneous reductions in smoke and NO_x could be achieved when the engine is operating with low pilot fuel quantity and high fuel injection pressure.

Further experimental work was carried out to investigate the effect of pilot fuel injection timing to the main combustion behaviour. As it is accepted, the pilot fuel injection is favoured for the main fuel combustion process. The results showed that the main ignition delay, BSFC, THCs, CO and smoke level are initially increased with retarded pilot fuel injection timing of -9 to -19 CAD and then decreased after an advanced of injection timing of -21 to -30 CAD for both engine loads. However, the effect on NO_x emissions is reversed. Therefore, it has been proven that advanced pilot fuel injection timings of -21, -24, -27 and -30 CAD are better for smoke, THCs and CO. Conversely, the pilot fuel injection timings of -9, -12, -15, and-19 are worse for those particular emissions. In terms of NO_x emissions, the pilot fuel injection timings of -21 and -19 CAD are the best for 30 Nm and 55 Nm respectively. In summary, advanced pilot fuel injection has promising emissions reduction in terms of smoke, THCs and CO but not for NO_x. The middle of pilot injection timings (-21 and -19 CAD) are also better for NO_x-smoke trade-off emissions for the engine loads of 30 Nm and 55 Nm, respectively.

CHAPTER 7

COMBUSTION BEHAVIOUR AND EMISSION CHARACTERISTICS OF TME BLENDS FUELLING

This chapter presents the experimental results of a modern 3.0l V6 diesel engine fuelling with 10% and 30% Tallow Methyl Ester (TME10 and TME30) blends with diesel. The study is designed to investigate the influence of the fuel properties by using TME blends with diesel on the combustion characteristics and emissions without any modification to the engine management system (EMS). Furthermore, the aim of this study is to understand more about the fuel economy, combustion and then emissions behaviour of TME blends. The details of the engine test conditions are described in section 7.1. Sections 7.2 and 7.3 discussed the details of the combustion behaviour and engine emissions respectively. The results are summarised in Section 7.4.

7.1 Engine Test Conditions

The experimental work is carried out based on 11 test points as displayed in Figure 7.1. Mode 11 is used to monitor the engine health condition. These conditions are recommended by Jaguar-Land Rover (JLR) taken from the NEDC (New European Driving Cycle). The inlet fuel temperature (35 ± 1 °C), inlet air temperature (30 ± 1 °C) and relative humidity (45-50%) were kept constant and monitored throughout the tests.

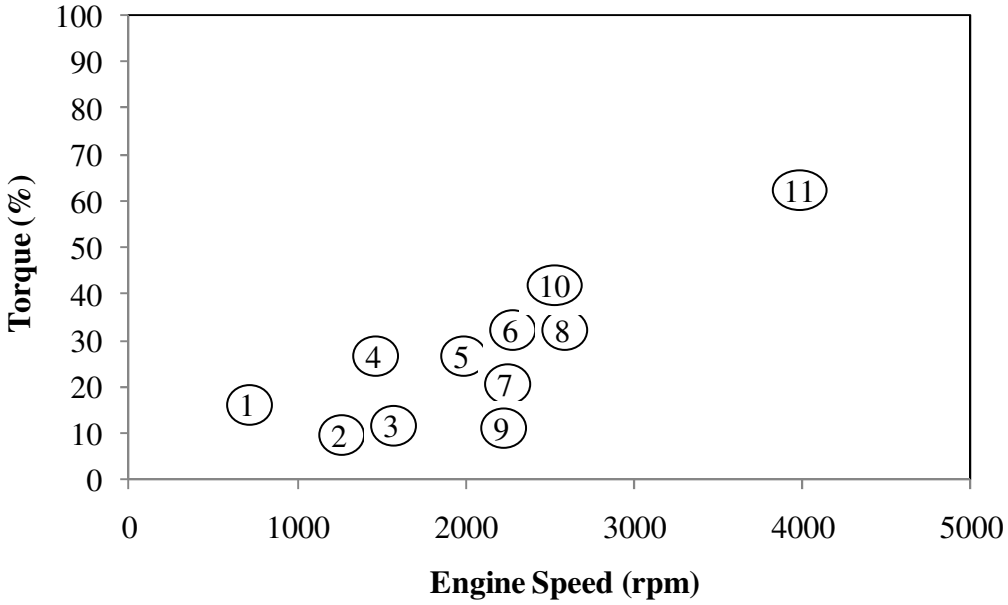

Figure 7.1. Engine test conditions

The injection strategy for each mode is different as clearly displayed in Table 7.1. For modes 1, 2 and 3, the injection strategy consists of pilot 1, pilot 2 and main fuel injection. However, modes 4–10 consist of all above with additional post 2 fuel injection. During high speed and high load (mode 11) the injection strategy only consists of main fuel injection. The fuel injection pressure for the pilot, main and post injections are the same.

Table 7.1. Injection strategy for each mode

Mode	Pilot 1	Pilot 2	Main	Post 1	Post 2
1,2,3	ON	ON	ON	OFF	OFF
4-10	ON	ON	ON	OFF	ON
11	OFF	OFF	ON	OFF	OFF

7.2 Combustion Behaviour of TME10 and TME30

The combustion behaviour of biodiesel-diesel blends (TME10 and TME30) in a diesel engine can be understood through the output responses such as rate of heat release, in-cylinder peak pressure, ignition delay, combustion duration, injection timing, mass fuel burnt, brake specific fuel consumption, and exhaust emissions. The results from this study will be able to provide useful information to evaluate the engine flexibility to the new fuel (TME10 and TME30). It can also be considered as a guideline for further development to the engine mapping for the engines fuelled with a wide range of fuels.

7.2.1 Engine Management System Responses to the Fuel Types

Figure 7.2 shows the EGR rate for different fuel types throughout the engine test conditions. The EGR rate was not affected as TME concentration increases in the blended fuel.

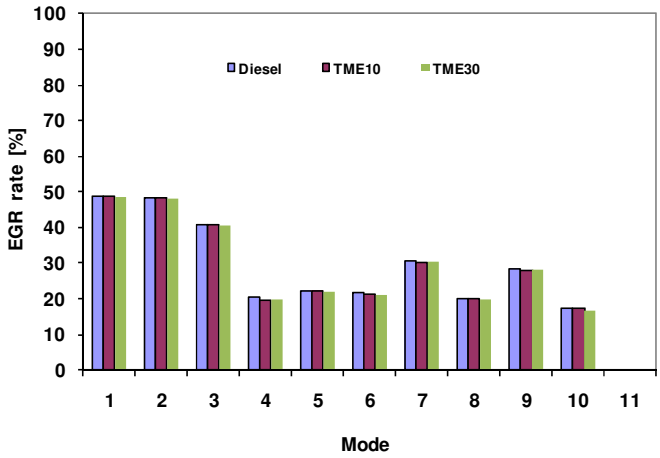

Figure 7.2. EGR rate at each engine test mode and engine fuelling.

Figures 7.3 and 7.4 show the start of main injection and fuel injection pressure respectively as a function of engine test conditions for each fuel. It is observed that the

start of injection (SOI) and fuel injection pressure are the same regardless of fuel type. Although as reported by other researchers [199, 200] higher fuel density and viscosity and lower compressibility influence significantly the injection process. As a result the injection system is capable of maintaining the same SOI and fuel injection pressure despite the variation in the fuel properties.

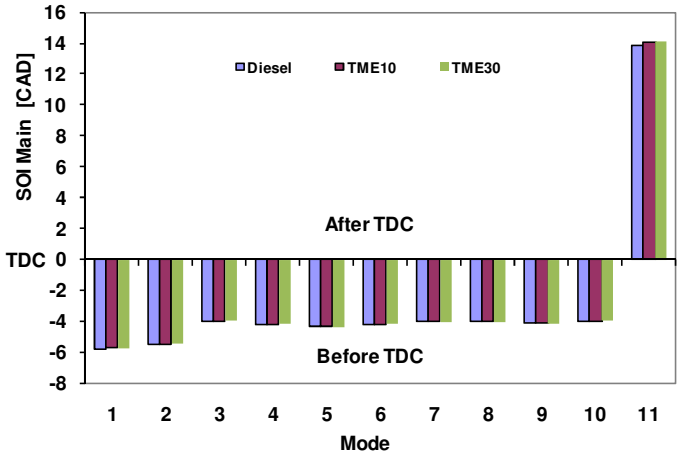

Figure 7.3. The start of main injection (SOI main) at each engine test mode and engine fuelling.

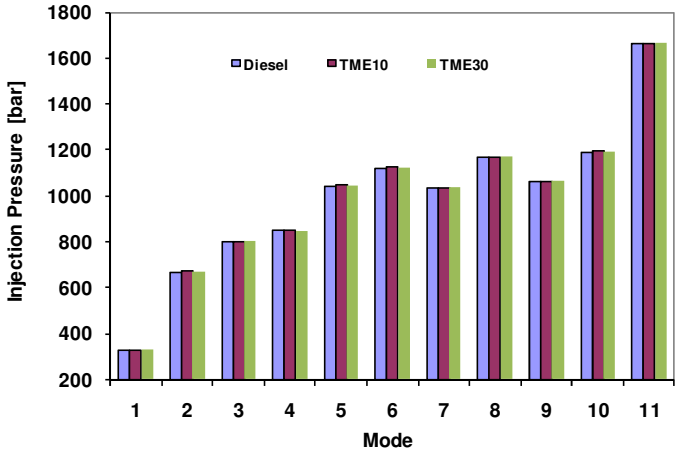

Figure 7.4. The fuel injection pressure at each engine test mode and engine fuelling.

7.2.2 Rate of Heat Release and In-cylinder Pressure Profiles

Figures 7.5a, 7.5b and 7.5c show the rate of heat release (ROHR) as a function of crank angle degree (CAD) for different fuel types. Figures 7.5 b and 7.5 c are closed up images of ROHR at peak 1 and peak 2 respectively. The start of combustion of TME-diesel blends was advanced as compared to diesel. This is mainly due to the higher cetane number i.e TME (58.8) as compared to ULSD (47) [172]. These results are in good agreement with Zhang et al. [33] who found that the combustion behaviour in biodiesel-diesel blends is dominated by a higher cetane number and higher oxygen content.

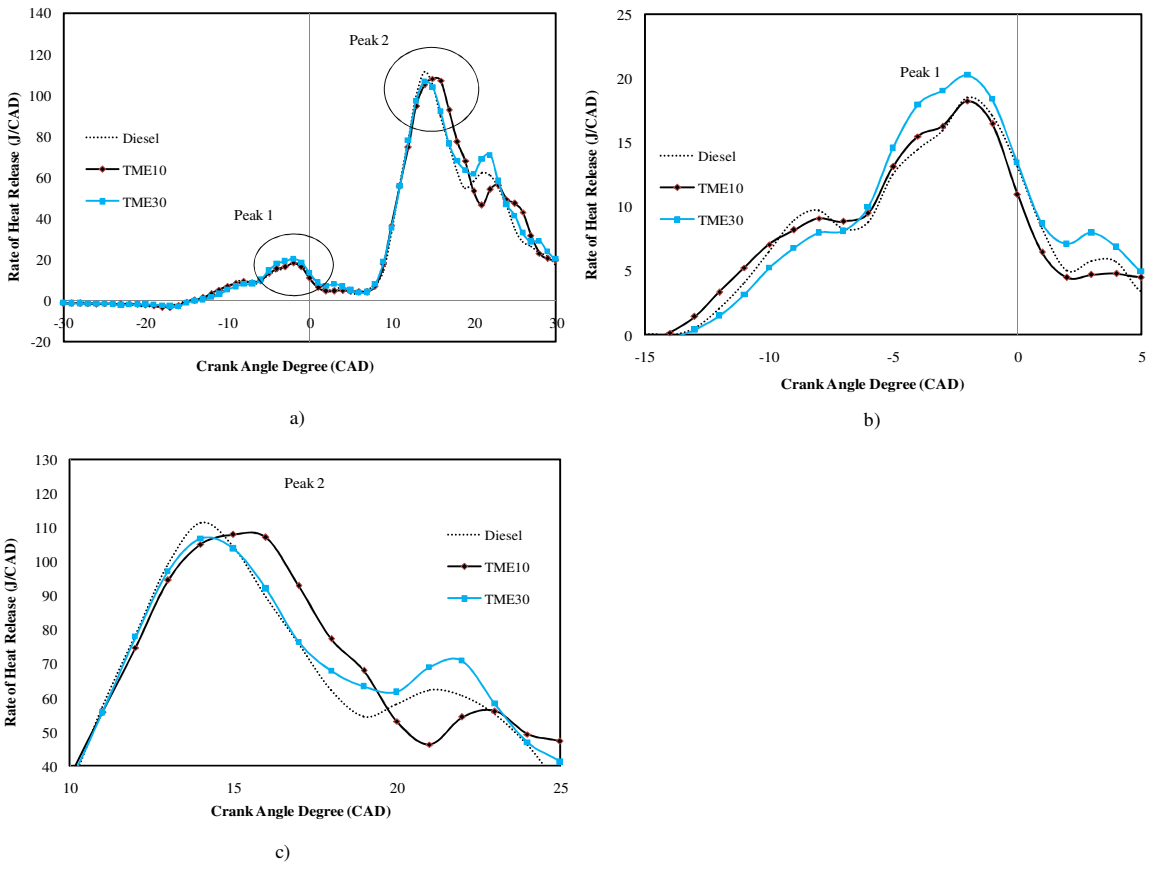

Figure 7.5. a) The rate of heat release for the three fuels at mode 4 b) closed-up peak 1 and c) closed-up peak 2

Figures 7.6a, 7.6b and 7.6c show the in-cylinder pressure profile as a function of crank angle degree (CAD) for three fuels. Figures 7.6b and 7.6c are closed up images of in-cylinder pressure at peak 1 and peak 2 respectively. The reduced ignition delay with TME-diesel blends fuelling results in higher peak in-cylinder pressure as compared to diesel (Figure 7.7). The higher oxygen content of the biodiesel can lead to the improved combustion process as mentioned by previous studies [2, 36, 69]. The increased peak in-cylinder pressure with TME10 and TME30 fuelling is a result of the different density and viscosity properties that are influencing injection rate and fuel atomisation.

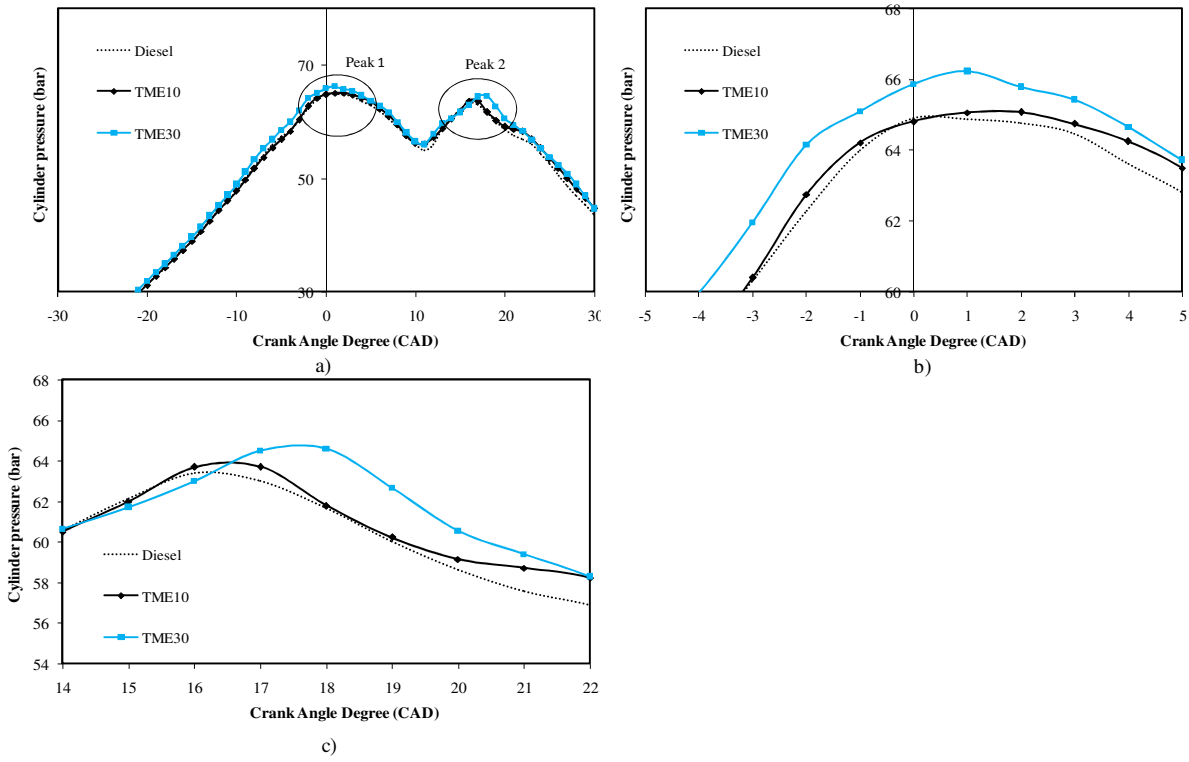

Figure 7.6. a) In-cylinder pressure profile for the three fuels at mode 4, b) closed-up peak 1 and c) closed-up peak 2

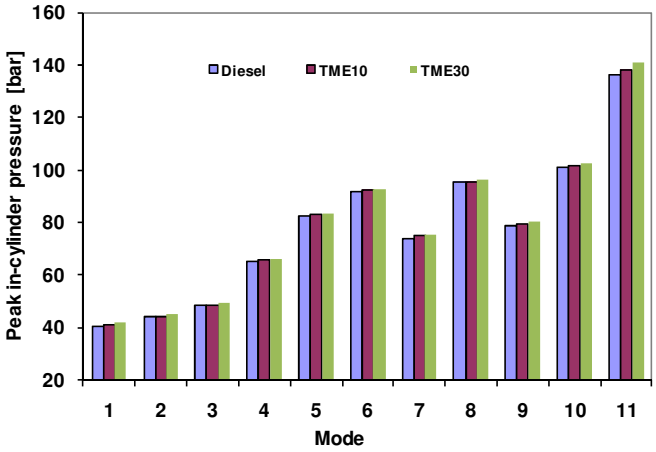

Figure 7.7. The peak in-cylinder pressure (peak 1) at each engine test mode and engine fuelling.

7.2.3 Fuel Consumption and Engine Thermal Efficiency.

Increasing the biodiesel concentration in the blend results in higher BSFC (Figure 7.8) as compared to diesel; most of the authors agree with these findings [33, 35, 143, 201, 202]. This is mainly due to the lower calorific value i.e TME (39.8 MJ/kg) as compared to diesel (42.7 MJ/kg) [150]. The higher biodiesel density can compensate for the significantly lower calorific value. The modified combustion patterns with TME-diesel blends fuelling led to reduced engine thermal efficiency (Figure 7.9).

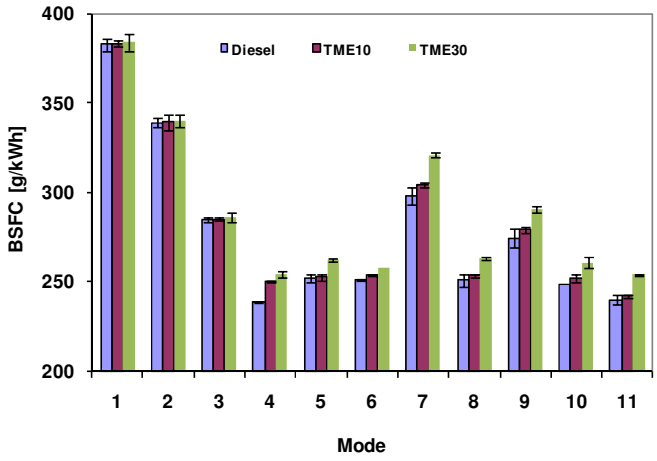

Figure 7.8. Brake specific fuel consumption (BSFC) at each engine test mode and engine fuelling, error bars represent 95 percent confidence.

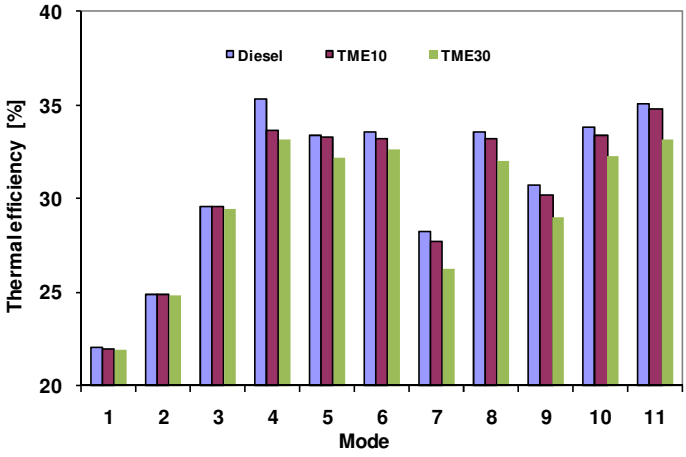

Figure 7.9. Engine thermal efficiency (%) at each engine test mode and engine fuelling.

7.2.4 Combustion Duration

Figure 7.10 shows the analysis of the combustion duration at a variation of engine test conditions for three fuels. The time period in CAD between 10.0% fuel burnt with 90.0% fuel burnt is considered as combustion duration. These values were recorded and analysed by using IndiCom 2010 software provided by AVL. Figure 7.10 shows that when the engine fuelled with TME-diesel blends, results in shorter combustion duration as

compared to diesel for all engine conditions. The higher oxygen content and high cetane number of TME-diesel blends contributes to the shorter combustion duration.

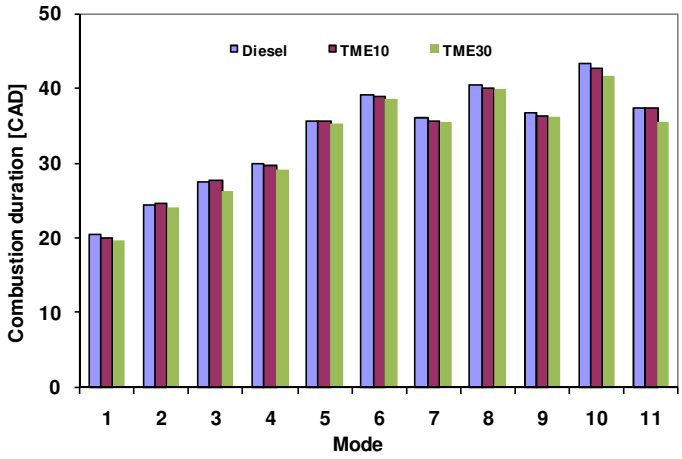

Figure 7.10. Combustion duration at each engine test mode and engine fuelling.

7.3 Engine Emissions

A number of research projects have been carried out on biodiesel combustion and have reported reductions in carbon monoxide, total hydrocarbons and smoke emissions [110, 203, 204], however there was an increase in NO_x emissions [15, 26, 30-33, 35, 109, 114, 205-207]. It has been reported that the higher NO_x with biodiesel is due to advanced combustion and higher oxygen content and in some cases increased flame temperatures. In this study, the injection timing of biodiesel is similar to diesel. Therefore the higher NO_x emissions from biodiesel fuelling due to advanced injection timing, is not applicable in this study.

7.3.1 Oxides of Nitrogen

The key influences of higher NO_x emissions seen from the biodiesel combustion (Figure 7.11) is a result to high peak in-cylinder pressure, temperature and oxygen content

[15, 33, 35, 109]. Previous studies have described that the advanced injection timing leading to higher NO_x emissions due to longer residence time in the combustion chamber [15, 31, 114, 208]. Although, in this work, the injection timing occurs at the same time regardless of fuel types, the reduced ignition delay and the start of combustion might be possible to explain the slightly higher NO_x emissions with TME-diesel blends. The existing nitrogen in fuel in the form of NH_3, NC and HCN might be a possible reason contributing to the higher NO_x emissions in biodiesel [209].

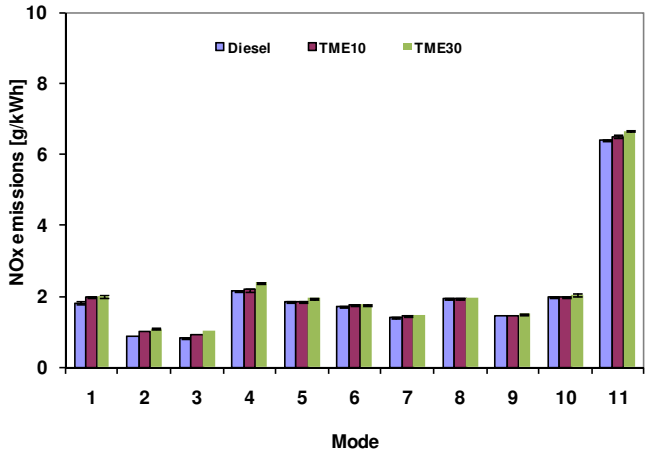

Figure 7.11. NO_x emissions at each engine test mode and engine fuelling, error bars represent 95 percent confidence.

7.3.2 Total Hydrocarbons (THCs) and Carbon Monoxide (CO)

Figures 7.12 and 7.13 show the total hydrocarbons (THCs) and carbon monoxide (CO) emissions respectively with different fuel types at different engine test conditions. The reduced THCs and CO are due to the oxygen availability that is favourable to improve the combustion efficiency [31, 35, 115-117, 149, 150]. In fact, CO and THCs emissions are greatly influenced by Fuel–Air mixing and the Air-Fuel ratio [36, 151]. The results are

also consistent with Abd-Alla et al. [57] who found out that biodiesel leads to higher combustion temperatures thus lowering the THCs emissions.

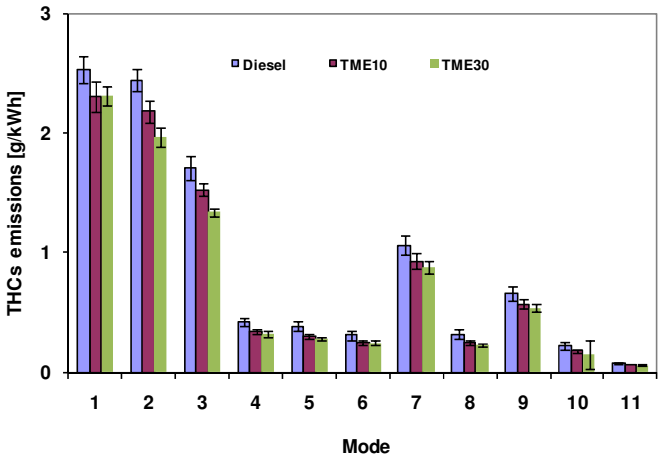

Figure 7.12. THCs emissions at each engine test mode and engine fuelling, error bars represent 95 percent confidence.

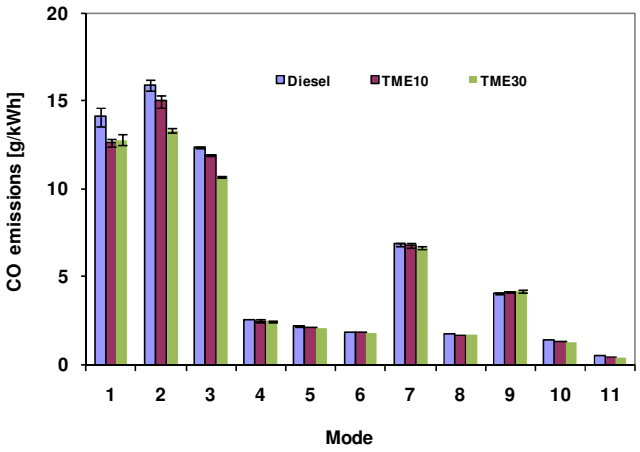

Figure 7.13. CO emissions at each engine test mode and engine fuelling, error bars represent 95 percent confidence.

7.3.3 Smoke Level

The variation of smoke level relative to the variation of fuel types at different engine test conditions is shown in the Figure 7.14. It is observed that when the engine is fuelled with TME-diesel blends, results in significantly less smoke as compared to diesel. This is due to improvement in combustion efficiency with TME-diesel blends. The higher oxygen content in biodiesel is favourable for the soot oxidation process (complete combustion) [26, 44, 149], while the absence of sulphur in the fuel can reduce carbon [35, 150, 202, 210]. In addition, the soot from biodiesel is easy to be oxidised, it has been reported biodiesel soot can oxidise up to six times faster than the soot emitted by diesel fuel [31].

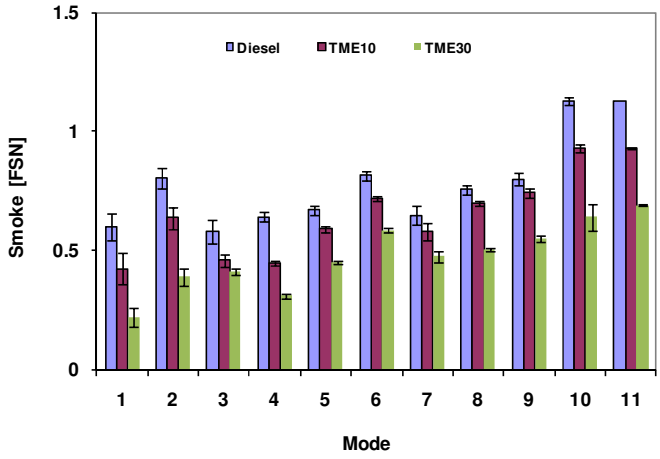

Figure 7.14. Smoke level at each engine test mode and engine fuelling, error bars represent 95 percent confidence.

7.4 Summary

Experimental work was carried out to investigate the influence of the fuel properties by using TME blends with diesel on the engine performance and emissions of a modern 3.0l V6 diesel engine. This did not involve any modification to the engine

management system (EMS). The results on the EMS responses such as EGR rate, SOI and fuel injection pressure are similar regardless of the fuel types. The overall results showed that TME-diesel blends (TME10 and TME30) have a potential to reduce exhaust emissions particularly smoke, THCs and CO emissions. In fact, blended fuels have a capability to produce a comparable engine performance to diesel. The engine fuelled with TME-diesel blends, results in higher peak in-cylinder pressure and rate of heat release as compared to diesel due to the high oxygen content and cetane number of the fuel, providing complete combustion. In the case of mode 4 (1500 rpm and 25 % of engine peak torque), engine fuelled with TME-diesel blends results in increased the BSFC by 4.9% and 6.5%, and reduced the thermal efficiency from 35.3 to 33.7% and 35.3 to 33.2% for TME10 and TME30 respectively. The engine fuelled with TME-diesel blends results in higher fuel consumption due to its higher density, high viscosity and lower heating value. These properties will influence both the size of the fuel droplets and fuel atomisation that leads to the poor evaporation process resulting to the incomplete combustion.

The combustion of TME-diesel blends in the case of mode 4 (1500 rpm and 25 % of engine peak torque) increased NO_x emissions by 1.8% and 10.0% and reduced CO by 0.9% and 1.8%, THCs by 18.0% and 23.9 %, smoke by 30% and 51.7% for TME10 and TME30 respectively. This is due to high oxygen content, no aromatic compounds and high cetane number of TME-diesel blends. The high NO_x emissions in TME-diesel blends are due to advanced combustion, high peak in-cylinder pressure, temperatures and oxygen availability. As it is well accepted, the major contribution to the higher NO_x emissions is the thermal effect. The higher oxygen content in the TME-diesel blends is favourable for smoke emissions. The reduction of smoke can also be observed at high engine load due to high combustion temperatures and better mixture formation. The fuel properties, engine

calibration and test conditions have influenced the engine performance and emissions characteristics. Therefore it can be concluded that, if the engine is fuelled with TME10 or TME30, engine thermal efficiency and BSFC could be improved and NO_x emissions minimised with the application of a new engine calibration. The author suggests that the combined effect of injection strategy (fuel injection pressure, dwell period, pilot fuel quantity) and EGR could be a potential solution to diesel engines fuelled with TME10 and TME30, as shown in the first phase of this study.

CHAPTER 8
CONCLUSIONS AND RECOMMENDATIONS

The main objectives of this study were to investigate the combined effect of injection strategy and EGR modes on engine performance and emissions when using mineral diesel (ULSD). A further study was carried out with the engine fuelled with tallow methyl ester (TME)-diesel blends in order to understand the effects of fuel properties on the combustion characteristics and exhaust emissions. Two phases of experimental work were conducted; in the first phase, the effect of injection strategies, i.e, variation of injection pressures, variation of dwell duration periods and variation of pilot quantities and EGR modes were carried out by using a modern 2.7l V6 Jaguar diesel engine fuelled with ULSD. The experimental work was carried out at a variation of engine speeds and loads. In the second phase, an updated 3.0l V6 Jaguar diesel engine was used to investigate the effects of TME-diesel blends on the combustion characteristics and exhaust emissions. The experiments were carried out by using mineral diesel, TME10 and TME30 at 11 modes of engine test conditions. The selected test conditions proposed by Jaguar Land Rover are based on the New European Driving Cycle. Finally, the study summarises the overall engine combustion characteristics and exhaust emissions from both types of V6 diesel engines (2.7l and 3.0l).

8.1 Concluding Remarks

The main outcomes of this study can be concluded as following.

8.1.1 Combined effect of Fuel Injection Pressure and EGR Modes on The Engine Performance and Emissions

The experimental results show that the performance and exhaust emissions of the engine fuelled with higher injection pressure are improved compared to the lower injection pressure. The effect of higher injection pressure is more important at the higher engine load compared with the lower loads. This is due to higher quantity of injected fuel at higher engine load that requires a longer time for a mixing process. The study of the combined effect of injection pressure and EGR modes showed that effect of injection pressure is more significant in the case of EGR ON compared with EGR OFF due to higher availability of oxygen in the charge air in the EGR OFF mode. The smoke level, CO and THCs are decreased by 74.6%, 22.7% and 29.4% respectively with the increase of injection pressure from 300 to 700 bar when the engine is operating with EGR ON at 1500 rpm, 35.1 Nm. Meanwhile, the smoke level, CO and THCs are decreased by 63.4%, 10.2% and 11% with the increase in injection pressure from 300 to 700 bar when the engine is operating with EGR OFF at the same engine condition. The BSFC is decreased by 2.7% and 5.1% respectively, while thermal efficiencies are increased from 18.5 to 19.0% and 19.0 to 20.0%. Lastly NO_x emissions are increased by 65% and 44% with the increase of injection pressure from 300 to 700 bar for the EGR ON and EGR OFF respectively.

The high injection pressure introduces a better mixing process to improve smoke emissions. Meanwhile, the application of EGR was used to reduce the higher NO_x emissions emitted as a result of complete combustion. The results show that fuel injections with higher injection pressure are a way to improve diesel engine performance and lower emissions of THCs, smoke and carbon monoxide (CO). However this strategy leads to a

higher level of NO_x emissions. Therefore, the application of a combination of higher fuel injection pressure and exhaust gas recirculation (EGR) has potential in controlling both smoke-NO_x emissions and improving engine performance simultaneously.

8.1.2 Combined effect of Fuel Injection Pressure, Dwell Period (Interval between Pilot and Main) and EGR Modes on The Engine Performance and Emissions

The study was designed to produce improvements in the fuel mixing process via the injection strategy (injection pressure and dwell duration period) and EGR modes. This would contribute to a minimum amount of fuel burnt in the premixed combustion phase, leading to a reduction in emissions. Six different injection pressures (300 – 800 bar) combined with a short and long dwell period were compared in an attempt to improve engine performance and exhaust emissions. The engine performance is measured in terms of brake specific fuel consumption, ignition delay, heat release and peak in-cylinder pressure and emissions, specifically those of oxides of nitrogen (NO_x), total unburned hydrocarbons (THCs), carbon monoxide (CO) and smoke emissions for each engine test condition. The combustion analysis showed that premixed combustion is important in the controlling of emissions of NO_x and smoke. The results also confirmed that the effect of injection pressure is more dominant than the dwell period in terms of peak cylinder pressure, heat release, brake specific fuel consumption and exhaust emissions.

However, the dwell period shows a strong effect at a higher engine speed. In the case of 1500 rpm, with the increase of injection pressure from 300 to 800 bar at short and long dwell period, the engine thermal efficiencies are increased from 16.5 to 19.1% and 17.1 to 19.7%, BSFC is decreased by 13.5% and 13.2%, smoke levels are decreased by 74.3% and 70.1% and NO_x emissions are increased by 69.6% and 68.0% respectively.

Meanwhile, at 2250 rpm, with the increase of injection pressure from 300 to 800 bar at short and long dwell period the engine thermal efficiencies are increased from 18.2 to 20.3% and 20.4 to 23.2% , BSFC is decreased by 10.4% and 12.4%, smoke levels are decreased by 49.6% and 67.7% and NO_x emissions are increased by 61.0% and 71.1% respectively. It therefore can be concluded that the longer dwell period is more effective at the higher engine speed particularly when the engine is operating with EGR ON.

8.1.3 Combined Effects of Pilot Fuel Quantity, Fuel Injection Pressure and Dwell Timing on The Engine Performance and Emissions

The overall results showed that when the engine is operated with a larger pilot quantity, higher BSFC, smoke level and NO_x emissions are the result; while the smaller pilot quantities tend to improve smoke, THCs and CO emissions. The engine thermal efficiencies are decreased from 15.9 to 13.3% and 17.6 to 14.0%, BSFC is increased by 19.6% and 25.9%, smoke levels are increased by 24.4% and 25.2% and NO_x emissions are increased by 26.67% and 60.0% with the increase of pilot quantity from 0.8 to 3.0 mg/stroke at low and high injection pressure with a short dwell period respectively. The experimental results also reveal that larger pilot quantity increased peak in-cylinder pressure and rate of heat release.

The results from the study of the effect of pilot injection timing showed that the main ignition delay, BSFC, THCs, CO and smoke level are initially increased with retarded pilot injection timing of -9 to -19 CAD and then decreased after an advanced pilot injection timing of -21 to -30 CAD for both engine loads. However, the effect on NO_x emissions is reversed. The middle of pilot injection timings (-21 and -19 CAD) are better for NO_x-smoke trade-off emissions for the engine loads of 30 Nm and 55 Nm, respectively. It therefore can be concluded that the most effective combination for improving engine

performance and minimising exhaust emissions is smaller pilot quantity, moderate dwell duration period and higher fuel injection pressure.

8.1.4 Combustion Behaviour and Emissions Characteristics of TME Blends Fuelling

The experimental results showed that saturated FAMEs from animals (Tallow Methyl Ester-diesel blends) showed better combustion characteristics and lower engine emissions as compared to diesel. Engine fuelling with TME-diesel blends (TME10 and TME30) results in higher peak in-cylinder pressure and rate of heat release as compared to diesel. In the case of mode 4 (1500 rpm and 25 % of engine peak torque), the combustion of TME-diesel blends increased the BSFC by 4.9% and 6.5%, and reduced the thermal efficiency from 35.3 to 33.7% and 35.3 to 33.2% for TME10 and TME30 respectively. The fuel properties such as high density and viscosity contribute to the poor fuel evaporation that leads to incomplete combustion of the fuel.

The combustion of TME-diesel blends in the case of mode 4 (1500 rpm and 25 % of engine peak torque) increased NO_x emissions by 1.8% and 10.0% and reduced CO by 0.9% and 1.8%, THC by 18.0% and 23.9 %, smoke by 30% and 51.7% for TME10 and TME30 respectively. This is strongly believed to be due to the higher oxygen content in TME-diesel blends that tends to produce the cleaner combustion and lower engine emissions. The higher level of NO_x with TME-diesel blends is due to high oxygen content and high combustion temperatures. It can be concluded that the formation of NO_x is influenced by the combustion temperatures and oxygen content in the fuel since the effect of changed residence time is not applicable in this study where injection timings were kept constant.

These findings show that TME10 and TME30 can be considered as a good alternative fuel for diesel engines. The fuel can be used to the engines even without any modification on hardware and engine mapping calibration. The results showed that the engine fuelled with TME10 and TME30 results in slightly higher BSFC and NO_x emissions. The author strongly believes that, with a new engine calibration, i.e the combined strategy between injection strategy and EGR which is obtained from the first phase study, both of these problems could be resolved.

8.2. Future Work

Through a series of experimental work done on 2.7l and 3.0l V6 Jaguar diesel engines, the author would suggest several areas of research work that can be considered for future work.

8.2.1 The Effect of Injection Strategy and EGR Modes on Engine Operated with TME-diesel Blends

The experiments were carried out with no modifications on hardware and EMS when the engine is fuelled with TME blends. Therefore, the results are based on the fossil diesel fuel's engine calibration. Engine fuelled with TME results in higher BSFC and NO_x. The results from the combined strategy between injection strategy (injection pressure, dwell period and pilot quantity) and EGR showed an improvement in BSFC and emissions when the engine is fuelled with fossil diesel. Based on that, it is worth to apply the combined injection and EGR strategies on engine when fuelled with TME-diesel blends. The strategy has the potential to enhance the combustion of TME-diesel blends, and improve engine fuel consumption and emissions.

8.2.2 The Study of Fuel Properties on TME-diesel Blend Fuels

The experiments were carried out by using TME-diesel blend fuels. However, the details about fuel properties have not been completely explored yet. The combustion in a diesel engine is strongly dependent on the air-fuel mixing process that results in longer or shorter premixed combustion. As it is well accepted, the premixed combustion has a significant effect to the engine performance and emissions. A further study should be carried out to understand the influence of the physical and chemical properties of TME fuel blends on the combustion characteristics. The fuel compositions such as (C: H: O) are significantly important to relate with the combustion behaviour.

8.2.3 A Variation of EGR Temperatures

The EGR temperature on this engine is automatically controlled by the engine management system. The engine coolant is used to cool the exhaust gas in the EGR pipe. Therefore, the effect of a variation of EGR temperatures is difficult to study. Additional pipeline needs to be attached into the existing EGR system in order to control the EGR temperature by controlling the water flow rate. The result from this study will elaborate more about the effect of EGR temperature to the ignition delay and premixed combustion.

8.2.4 After-Treatment Performance with TME-diesel Blend fuels

In this research work, the samples of the exhaust emissions are taken upstream of the after-treatment devices (DOCs and DPFs). Therefore, the results are not comparable with the actual vehicle on the road. In fact, the exhaust emissions are quite unpredictable after passing through such devices as the DOC and DPF. A further investigation from the complete exhaust system is required in order to compare the experimental results to actual on road vehicles. At the same time, the results from the study can be used to evaluate the performance of after-treatment devices with TME-diesel blends.

APPENDIX A

ENGINE MANAGEMENT SYSTEM

A.1. Engine Measurement and Calibration Variables

Table A.1. Engine measurement variables

	Abbreviation	Description	Unit
1	Epm_n	Engine Speed	rpm
2	InjCrv_phiPil1Des	Pilot Injection Timing 1	^{o}CRK
3	InjCrv_phiPil2Des	Pilot Injection Timing 2	^{o}CRK
4	InjCrv_phiMI1Des	Main Injection Timing 1	^{o}CRK
5	InjCrv_phiPol1Des	Post Injection Timing 1	^{o}CRK
6	InjCrv_phiPol2Des	Post Injection Timing 2	^{o}CRK
7	InjCrv_qPil1Des_mp	Pilot Injection Quantity 1	mg/stk
8	InjCrv_qPil2Des_mp	Pilot Injection Quantity 2	mg/stk
9	InjCrv_qMI1Des_mp	Main Injection Quantity 1	mg/stk
10	InjCrv_qPol1Des_mp	Post Injection Quantity 1	mg/stk
11	InjCrv_qPol2Des_mp	Post Injection Quantity 2	mg/stk
12	InjSys_qTot	Total Injected Quantity	mg/stk
13	EGRVlv_rActB2	EGR Right Hand Side (RHS)	%
14	EGRVlv_rActB1	EGR Left Hand Side (LHS)	%
15	EGRVlv_rActB2	EGR RHS Feedback Voltage	V
16	EGRVlv_rActB1	EGR LHS Feedback Voltage	V
17	AirCtl_rEGREst_r32	EGR Desired	%
18	Air_pCmpr2Us	Ambient Pressure	hPa
19	Air_tAFS	Inlet Air Temperature	^{o}C
20	AFS_dmB2 RLH	RHS Mass Air Flow	mg/stk
21	AFS_dmB1 LH	LHS Mass Air Flow	mg/stk
22	AirCtl_rRatDesDyn_	Total Mass Air Flow Desired	mg/stk
23	Air_tCACDs	Total Mass Air Flow Actual	mg/stk
24	PCR_pDesVal	Manifold Pressure Desired	hPa
25	Air_pCACDs	Manifold Pressure Actual	hPa
26	TrbCh_rB2	Turbocharger RHS	%
27	TrbCh_rB1	Turbocharger LHS	%
28	Exh_pPFitDiff	Exhaust Back Pressure	hPa
29	Oil_tSwmp	Oil Temperature	^{o}C
30	FuelT_t	Fuel Temperature	^{o}C
31	APP_r	Pedal Value	%
32	Rail_pSetPoint	Fuel Pressure Desired	MPa
33	RailP-pCurr_mp	Fuel Pressure Actual	MPa

APPENDIX B

BASIC EQUATIONS OF COMBUSTION ANALYSIS

The Indicated Work

The indicated work per engine cycle can be calculated as below:

$$\text{IMEP} = \frac{\text{Indicated work per cycle}}{\text{Displaced volume}} = \frac{\oint pdV}{V_d} \quad (1)$$

The Exhaust Gas Recirculation (EGR) Rate (%)

The exhaust gas recirculation EGR rate (%) can be calculated as below [211]:

$$\text{EGR}\ (\%) = \frac{m_{EGR}}{m_{Total}} \times 100 \quad (2)$$

Where m_{EGR} and m_{Total} represent the mass of EGR and the mass of total intake, respectively. The mass of total intake consists of mass of air, mass of fuel and mass of EGR as shown in equation 3.

$$\text{m}_{\text{Total}} = m_a + m_f + m_{EGR} \quad (3)$$

Where, m_a, m_f and m_{EGR} represent the mass of air, the mass of fuel and the mass of EGR respectively.

The Rate of Heat Release (ROHR)

The equation of the heat release rate $dQ/d\theta$ is taken from Heywood [145].

$$\mathrm{dQ} = dU + PdV \tag{i}$$

Heat capacity per crank angle is given by

$$\frac{dQ}{d\theta} = \frac{dU}{d\theta} + P\frac{dV}{d\theta} \tag{ii}$$

Consider the gas in a cylinder as ideal gas, $\mathrm{dU} = mCvdT$ and $Cv = \frac{R}{\gamma - 1}$. Substitute these in equation ii.

$$\frac{dQ}{d\theta} = \frac{mR}{\gamma - 1}\frac{dT}{d\theta} + P\frac{dV}{d\theta} \tag{iii}$$

By substituting the ideal gas equations ($PV = mRT$ and $V.dP + P.dV = m.R.T$) in equation iii, the final equation of the rate of heat release can be simplified as below.

$$\frac{dQ}{d\theta} = \frac{\gamma}{\gamma - 1}p\frac{dV}{d\theta} + \frac{1}{\gamma - 1}V\frac{dp}{d\theta} \tag{4}$$

Where:

Q : Heat

$d\Theta$: Crank angle degree

γ: the ratio of specific heats (c_p/c_v),

V: the instantaneous volume of the engine cylinder

p: the instantaneous cylinder pressure,

The γ values before and after combustion are calculated based on actual *p-V* diagram.

The Engine Brake Power

The engine brake power P_b in kW delivered by the engine and absorbed by the dynamometer is the product of brake torque (T_b, in Nm) and the crankshaft rotational speed *(N*, in revolution per second).

$$P_b = \frac{2\pi N T_b}{1000} \tag{5}$$

The Brake Specific Fuel Consumption

The brake specific fuel consumption (bsfc, in g/kWh)

$$\text{bsfc} = \frac{\dot{m}_f}{P_b} \tag{6}$$

The Engine Thermal Efficiency

The engine thermal efficiency η_{th} is given by:

$$\eta_{th}(\%) = \frac{P_b}{\dot{m}_f(\text{LHV})} \times 100 \tag{7}$$

where $\dot{m}_f$ is the fuel mass flow rate per cycle, P_b is the brake power and LHV is the lower heating value of the fuel used.

The Reduction of Theoretical Heating Value

The theoretical heating value of TME30 was reduced by ~2.562% (Eq.8).

$$\mathrm{LHV_{B30}\,Reduction}(\%) = \left(1 - \frac{0.3\times \mathrm{LHV_{TME}} + 0.7\times \mathrm{LHV_{ULSD}}}{\mathrm{LHV_{ULSD}}}\right)\times 100 \qquad (8)$$

APPENDIX C

TEMPERATURE AND PRESSURE ACQUISITION

Table C.1. Channel designation for the temperature data acquisition

	Abbreviation (CADET V14)	Description	Unit
1	TC1	Air Inlet	°C
2	TC2	Pre Compressor RH	°C
3	TC3	Pre Compressor LH	°C
4	TC4	Compressor Out RH	°C
5	TC5	Compressor Out LH	°C
6	TC6	Intercooler In	°C
7	TC7	Intercooler Out	°C
8	TC8	Intake Manifold	°C
9	TC9	Exhaust port 1	°C
10	TC10	Exhaust port 2	°C
11	TC11	Exhaust port 3	°C
12	TC12	Exhaust port 4	°C
13	TC13	Exhaust port 5	°C
14	TC14	Exhaust port 6	°C
15	TC15	Turbocharger In RH	°C
16	TC16	Turbocharger In LH	°C
17	TC17	Exhaust Pre DOC RH	°C
18	TC18	Exhaust Pre DOC LH	°C
19	TC19	Fuel In	°C
20	TC20	Coolant In	°C
21	TC21	Oil Gallery	°C
22	TC22	Turbo Oil	°C

Table C.2. Channel designation for the pressure data acquisition

	Abbreviation (CADET V14)	Description	Unit
1	PTX 1	Oil Gallery	Bar
2	PTX 2	Coolant Inlet	Bar
3	PTX 3	Manifold RH	Bar
4	PTX 4	Manifold LH	Bar
5	PTX 5	Crankcase	Bar
6	PTX 6	Exhaust Pre DOC RH	Bar
7	PTX 7	Exhaust Pre DOC LH	Bar
8	PTX8	Intercooler Outlet	Bar

Right and left bank of the V6 engine when looking from flywheel (driver position)

APPENDIX D

SPECIFICATION OF AVL PRESSURE TRANSDUCER

Table D.1. AVL pressure transducer (GU 13P)

Sensitivity	15,53 pC/Bar
Linearity	≤± 0.3%
Measurement range	200 Bar
Temperature range	400 deg C
Natural frequency	130 kHz
Tight torque	1.5 Nm

APPENDIX E

ENGINE TEST CONDITIONS

Table E.1. Engine test conditions

Mode Label	Engine Speed (rpm)	Peak Torque (%)
Mode 1	750	16
Mode 2	1250	10
Mode 3	1500	13
Mode 4	1500	25
Mode 5	2000	27
Mode 6	2280	33
Mode 7	2250	16
Mode 8	2500	32
Mode 9	2250	20
Mode 10	2500	40
Mode 11	4000	63

APPENDIX F

LIST OF PUBLICATIONS DURING PHD PERIOD

1. Soot emissions control using diesel particulate filter and fuel-borne additives.
   N.R. Abdullah, M.L. Wyszynski and A.Tsolakis (December 2007)
   Poster Presentation Organized by Graduate School, University of Birmingham, December 2007.

2. Thermal Stress Analysis on Diesel Particulate Filter Using CFD Modeling
   N.R. Abdullah, M.L. Wyszynski and A.Tsolakis (April 2008)
   Poster Presentation Organized by Graduate School, University of Birmingham, April 2008.

3. Effect of Air Intake Pressure Drop on Performance and Emissions of a Diesel Engine Operating with Biodiesel and Ultra Low Sulphur Diesel (ULSD)
   R. Mamat, N.R.Abdullah, H.M. Xu, M.L.Wyszynski A.Tsolakis (2009), International Conference on Renewable Energy and Power Quality, 15-17 April 2009, Valencia, Spain

4. Effects of Pilot Injection Timing on Main Combustion Behaviour in Multi Cylinder V6 Diesel Engine.
   N.R. Abdullah, M.L. Wyszynski and A.Tsolakis (June 2009)
   Poster Presentation Organized by Graduate School, University of Birmingham, June 2009

5. Effect of Fuel Temperature on Combustion and Emissions of a Common Rail Diesel Engine

   R. Mamat, N.R.Abdullah, H.M. Xu, M.L.Wyszynski, A.Tsolakis

   International Powertrains, Fuels and Lubricants Meeting June 15-17, 2009 Florence, SAE Paper No. 2009-01-1896

6. Effect of Exhaust Gas Recirculation (EGR) with Multiple Injections on Combustion Pattern in a Common Rail Diesel Engine .

   R. Mamat, N.R.Abdullah, H.M. Xu, M.L.Wyszynski, A.Tsolakis.

   12th EAEC European Automotive Congress 2009, 29th June - 1st July 2009, Bratislava, Slovak Republic

7. Effect of Injection Pressure with Split Injection in a V6 Diesel Engine.

   N.R.Abdullah, R. Mamat, P. Rounce , A.Tsolakis, M.L.Wyszynski, H.M. Xu (2009) . International Conference, Capri Italy. SAE 2009-24-0049 September 2009.

8. The Effect of Injection Pressure and Strategy in a Jaguar V6 Diesel Engine

   N.R.Abdullah, R. Mamat, P. Rounce , A.Tsolakis, M.L.Wyszynski, H.M. Xu, G.Tian

   Journal of KONES (Internal Combustion Engines, European Science Society of Power train and Transport Publication) ISSN 1231-4005, pp 9-22, Vol 16, September 2009

9. Optimisation of Premixed Combustion on V6 Diesel Engine Through The Variation of Pilot Injection Timings Combined with EGR.
   N.R.Abdullah, R. Mamat, P. Rounce , A.Tsolakis, M.L.Wyszynski, H.M. Xu, G.Tian
   United Kingdom-Malaysia Engineering Conference, April 2010

10. Effect of Boost Temperature on the Performance and Emissions of a Common Rail Diesel Engine Operating with Rapeseed Methyl Ester (RME)
    Rizalman Mamat, Nik Rosli Abdullah, Hongming Xu, Miroslaw L. Wyszynski, A. Tsolakis
    World Congress on Engineering, 30 June - 2 July 2010, London.

11. Combined effects of pilot quantity, injection pressure and dwell periods on the combustion and emissions behaviour of a modern V6 diesel engine.
    N.R.Abdullah, M.L.Wyszynski, A.Tsolakis, R.Mamat, H.M.Xu, G.Tian.
    Journal of Archivum Combustions , ISSN 0208-4198, pp 481-495, Vol 30-2010-No.4, September 2010.

12. Emissions of a single cylinder Diesel engine operating with Ethanol.
    R.Mamat, N.R. Abdullah, N. Tamaldin.
    2nd International Youth Science Festival, November 2010.

13. A variation of pilot injection timing on V6 diesel engine fuelled with ULSD.
    N.R.Abdullah, , A.Tsolakis, M.L.Wyszynski R.Mamat, H.M.Xu, G.Tian
    Paper preparation for SAE Technical Paper (Ready for submission)

14. Control of premixed combustion behaviour in a multiple injections diesel engine fuelled with biodiesel.
    N.R.Abdullah, A.Tsolakis, M.L.Wyszynski, H.M. Xu, S.Chuepeng
    Paper preparation for The Journal of Combustion and Flame.

15. Combustion and emissions characteristics of a modern V6 diesel engine fuelling with Tallow Methyl Ester (TME)
    N.R.Abdullah, H.M.Xu, M.L.Wyszynski, A.Tsolakis, G.Tian, T.Garderner.
    Paper preparation for the Journal of Fuels (Ready for submission)

REFERENCES

1. Marques, A., E. Monterio, N.A. Moreira and S. Malheiro, *NOx emissions Reduction in a Biodiesel Engine by Means of EGR Technology.* SAE Paper 2007-01-0078, 2007.
2. An, B.-I., Y. Sato, S.-W. Lee and T. Takayanagi, *Effects of Injection Pressure on Combustion of a Heavy Duty Diesel Engine With Common Rail DME Injection Equipment.* SAE Paper 2004-01-1864, 2004.
3. Beatrice, C., P. Belardini and C. Bertoli, *Diesel Combustion Control in Common Rail Engines by New Injection Strategies.* Int J Engine Research Vol 3 p 23-36, 2002.
4. Ganser, M.A., *Common Rail Injectors for 2000 bar and Beyond.* SAE Paper 2000-01-0706, 2000.
5. Dober, G., S. Tullis, G. Greeves, N. Milovanovic, M. Hardy and S. Zuelch, *The Impact of Injection Strategies on Emissions Reduction and Power Output of Future Diesel Engines.* SAE Paper 2008-01-0941, 2008.
6. Lee, J., J. Jeon, J. Park and C. Bae, *Effect of Multiple Injection Strategies on Emission and Combustion Characteristics in a Single Cylinder Direct-Injection Optical Engine.* SAE Paper 2009-01-1354, 2009.
7. Shayler, P.J., T.D. Brooks, G.J. Pugh and R. Gambrill, *The Influence of Pilot and Split-Main Injection Parameters on Diesel Emissions and Fuel Consumption.* SAE Paper 2005-01-0375, 2005.
8. Vanegas, A., H. Won, C. Felsch, M. Gauding and N. Peters, *Experimental Investigation of the Effect of Multiple Injections on Pollutant Formation in a Common-Rail DI Diesel Engine.* SAE Paper 2008-01-1191, 2008.

9. Eastwood, P.G., T. Morris, K. Tufail, T. Winstanley, Y.Hardalupas and A.M.K.P. Taylor, *The Effects of Fuel-Injection Schedules on Emissions of NOx and Smoke in a Diesel Engine during.* SAE paper 2007-24-0011, 2007.

10. Idicheria, C.A. and L.M. Pickett, *Soot Formation in Diesel Combustion under High-EGR Conditions.* SAE Paper 2005-01-3834, 2005.

11. Morgan, R.E., M.R. Gold, O. Laguitton, C. Crua and M.R. Heikal, *Characterisation of the Soot Formation Processes in a High Pressure Combusting Diesel Fuel Spray.* SAE Paper 2003-01-3086, 2003.

12. Dec, J.E., *Advanced Compression-Ignition Engines - Understanding The In-cylinder Processes.* Proceedings of the Combustion Institute,Vol 32, p 2727-2742, 2009.

13. Tree, D.R. and K.I. Svensson, *Soot Processes in compression ignition engines.* Progress in Energy and Combustion Science, Vol 33, p 272-309, 2007.

14. Knecht, W., *Diesel engine development in view of Reduced Emission Standards.* Energy, Vol 33 p. 264-271, 2008.

15. Tsolakis, A. and A. Megaritis, *Partially Premixed Charge Compression Ignition Engine With On-Board H_2 Production by Exhaust Gas Fuel Reforming of Diesel and Biodiesel.* International Journal of Hydrogen Energy, Vol 30, p. 731-745, 2005.

16. Kegl, B., *Effects of Biodiesel on Emissions of a Bus Diesel Engine.* Bioresource Technology, Vol 99, p. 863-873, 2008.

17. Hazar, H., *Effects of Biodiesel on a Low Heat Loss Diesel Engine.* Renewable Energy, Vol 34, p. 1533-1537, 2009.

18. Szybist, J.P. and A.L. Boehman, *Behavior of a Diesel Injection System with Biodiesel Fuel.* SAE Paper 2003-01-1039, 2003.

19. Monyem, A. and J. H. Van Gerpen, *The Effect of Biodiesel Oxidation on Engine Performance and Emissions.* Biomass and Bioenergy, Vol 20, p 317-325, 2001.

20. Payri, F., V.R. Bermúdez, B. Tormos and W.G. Linares, *Hydrocarbon Emissions Speciation in Diesel and Biodiesel Exhausts.* Atmospheric Environment,Vol 43, p. 1273-1279, 2009.

21. Mamat, R., N.R. Abdullah, H.M. Xu, M. L.Wyszynski and A. Tsolakis, *Effect of Air Intake Pressure Drop on Performance and Emissions of Diesel Engine Operating with Biodiesel and Ultra Low Sulphur Diesel (ULSD).* International Conference on Renewable Energies and Power Quality 2009, 2009.

22. Mamat, R., S. Chuepeng, H. Xu, M.L. Wyszynski and J. Qiao, *Effect of Exhaust Gas Temperature on Engine Performance and Emissions of a Conventional V6 Diesel Engine Operating on Biodiesel and Diesel Fuel with Exhaust Gas Recirculation (EGR).* United Kingdom-Malaysia Engineering Conference 2008, 2008.

23. Chuepeng, S., H.M. Xu, A. Tsolakis, M.L. Wyszynski, P. Price, R. Stone, J.C. Hartland and J. Qiao, *Particulate Emissions from a Common Rail Fuel Injection Diesel Engine with RME-based Biodiesel Blended Fuelling Using Thermo-gravimetric Analysis.* SAE Paper 2008-01-0074, 2008.

24. Cheng, W.L., C.F. Lee and F. Ruan, *Comparisons of Combustion Characteristics of Biodiesels in a High Speed Direct Injection Diesel Engine.* SAE Paper 2008-01-1638, 2008.

25. Desantes, J.M., J. Arregle, S. Ruiz and A. Delage, *Characterisation of the Injection-Combustion Process in a D.I. Diesel Engine Running with Rape Oil Methyl Ester.* SAE Paper 1999-01-1497, 1999.

26. Labeckas, G. and S. Slavinskas, *The Effect of Rapeseed Oil Methyl Ester on Direct Injection Diesel Engine Performance and Exhaust Emissions.* Energy Conversion and Management Vol 47, p 1954-1967, 2006.

27. Szybist, J.P., J. Song, M. Alam and A.L. Boehman, *Biodiesel Combustion, Emissions and Emission Control.* Fuel Processing Technology, Vol 88, p 679–691, 2007.

28. Kahraman, B., *Biodiesel as an Alternative Motor Fuel: Production and Policies in the European Union.* Renewable and Sustainable Energy Reviews, Vol 12, p. 542-552, 2008.

29. Raheman, H. and S.V. Ghadge, *Performance of Diesel Engine with Biodiesel at Varying Compression Ratio and Ignition Timing*. Fuel, Volume 87, Vol 87, p 2659-2666, 2008.

30. Szybist, J.P., J. Song, M. Alam and A.L. Boehman, *Biodiesel Combustion, Emissions and Emission Control.* Fuel Processing Technology, Vol 88, p. 679-691, 2007.

31. Lapuerta, M., O. Armas and J.R. Fernández, *Effect of Biodiesel Fuels on Diesel Engine Emissions.* Progress in Energy and Combustion Science, Vol 34, p. 198-223, 2008.

32. Lapuerta, M., O. Armas and J.R. Fernández, *Effect of the Degree of Unsaturation of Biodiesel Fuels on NOx and Particulate Emissions.* SAE Paper, 2008-01-1676, 2008.

33. Zhang, X., G.G.L. Li, Z. Wu, Z. Hu and J. Deng, *Characteristics of Combustion and Emissions in a DI Engine Fueled with Biodiesel Blends from Soybean Oil.* SAE, 2008-01-1832.

34. Zheng, M., M.C. Mulenga, G.T. Reader, M. Wang, D.S. K.Ting and J. Tjong, *Biodiesel Engine Performance and Emissions in Low Temperature Combustion.* Fuel, Vol 87, p. 714-722, 2008.

35. Bielaczyc, P. and A. Szczotka, *A Study of RME-Based Biodiesel Blend Influence on Performance, Reliability and Emissions from Modern Light-Duty Diesel Engines.* SAE Paper 2008-01-1398, 2008.

36. Bhusnoor, S.S., M.K.G. Babu and J.P. Subrahmanyam, *Studies on Performance and Exhaust Emissions of a CI Engine Operating on Diesel and Diesel Biodiesel Blends at Different Injection Pressures and Injection Timings.* SAE Paper 2007-01-0613, 2007.

37. Oguma, M., S. Goto and Z. Chen, *Fuel Characteristics Evaluation of GTL for DI Diesel Engine* SAE Paper 2004-01-0088, 2004.

38. Oguma, M., S. Goto, M. Konno, K. Sugiyama and M. Mori, *Experimental Study of Direct Injection Diesel Engine Fueled with Two Types of Gas To Liquid (GTL).* SAE Paper 2002-01-2691, 2002.

39. Tsolakis, A., A. Megaritis, M.L. Wyszynski and K. Theinnoi, *Engine Performance and Emissions of a Diesel Engine Operating on Diesel-RME (Rapeseed Methyl Ester) Blends with EGR (Exhaust Gas Recirculation).* Energy, Vol 32, p 2072-2080, 2007.

40. Ban-Weiss, G.A., J.Y. Chen, B.A. Buchholz and R.W. Dibble, *A Numerical Investigation into the Anomalous Slight NOx Increase When Burning Biodiesel; A New (Old) Theory.* Fuel Processing Technology, Vol 88, p. 659-667, 2007.

41. Maiboom, A., X. Tauzia and J.-F. Hétet, *Experimental Study of Various Effects of Exhaust Gas Recirculation (EGR) on Combustion and Emissions of an Automotive Direct Injection Diesel Engine.* Energy, Vol 33, p. 22-34, 2008.

42. Horibe, N. and T. Ishiyama, *Relations among NOx, Pressure Rise Rate, HC and CO in LTC Operation of a Diesel Engine.* SAE Paper 2009-01-1443, 2009.

43. Aldajah, S., O.O. Ajayi, G.R. Fenske and I.L. Goldblatt, *Effect of Exhaust Gas Recirculation (EGR) Contamination of Diesel Engine Oil on Wear.* Wear, Vol 263, p. 93-98, 2007.

44. Husberg, T., S. Gjirja, I. Denbratt and J. Engstrom, *Visualization of EGR on Diesel Combustion with Long Ignition Delay in a Heavy-duty Engine.* SAE Technical Paper 2004-01-2947, 2004.

45. Chuepeng, S., A. Tsolakis, K. Theinnoi, H.M. Xu and M.L. Wyszynski, *A Study of Quantitative Impact on Emissions of High Proportion RME-Based Biodiesel Blends.* SAE Paper 2007-01-0072, 2007.

46. Ladommatos, N., S. Abdelhalim and H. Zhao, *The Effects Of Exhaust Gas Recirculation On Diesel Combustion And Emissions.* Int. J Engine Research, IMechE, Vol 1, p. 107-126, 1999.

47. *Euro 5 and Euro 6 Emissions Legislation Passenger Cars, Directive 2007/715/EC.* 2007.

48. Baumgarten, C., D. Mewes and F. Mayinger, *Mixture Formation in Internal Combustion Engines.* Springer-Verlag Berlin Heidelberg New York, 2006.

49. Zheng, M., G.T. Reader and J.G. Hawley, *Diesel Engine Exhaust Gas Recirculation-A Review on Advanced and Novel Concepts.* Energy Conversion and Management, Vol 45, p. 883-900, 2004.

50. Horn, U., R. Egnell, B. Johansson and Ö. Andersson, *Detailed Heat Release Analyses with Regard to Combustion of RME and Oxygenated Fuels in an HSDI Diesel Engine.* SAE Paper 2007-01-0627, 2007.

51. Dober, G., S. Tullis, G. Greeves, N. Milovanovic, M. Hardy and S. Zuelch, *The Impact of Injection Strategies on Emissions Reduction and Power Output of Future Diesel Engines.* SAE Paper 2008-01-0941, 2008.

52. GmbH., R.B., *Diesel-Engine Management.* Book, 2005.

53. Tanaka, T., A. Ando and K. Ishizaka, *Study on Pilot Injection of DI Diesel Engine Using Common-Rail Injection System.* JSAE Review, Vol 23, p 297-302, 2002.

54. Zhang, L., *A Study of Pilot Injection in a DI Diesel Engine.* SAE Paper 1999-01-3493, 1999.

55. Kegl, B., *Biodiesel Usage At Low Temperature.* Fuel, Vol 87, p. 1306-1317, 2008.

56. Sayin, C., K. Uslu and M. Canakci, *Influence of Injection Timing on the Exhaust Emissions of a Dual-Fuel CI Engine.* Renewable Energy, Vol 33, p. 1314-1323, 2008.

57. Abd-Alla, G.H., H.A. Soliman, O.A. Badr and M.F.A. Rabbo, *Effect of Injection Timing on the Performance of a Dual Fuel Engine.* Energy Conversion and Management, Vol 43, p. 269-277, 2002.

58. Okude, K., K. Mori, S. Shiino, K. Yamada and Y. Matsumoto, *Effects of Multiple Injections on Diesel Emission and Combustion Characteristics.* SAE Paper 2007-01-4178, 2007.

59. Hountalas, D.T., D.A. Kouremenos, K.B. Binder, V. Schwarz and G.C. Mavropoulos, *Effect of Injection Pressure on the Performance and Exhaust Emissions of a Heavy Duty DI Diesel Engine.* SAE Paper 2003-01-0340, 2003.

60. Choi, C.Y. and R.D. Reitz, *An Experimental Study on the Effects of Oxygenated Fuel Blends and Multiple Injection Strategies on DI Diesel Engine Emissions.* Fuel, Vol 78, p. 1303-1317, 1999.

61. Benajes, J., S. Molina, J.M. García and R. Novella, *Influence of Boost Pressure and Injection Pressure on Combustion Process and Exhaust Emissions in a HD Diesel Engine.* SAE Paper 2004-01-1842, 2004.

62. Arrègle, J., J.V. Pastor and S. Ruiz, *The Influence of Injection Parameters on Diesel Spray Characteristics.* SAE Paper 1999-01-0200, 1999.

63. Delacourt, E., B. Desmet and B. Besson, *Characterisation of Very High Pressure Diesel Sprays Using Digital Imaging Techniques.* Fuel, Vol 84, p. 859-867, 2005.

64. Dhananjaya, D.A., P. Mohanan and C.V. Sudhir, *Effect of Injection Pressure and Injection Timing on a Semiadiabatic CI Engine Fuelled with Blends of Jatropha Oil Methyl Esters.* SAE Paper 2008-28-0070, 2008.

65. Abdullah, N.R., R. Mamat, P. Rounce, M.L. Wyszynski, A. Tsolakis, H.M. Xu and G. Tian, *The Effect of Injection Pressure and Strategy in a Jaguar V6 Diesel*

Engine. Journal of International Combustion Engines (KONES 2009), p 9-24, 2009.

66. Shimazaki, N., A. Minato and T. Nishimura, *Premixed Diesel Combustion Using Direct Injection Near Top Dead Centre.* IMechE Int. J. Engine Res. Vol 8., p 259-270, 2007.

67. Kimura, S., O. Aoki, Y. Kitahara and E. Aiyoshizawa, *Ultra-Clean Combustion Technology Combining a Low-Temperature and Premixed Combustion Concept for Meeting Future Emission Standards.* SAE Paper 2001-01-0200, 2001.

68. Benajes, J., S. Molina, R. Novella and K. DeRudder, *Influence of Injection Conditions and Exhaust Gas Recirculation in a High-Speed Direct-Injection Diesel Engine Operating with a Late Split Injection.* Proc. IMechE Part D: J. Automobile Engineering, Vol 222, p 629-641, 2008.

69. Badami, M., P. Nuccio and G. Trucco, *Influence of Injection Pressure on the Performance of a DI Diesel Engine with a Common Rail Fuel Injection System.* SAE Paper 1999-01-0193, 1999.

70. Roy, M.M. and H. Tsunemoto, *Effect of Injection Pressure and Split Injection on Exhaust Odor and Engine Noise in DI Diesel Engines.* SAE Paper 2002-01-2874, 2002.

71. Iwabuchi, Y., K. Kawai, T. Shoji and Y. Takeda, *Trial of New Concept Diesel Combustion System (Premixed Compression-Ignited Combustion).* SAE Paper 1999-01-0185, 1999.

72. Park, C., S. Kook and C. Bae, *Effects of Multiple Injections in a HSDI Diesel Engine Equipped With Common Rail Injection System.* SAE Paper 2004-01-0127, 2004.

73. Carlucci, P., A. Ficarella and D. Laforgia, *Effects on Combustion and Emissions of Early and Pilot Fuel Injections in Diesel Engines.* Int. J. Engine, Res.Vol 6, p 43-60, 2004.

74. Ghaffarpour, M. and A.R. Noorpoor, *NO_x Reduction in Diesel Engines Using Rate Shaping and Pilot Injection.* Int. J. Automotive Technology and Management, Vol 7, p 17-31, 2007.

75. Badami, M., F. Mallamo, F. Millo and E.E. Rossi, *Influence of Multiple Injection Strategies on Emissions, Combustion Noise and BSFC of a DI Common Rail Diesel Engine.* SAE Paper 2002-01-0503, 2002.

76. Lee, T. and R.D. Reitz, *The Effects of Split Injection and Swirl on a HSDI Diesel Engine Equipped with a Common Rail Injection System.* SAE Paper 2003-01-0349, 2003.

77. Montgomery, D.T. and R.D. Reitz, *Effects of Multiple Injections and Flexible Control of Boost and EGR on Emissions and Fuel Consumption of a Heavy-Duty Diesel Engine.* SAE Paper 2001-01-0195, 2001.

78. Dronniou, N., M. Lejeune, I. Balloul and P. Higelin, *Combination of High EGR Rates and Multiple Injection Strategies to Reduce Pollutant Emissions.* SAE Paper 2005-01-3726, 2005.

79. Hardy, W.L. and R.D. Reitz, *An Experimental Investigation of Partially Premixed Combustion Strategies Using Multiple Injections in a Heavy-Duty Diesel Engine.* SAE Paper 2006-01-0917, 2006.

80. Peng, H., Y. Cui, L. Shi and K. Deng, *Effects of Exhaust Gas Recirculation (EGR) on Combustion and Emissions During Cold Start of Direct Injection (DI) Diesel Engine.* Energy, Vol 33, p 471-479, 2008.

81. Baik, D.S., Y.C. Han and S.K. Oh, *A Study on Spray and Combustion Behavior in Heavy-Duty Diesel Engine Equipped with EGR.* SAE Paper 2001-01-3749, 2001.

82. Idicheria, C.A. and L.M. Pickett, *Effect of EGR on Diesel Premixed-Burn Equivalence Ratio.* Proceedings of the Combustion Institute, Vol 31, p 2931-2938, 2007.

83. Hountalas, D.T., G.C. Mavropoulos and K.B. Binder, *Effect of Exhaust Gas Recirculation (EGR) Temperature for Various EGR Rates on Heavy Duty DI Diesel Engine Performance and Emissions.* Energy, Vol 33, p. 272-283, 2008.

84. Tao, F. and P. Bergstrand, *Effect of Ultra-High Injection Pressure on Diesel Ignition and Flame under High-Boost Conditions.* SAE Paper 2008-01-1603, 2008.

85. Horibe, N., K. Takahashi, S.-S. Kee, T. Ishiyama and M. Shioji, *The Effects of Injection Conditions and Combustion Chamber Geometry on Performance and Emissions of DI-PCCI Operation in a Diesel Engine.* SAE paper 2007-01-1874, 2007.

86. Kawano, D., H. Ishii, Y. Goto, A. Noda and Y. Aoyagi, *Effect of Exhaust Gas Recirculation on Exhaust Emissions from Diesel Engines Fuelled with Biodiesel.* SAE Paper 2007-24-0128, 2007.

87. Okude, K., K. Mori, S. Shiino and T. Moriya, *Premixed Compression Ignition (PCI) Combustion for Simultaneous Reduction of NOx and Soot in Diesel Engine.* SAE Paper, 2004-01-1907, 2004.

88. Fang, T., R.E. Coverdill, C.-F.F. Lee and R.A. White, *Effects of Injection Angles on Combustion Processes Using Multiple Injection Strategies In An HSDI Diesel Engine.* Fuel, Vol 87, p. 3232-3239, 2008.

89. Ladommatos, N., S.M. Abdelhalim, H. Zhao and Z. Hu, *The Effects of Carbon Dioxide in Exhaust Gas Recirculation on Diesel Engine Emissions.* Proc Instn Mech Engrs.IMechE, Part D J. Automobile Engineering, Vol 212, p 25-42, 1998.

90. Desantes, J.M., J. Arrègle, S. Molina and M. Lejeune, *Influence of the EGR Rate, Oxygen Concentration and Equivalent Fuel/Air Ratio on the Combustion Behaviour and Pollutant Emissions of a Heavy-Duty Diesel Engine.* SAE paper 2000-01-1813, 2000.

91. Nikolic, D. and N. Iida, *Effects of Intake CO_2 Concentrations on Fuel Spray Flame Temperatures and Soot Formations.* Proc. IMechE Part D: J. Automobile Engineering, Vol. 221, p 1567-1573, 2006.

92. Çinar, C., T. Topgül, M. Ciniviz and C. Hasimoglu, *Effects of Injection Pressure and Intake CO_2 Concentration on Performance and Emission Parameters of An IDI Turbocharged Diesel Engine.* Applied Thermal Engineering, Vol 25, p. 1854-1862, 2005.

93. Buchwald, R., M. Brauer, A. Blechstein, A. Sommer and J. Kahrstedt, *Adaption of Injection System Parameters to Homogeneous Diesel Combustion.* SAE Paper 2004-01-0936, 2004.

94. Sen, A.K., R. Longwic, G. Litak and K. Górski, *Analysis of Cycle-to-Cycle Pressure Oscillations in a Diesel Engine.* Mechanical Systems and Signal Processing, Vol 22, p 362-373, 2008.

95. Bouchez, M. and J.B. Dementhon, *Strategies for the Control of Particulate Trap Regeneration.* SAE Paper 2000-01-0472, 2000.

96. Wagner, R.M., J.B.G. Jr, T.Q. Dam, K.D. Edwards and J.M. Storey, *Simultaneous Low Engine-Out NOx and Particulate Matter with Highly Diluted Diesel Combustion.* SAE Paper 2003-01-0262, 2003.

97. Akihama, K., Y. Takatori, K. Inagaki, S. Sasaki and A.M. Dean, *Mechanism of the Smokeless Rich Diesel Combustion by Reducing Temperature.* SAE Paper 2001-01-0655, 2001.

98. Horibe, N., S. Harada, T. Ishiyama and M. Shioji, *Improvement of Premixed Charge Compression Ignition Based Combustion by Two-Stage Injection.* Int. J. Engine Res. IMechE, Vol 10, p 71-80, 2009.

99. Jacobs, T., D. Assanis and Z. Filipi, *The Impact of Exhaust Gas Recirculation on Performance and Emissions of a Heavy-Duty Diesel Engine.* SAE Paper 2003-01-1068, 2003.

100. Dennis, A.J., C.P. Garner and D.H.C. Taylor, *The Effect of EGR on Diesel Engine Wear.* SAE Paper 1999-01-0839, 1999.

101. Bae, M.W., J.H. Ha and K. Tsuchiya, *The Characteristics of Wear in Diesel Engines with Scrubber EGR System.* SAE Paper 2000-05-0122, 2000.

102. Ishiki, K., S. Oshida, M. Takiguchi and M. Urabe, *A Study of Abnormal Wear in Power Cylinder of Diesel Engine with EGR-Wear Mechanism of Soot Contaminated in Lubricating Oil.* SAE Paper 2000-01-0925, 2000.

103. Li, S., A.A. Csontos, B.M. Gable, C.A. Passut and T.-C. Jao, *Wear in Cummins M-11/EGR Test Engines.* SAE Paper 2002-01-1672, 2002.

104. Takakura, T., Y. Ishikawa and K. Ito, *The Wear Mechanism of Piston Rings and Cylinder Liners Under Cooled-EGR Condition and the Development of Surface Treatment Technology for Effective Wear Reduction.* SAE Paper 2005-01-1655, 2005.

105. Tanin, K.V., D.D. Wickman, D.T. Montgomery, S. Das and R.D. Reitz, *The Influence of Boost Pressure on Emissions and Fuel Consumption of a Heavy-Duty Single-Cylinder D.I. Diesel Engine.* SAE Paper 1999-01-0840, 1999.

106. Arnold, S., K. Slupski, M. Groskreutz, G. Vrbas, R. Cadle and S.M. Shaded, *Advanced Turbocharging Technologies for Heavy-Duty Diesel Engines.* SAE Paper 2001-01-3260, 2001.

107. Lapuerta, M., O. Armas and R. Ballesteros, *Diesel Particulate Emissions from Biofuels Derived from Spanish Vegetable Oils.* SAE Paper 2002-01-1657, 2002.

108. Agarwal, D., L. Kumar and A.K. Agarwal, *Performance Evaluation of a Vegetable Oil Fuelled Compression Ignition Engine.* Renewable Energy, Vol 33, p 1147-1156, 2008.

109. Cho, H.M., S. Maji and B.D. Pathak, *Waste Cooking Oil as Fuel in Diesel Engines.* SAE Paper 2008-28-0013, 2008.

110. Kalligeros, S., F. Zannikos, S. Stournas, E. Lois, G. Anastopoulos, C. Teas and F. Sakellaropoulos, *An Investigation of Using Biodiesel/Marine Diesel Blends on the Performance of a Stationary Diesel Engine.* Biomass and Bioenergy, Vol 24, p 141-149, 2003.

111. Mittelbach, M., *Diesel Fuel Derived from Vegetable Oils, VI: Specifications and Quality Control of Biodiesel.* Bioresource Technology, Vol 56, p 7-11, 1996.

112. Szybist, J.P., A.L. Boehman, J.D. Taylor and R.L. McCormick, *Evaluation of Formulation Strategies to Eliminate the Biodiesel NO_x Effect.* Fuel Processing Technology, Vol 86, p 1109-1126, 2005.

113. Tsolakis, A., A. Megaritis and D. Yap, *Application of Exhaust Gas Fuel Reforming in Diesel and Homogeneous Charge Compression Ignition (HCCI) Engines Fuelled with Biofuels.* Energy Vol 33, p 462-470, 2008.

114. Hess, M.A., M.J. Haas and T.A. Foglia, *Attempts to Reduce NOx Exhaust Emissions by Using Reformulated Biodiesel.* Fuel Processing Technology, Vol 88, p 693-699, 2007.

115. Karavalakis, G., S. Stournas and E. Bakeas, *Effects of Diesel/Biodiesel Blends on Regulated and Unregulated Pollutants from a Passenger Vehicle Operated Over The European and the Athens Driving Cycles.* Atmospheric Environment, Vol 43, p 1745-1752, 2009.

116. Canakci, M., A. Erdil and E. Arcaklioglu, *Performance and Exhaust Emissions of a Biodiesel Engine.* Applied Energy, Vol 83, p 594-605, 2006.

117. Ramadhas, A.S., C. Muraleedharan and S. Jayaraj, *Performance and Emission Evaluation of a Diesel Engine Fueled with Methyl Esters of Rubber Seed Oil.* Renewable Energy, Vol 30, p 1789-1800, 2005.

118. Demirbas, A., *Progress and Recent Trends in Biodiesel Fuels.* Energy Conversion and Management, Vol 50, p 14-34, 2009.

119. Bozbas, K., *Biodiesel as an Alternative Motor Fuel: Production and Policies in the European Union.* Renewable and Sustainable Energy Reviews, Vol 12, p 542-552, 2008.

120. Canakci, M., *Performance and Emissions Characteristics of Biodiesel from Soybean Oil.* Proc. IMechE, Part D: J. Automobile Engineering, Vol 219, p 915-922, 2005.

121. Haas, J.M., K.M. Scott, T.L. Alleman and R.L. McCormick, *Engine Performance of Biodiesel Fuel Prepared from Soybean Soapstock: A High Quality Renewable Fuel Produced from a Waste Feedstock.* Energy Fuels, Vol 15, p 1207-1212, 2001.

122. Usta, N., *An Experimental Study on Performance and Exhaust Emissions of a Diesel Engine Fuelled with Tobacco Seed Oil Methyl Ester.* Energy Conversion and Management, Vol 46, p 2373-2386, 2005.

123. Canakci, M., *Combustion Characteristics of a Turbocharged DI Compression Ignition Engine Fuelled with Petroleum Diesel Fuels and Biodiesel.* Bioresource Technology, Vol 98, p 1167-1175, 2007.

124. Lin, C.-Y. and H.-A. Lin, *Diesel Engine Performance and Emission Characteristics of Biodiesel Produced by the Peroxidation Process.* Fuel, Vol 85, p 298-305, 2006.

125. Carraretto, C., A. Macor, A. Mirandola, A. Stoppato and S. Tonon, *Biodiesel as Alternative Fuel: Experimental Analysis and Energetic Evaluations.* Energy, Vol 29, p 2195- 2211, 2004.

126. Lin, C.-Y., H.-A. Lin and L.-B. Hung, *Fuel Structure and Properties of Biodiesel Produced by the Peroxidation Process.* Fuel, Vol 85, p 1743-1749, 2006.

127. Sinha, S. and A.K. Agarwal, *Performance Evaluation of a Biodiesel (Rice Bran Oil Methyl Ester) Fuelled Transport Diesel Engine.* SAE Paper 2005-01-1730, 2005.

128. McCormick, R.L., C.J. Tennant, R. R.Hayes, S.Black, J.Ireland, T. McDaniel, A.Williams, M. Frailey and C.A. Sharp, *Regulated Emissions from Biodiesel Tested*

in Heavy-Duty Engines Meeting 2004 Emission Standards. SAE Paper 2005-01-2200, 2005.

129. Senatore, A., M. Cardone, V. Rocco and M.V. Prati, *A Comparative Analysis of Combustion Process in D.I. Diesel Engine Fuelled with Biodiesel and Diesel Fuel.* SAE Paper 2000-01-0691, 2000.

130. Szybist, J.P. and A.L. Boehman, *Behavior of a Diesel Injection System with Biodiesel Fuel.* SAE Paper 2003-01-1039, 2003.

131. Chuepeng, S., *Quantitative Impact on Engine Performance and Emissions of High Proportion Biodiesel Blends and the Required Engine Control Strategies*, PhD Thesis, The University of Birmingham, 2008.

132. Hasimoglu, C., M. Ciniviz, I. Özsert, Y. Içingür, A. Parlak and M.S. Salman, *Performance Characteristics of a Low Heat Rejection Diesel Engine Operating with Biodiesel.* Renewable Energy, Vol 33, p 1709-1715, 2008.

133. Nelson, R.G. and M.D. Schrock, *Energetic and Economic Feasibility Associated with the Production, Processing, and Conversion of Beef Tallow to a Substitute Diesel Fuel.* Biomass and Bioenergy, Vol 30, p. 584-59, 2006.

134. Ma, F. and M.A. Hanna, *Biodiesel Production: A Review.* Bioresource Technology, Vol 70, p 1-15, 1999.

135. Winther, K., *Large Scale Fleet Demonstration of TME Biodiesel in Northern Europe.* SAE Paper 2010-01-0474, 2010.

136. Zheng, D. and M. A.Hanna, *Preparation and Properties of Methyl Esters of Beef Tallow.* Bioresource Technology, Vol 57, p 137-142,1996.

137. Oner, C. and S. Altun, *Biodiesel Production from Inedible Animal Tallow and an Experimental Investigation of Its Use as Alternative Fuel in a Direct Injection Diesel Engine.* Applied Energy, Vol 86, p 2114-2120, 2009.

138. Kumar, M.S., A. Kerihuel, J. Bellettre and M. Tazerout, *Ethanol Animal Fat Emulsions as a Diesel Engine Fuel - Part 2: Engine Test Analysis.* Fuel, Vol 85, p 2646-2652, 2006.

139. Nuszkowski, J., G.J. Thompson, R. Tincher and N.N. Clark, *Heat Release and Emission Characteristics of B20 Biodiesel Fuels During Steady State and Transient Operation.* SAE Paper 2008-01-1377, 2008.

140. Lidstone, L., G.D. Harris, F. Gu and A. Ball, *An Experimental Study of NOx Emissions for the Development of an Emission Analysis Tool.* SAE Paper 2007-01-0065, 2007.

141. Ueki, S., Miura, Akinori, *Effect of Difference of High Pressure Fuel Injection Systems on Exhaust Emissions from HDDI Diesel Engine.* JSAE Review, Vol 20, p 555-557, 1999.

142. Can, Ö., I. Çelikten and N. Usta, *Effects of Ethanol Addition on Performance and Emissions of a Turbocharged Indirect Injection Diesel Engine Running at Different Injection Pressures.* Energy Conversion and Management, Vol 45, p 2429-2440, 2004.

143. Camobreco, V., J. Sheehan, J. Duffield and M. Graboski, *Understanding the Life-Cycle Costs and Environmental Profile of Biodiesel and Petroleum Diesel Fuel.* SAE Paper 2000-01-1487, 2000.

144. Svensson, K.I., M.J. Richards, A.J. Mackrory and D.R. Tree, *Fuel Composition and Molecular Structure Effects on Soot Formation in Direct-Injection Flames Under Diesel Engine Conditions.* SAE Paper 2005-01-0381, 2005.

145. Heywood, J.B., *Internal Combustion Engine Fundamentals.* Ed McGraw-Hill International Editions, Automotive Technology Series, 1988.

146. Kittelson, D.B., *Engines and Nanoparticles: A Review.* Journal of Aerosol Science, Vol 29, p 575-588, 1998.

147. Musculus, M.P.B., T. Lachaux, L.M. Pickett and C.A. Idicheria, *End-of-Injection Over-Mixing and Unburned Hydrocarbon Emissions in Low-Temperature-Combustion Diesel Engines.* SAE Paper 2007-01-0907, 2007.

148. Kashdan, J.T., S. Mendez and G. Bruneaux, *On the Origin of Unburned Hydrocarbon Emissions in a Wall Guided, Low NOx Diesel Combustion System.* SAE Paper 2007-01-1836, 2007.

149. Lapuerta, M., O. Armas and R. Ballesteros, *Diesel Particulate Emissions from Biofuels Derived from Spanish Vegetable Oils.* SAE Paper 2002-01-1657, 2002.

150. Chuepeng, S., H.M. Xu, A. Tsolakis, M.L. Wyszynski, P. Price, R. Stone, J.C. Hartland and J. Qiao, *Particulate Emissions from a Common Rail Fuel Injection Diesel Engine with RME-based Biodiesel Blended Fuelling Using Thermo-gravimetric Analysis.* SAE Paper 2008-01-0074, 2008.

151. Canakci, M., A.N. Ozsezen, E. Arcaklioglu and A. Erdil, *Prediction of Performance and Exhaust Emissions of a Diesel Engine Fuelled with Biodiesel Produced from Waste Frying Palm Oil.* Expert Systems with Applications, Vol 36, p 9268-9280, 2009.

152. Kook, S., C. Bae, P.C. Miles, D. Choi and L.M. Pickett, *The Influence of Charge Dilution and Injection Timing on Low-Temperature Diesel Combustion and Emissions.* SAE Paper 2005-01-3837, 2005.

153. Kook, S., C. Bae, P.C. Miles, D. Choi, M. Bergin and R.D. Reitz, *The Effect of Swirl Ratio and Fuel Injection Parameters on CO Emission and Fuel Conversion Efficiency for High-Dilution, Low-Temperature Combustion in an Automotive Diesel Engine.* SAE Paper 2006-01-0197, 2006.

154. Opat, R., Y. Ra, M.A. Gonzalez, D.R. Krieger, R.D. Reitz, D.E. Foster, R.P. Durrett and R.M. Siewert, *Investigation of Mixing and Temperature Effects on HC/CO Emissions for Highly Dilute Low Temperature Combustion in a Light Duty Diesel Engine.* SAE Paper 2007-01-0193, 2007.

155. Noehre, C., M. Andersson, B. Johansson and A. Hultqvist, *Characterization of Partially Premixed Combustion.* SAE Paper 2006-01-3412, 2006.

156. Henein, N.A., A. Bhattacharyya, J. Schipper, A. Kastury and W. Bryzik, *Effect of Injection Pressure and Swirl Motion on Diesel Engine-out Emissions in Conventional and Advanced Combustion Regimes.* SAE Paper 2006-01-0076, 2006.

157. Alkemade, U.G.S., Bernd, *Engines and Exhaust After Treatment Systems for Future Automotive Applications.* Solid State Ionics, Vol 177, p 2291-2296, 2006.

158. Mayer, A., U. Matter, G. Scheidegger, J. Czerwinski, M. Wyser, D. Kieser and J. Weidhofer, *Particulate Traps for Retro-Fitting Construction Site Engines - VERT: Final Measurements and Implementation.* SAE Paper 1999-01-0116, 1999.

159. Mazzarella, G., F. Ferraraccio, M.V. Prati, S. Annunziata, A. Bianco, A. Mezzogiorno, G. Liguori, I.F. Angelillo and M. Cazzola, *Effects of Diesel Exhaust Particles on Human Lung Epithelial Cells: An in Vitro Study.* Respiratory Medicine, Vol 101, p 1155-1162, 2007.

160. Kumfer, B.M.S., S. A. Chen, R. Axelbaum, R. L., *Measurement and Analysis of Soot Inception Limits of Oxygen-Enriched Coflow Flames.* Combustion and Flame, Vol 147, p 233-242, 2006.

161. Fino, D., *Diesel Emission Control: Catalytic Filters for Particulate Removal.* Science and Technology of Advanced Materials, Vol 8, p 93-100, 2007.

162. Khair, M.K., *A Review of Diesel Particulate Filter Technologies.* SAE Paper 2003-01-2303, 2003.

163. Masoudi, M., *Pressure Drop of Segmented Diesel Particulate Filters.* SAE Paper 2005-01-0971, 2005.

164. Guo, Z. and Z. Zhang, *Multi-Dimensional Modeling and Simulation of Wall-Flow Diesel Particulate Filter During Loading and Regeneration.* SAE Paper 2006-01-0265, 2006.

165. Donga, H., S. Shuai, R. Li, J. Wang, X. Shi and H. He, *Study of NOx Selective Catalytic Reduction by Ethanol Over Ag/Al2O3 Catalyst on a HD Diesel Engine.* Chemical Engineering Journal, Vol 135, p 195-201, 2008.

166. Arous, W., H. Tounsi, S. Djemel, A. Ghorbel and G. Delahay, *Selective Catalytic Reduction of Nitric Oxide with Ammonia on Copper (II) Ion-Exchanged Offretite.* Catalysis Communications, Vol 6, p 281-285, 2005.

167. Yan, H., T. Zhi-quan, W. Bing and Z. Jun-feng, *Low Temperature Selective Catalytic Reduction of NO by Ammonia Over V2O5-Ceo2/Tio2.* Journal of Fuel Chemistry and Technology, Vol 36, p 616-620, 2008.

168. Moreno-Tost, R., E.R. Castellon and A. Jimenez-Lopez, *Cobalt-Iridium Impregnated Zirconium-Doped Mesoporous Silica as Catalysts for the Selective Catalytic Reduction of NO with Ammonia.* Journal of Molecular Catalysis A: Chemical, Vol 248, p 126-134, 2006.

169. Wang, Q., J.H. Sohn and J.S. Chung, *Thermally Stable Pt/K2Ti2O5 as High-Temperature NOx Storage and Reduction Catalyst.* Applied Catalysis B: Environmental, Vol 89, p 97-103, 2009.

170. Liu, Y., M. Meng, X.-G. Li, L.-H. Guo and Y.-Q. Zha, *NOx Storage Behavior and Sulfur-Resisting Performance of the Third-Generation NSR Catalysts Pt/K/Tio2-Zro2.* Chemical Engineering Research and Design, Vol 86, p 932-940, 2008.

171. Ji, Y., T.J. Toops, J.A. Pihl and M. Crocker, *NOx Storage and Reduction in Model Lean NOx Trap Catalysts Studied By In Situ DRIFTS.* Applied Catalysis B: Environmental, Vol 91, p 329-338, 2009.

172. Graboski, M.S. and R.L. McCormick, *Combustion of Fat and Vegetable Oil Derived Fuels in Diesel Engines.* Progress in Energy and Combustion Science, Vol 24, p 125-164, 1998.

173. Öner, C. and S. Altun, *Biodiesel Production from Inedible Animal Tallow and an Experimental Investigation of Its Use as Alternative Fuel in a Direct Injection Diesel Engine.* Applied Energy, Vol 86, p 2114-2120, 2009.

174. Azmi, Y. and J.M. Stephen, *Physical and Chemical Characterization of Methyl Soyoil and Methyl Tallow Esters as CI Engine Fuels.* Biomass and Bioenergy, Vol 4, p 321-328, 1994.

175. Buyukkaya, E. and M. Cerit, *Experimental Study of NOx Emissions and Injection Timing of a Low Heat Rejection Diesel Engine.* International Journal of Thermal Sciences, Vol 47, p 1096-1106, 2008.

176. Hountalas, D.T., G.C. Mavropoulos, T.C. Zannis and V. Schwarz, *Possibilities to Achieve Future Emission Limits for HD DI Diesel Engines Using Internal Measures.* SAE Paper 2005-01-0377, 2005.

177. Zheng, M., G.T. Reader and J.G. Hawley, *Diesel Engine Exhaust Gas Recirculation - A Review on Advanced and Novel Concepts.* Energy Conversion and Management, Vol 45, p 883-900, 2004.

178. Ladommatos, N., S.M. Abdelhalim, H. Zhao and Z. Hu, *Effects of EGR on Heat Release in Diesel Combustion.* SAE Paper 980184, 1998.

179. Ladommatos, N., S. Abdelhalim and H. Zhao, *Control of Oxides of Nitrogen from Diesel Engines Using Diluents While Minimising the Impact on Particulate Pollutants.* Applied Thermal Engineering, Vol 18, p 963- 980,1998.

180. Ishida, M., S. Yamamoto, H. Ueki and D. Sakaguchi, *Remarkable Improvement of NOx-PM Trade-Off in a Diesel Engine by Means of Bioethanol and EGR.* Energy, Vol 35, p 4572-4581, 2010.

181. Abu-Hamdeh, N.H., *Effect of Cooling the Recirculated Exhaust Gases on Diesel Engine Emissions.* Energy Conversion and Management, Vol 44, p 3113-3124, 2003.

182. Turner, D., G. Tian, H. Xu and M.L. Wyszynski, *An Experimental Study of Dieseline Combustion in a Direct Injection Engine.* SAE Paper 2009-01-1101, 2009.

183. Roy, M.M., *Effect of Exhaust Gas Recirculation on Combustion and Odorous Emissions in Direct Injection Diesel Engines.* SAE Paper 2008-01-2482, 2008.

184. Ogawa, H., N. Miyamoto, H. Shimizu and S. Kido, *Characteristics of Diesel Combustion in Low Oxygen Mixtures with Ultra-High EGR.* SAE Paper 2006-01-1147, 2006.

185. Dec, J.E., *Advanced Compression-Ignition Engines - Understanding the In-Cylinder Processes.* Proceedings of the Combustion Institute. Vol 32, p. 2727-2742, 2009.

186. Sayin, C. and M. Canakci, *Effects of Injection Timing on the Engine Performance and Exhaust Emissions of a Dual-Fuel Diesel Engine.* Energy Conversion and Management, Vol 50, p 203-213, 2009.

187. Kegl, B., *NOx and Particulate Matter (PM) Emissions Reduction Potential by Biodiesel Usage.* Energy & Fuels, Vol 21, p 3310-3316, 2007.

188. Fang, T. and C.-F.F. Lee, *Bio-diesel Effects on Combustion Processes in an HSDI Diesel Engine Using Advanced Injection Strategies.* Proceedings of the Combustion Institute, Vol 32, p 2785-2792, 2009.

189. Kimura, S., O. Aoki, H. Ogawa, S. Muranaka and Y. Enomoto, *New Combustion Concept for Ultra-Clean and High-Efficiency Small DI Diesel Engines.* SAE Paper 1999-01-3681, 1999.

190. Badami, M., F. Millo and D.D. D'Amato, *Experimental Investigation on Soot and NOx Formation in a DI Common Rail Diesel Engine with Pilot Injection.* SAE Paper 2001-01-0657, 2001.

191. Fang, T., R.E. Coverdill, C.-F.F. Lee and R.A. White, *Low Temperature Combustion within a Small Bore High Speed Direct Injection (HSDI) Diesel Engine.* SAE Paper 2005-01-0919, 2005.

192. Jacobs, T.J., S.V. Bohac, D.N. Assanis and P.G. Szymkowicz, *Lean and Rich Premixed Compression Ignition Combustion in a Light-Duty Diesel Engine.* SAE Paper 2005-01-0166, 2005.

193. Nwafor, O.M.I., G. Rice and A.I. Ogbonna, *Effect of Advanced Injection Timing on the Performance of Rapeseed Oil in Diesel Engines.* Renewable Energy, Vol 21, p 433-444, 2000.

194. Nwafor, O.M.I., *Effect of Choice of Pilot Fuel on the Performance of Natural Gas in Diesel Engines.* Renewable Energy, Vol 21, p 495-504, 2000.

195. Lechner, G.A., T.J. Jacobs, C.A. Chryssakis and D.N. Assanis, *Evaluation of a Narrow Spray Cone Angle, Advanced Injection Timing Strategy to Achieve Partially Premixed Compression Ignition Combustion in a Diesel Engine.* SAE Paper 2005-01-0167, 2005.

196. Sayin, C., M. Ilhan, M. Canakci and M. Gumus, *Effect of Injection Timing on the Exhaust Emissions of a Diesel Engine Using Diesel-Methanol Blends.* Renewable Energy, Vol 34, p 1261-1269, 2009.

197. Verbiezen, K., A.J. Donkerbroek, R.J.H. Klein-Douwel, A.P.V. Vliet, P.J.M. Frijters, X.L.J. Seykens, R.S.G. Baert, W.L. Meerts, N.J. Dam and J.J.T. Meulen, *Diesel Combustion: In-cylinder NO Concentrations in Relation to Injection Timing.* Combustion and Flame, Vol 151, p 333-346, 2007.

198. Ren, Y., Z. Huang, D. Jiang, L. Liu, K. Zeng, B. Liu and X. Wang, *Combustion Characteristics of a Compression-Ignition Engine Fuelled with Diesel-Dimethoxy Methane Blends Under Various Fuel Injection Advance Angles.* Applied Thermal Engineering, Vol 26, p 327-337, 2006.

199. Ozsezen, A.N., M. Canakci, A. Turkcan and C. Sayin, *Performance and Combustion Characteristics of a DI Diesel Engine Fuelled with Waste Palm Oil and Canola Oil Methyl Esters.* Fuel, Vol 88, p 629-636, 2009.

200. Lapuerta, M., J.M. Herreros, L.L. Lyons, R.G. Contreras and Y. Briceño, *Effect of the Alcohol Type Used in the Production of Waste Cooking Oil Biodiesel on Diesel Performance and Emissions.* Fuel, Vol 87, p 3161-3169, 2008.

201. Lapuerta, M., J. Rodríguez-Fernández and J.R. Agudelo, *Diesel Particulate Emissions from Used Cooking Oil Biodiesel.* Bioresource Technology, Vol 99, p 731-740, 2008.

202. Di, Y., C.S. Cheung and Z. Huang, *Experimental Investigation on Regulated and Unregulated Emissions of a Diesel Engine Fuelled with Ultra-Low Sulfur Diesel Fuel Blended with Biodiesel from Waste Cooking Oil.* Science of the Total Environment, Vol 407, p 835-846, 2009.

203. Puhan, S., N. Vedaraman, G. Sankaranarayanan and B.V.B. Ram, *Performance and Emission Study of Mahua Oil (Madhuca Indica Oil) Ethyl Ester in a 4-Stroke Natural Aspirated Direct Injection Diesel Engine.* Renewable Energy, Vol 30, p 1269-1278, 2005.

204. AltIparmak, D., A. Keskin, A. Koca and M. Gürü, *Alternative Fuel Properties of Tall Oil Fatty Acid Methyl Ester-Diesel Fuel Blends.* Bioresource Technology, Vol 82, p 241-246, 2007.

205. Dorado, M.P., E. Ballesteros, J.M. Arnal, J. Gómez and F.J. López, *Exhaust Emissions from a Diesel Engine Fuelled with Transesterified Waste Olive Oil (Small Star, Filled).* Fuel, Vol 82, p 1311-1315, 2003.

206. Nabi, M.N., M.S. Akhter and M.M.Z. Shahadat, *Improvement of Engine Emissions with Conventional Diesel Fuel and Diesel-Biodiesel Blends.* Bioresource Technology, Vol 97, p 372-378, 2006.

207. Lin, Y.-F., Y.-P.G. Wu and C.-T. Chang, *Combustion Characteristics of Waste-Oil Produced Biodiesel/Diesel Fuel Blends.* Fuel, Vol 86, p 1772-1780, 2007.

208. Nagaraju, V., N. Henein, A. Quader, M. Wu and W. Bryzik, *Effect of Biodiesel (B-20) on Performance and Emissions in a Single Cylinder HSDI Diesel Engine.* SAE Paper 2008-01-1401, 2008.

209. Ganesan, V., *Internal Combustion Engines*, New Delhi: McGraw Hill, 2003.

210. Lapuerta, M., O. Armas and J.M. Herreros, *Emissions from a Diesel-Bioethanol Blend in an Automotive Diesel Engine.* Fuel, Vol 87, p 25-31, 2008.

211. Abd-Alla, G.H., *Using Exhaust Gas Recirculation in Internal Combustion Engines: A Review.* Energy Conversion and Management, Vol 43, p 1027-1042, 2002.